ALDOT Project 931-045 Final Report

March 2024

National Center for Asphalt Technology
NCAT
at AUBURN UNIVERSITY

A METHOD OF MAXIMUM THICKNESS FOR FLEXIBLE PAVEMENT DESIGN

Dr. Suri Gatiganti, Dr. David Timm, P.E., Dr. Nam Tran, P.E.

ALDOT Project 931-045

A Method of Maximum Thickness for Flexible Pavement Design

Final Report

Submitted to

Alabama Department of Transportation

1409 Coliseum Boulevard

Montgomery, Alabama

by

Dr. Suri Gatiganti

Dr. David Timm, P.E.

Dr. Nam Tran, P.E.

National Center for Asphalt Technology

Auburn University

277 Technology Parkway

Auburn, AL 36830

March, 2024

TABLE OF CONTENTS

LIST OF FIGURES

LIST OF TABLES

CHAPTER 1
INTRODUCTION

Asphalt pavement thickness design, for both new and overlay scenarios, has been evolving since the 1960's from empirical to mechanistic-empirical design frameworks. Regardless of the design methodology, the fundamental goal of thickness design has been to determine the optimum cross-section to achieve the desired performance under the prevailing conditions (i.e., traffic, climate and materials). Central to that effort has been the calibration of design systems to accurately predict pavement deterioration over time. While calibration can be effective in developing more accurate predictions and, therefore, optimizing cross-sections, most design systems do not have a maximum thickness built into the procedure, which can yield unreasonably thick cross-sections. Figure 1.1 shows a simple example, developed with the AASHTO 1993 Design Guide, where the Asphalt Concrete (AC) layer thickness is plotted against the design traffic, expressed in terms of Equivalent Single Axle Loads (ESALs). Clearly, the AC layer thickness increases indefinitely with traffic to overly thick sections that are likely overdesigned and impractical to build. This problem also exists with mechanistic-empirical design approaches such as the Mechanistic-Empirical Pavement Design Guide (AASHTO, 2008). Each design approach is simply a set of mechanistic and empirical equations that yield recommended design thicknesses given a set of material, structural, traffic, and climate inputs and leaves it to the designer, or written policy, to decide when it is sufficiently thick.

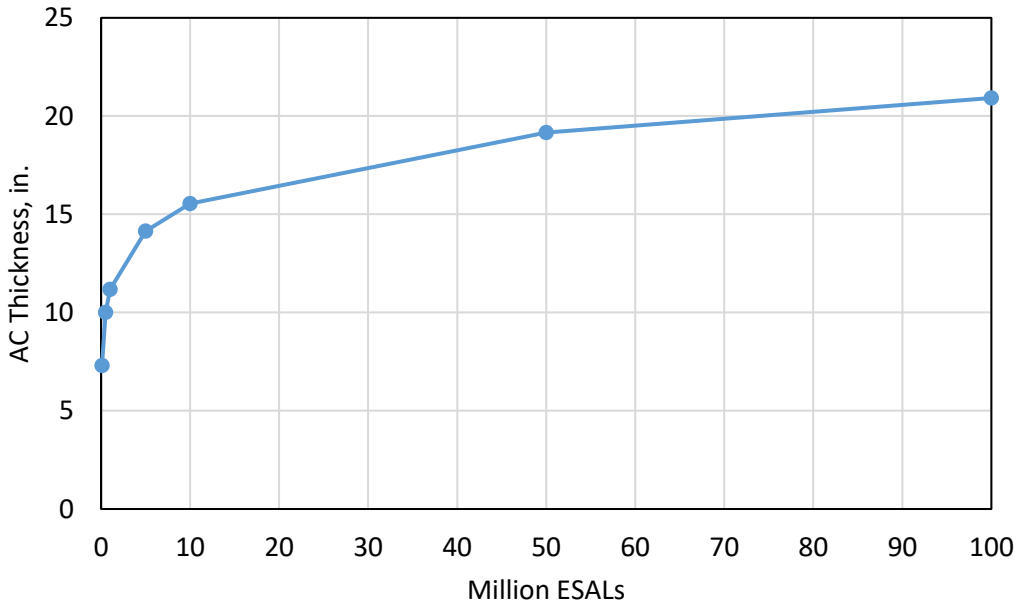

Figure 1.1 Thickness Design Example Using 1993 AASHTO Design Guide

Recent research and advancements in the field of long-life pavements have led to the development of perpetual pavement design procedures (TRC, 2001; Timm and Newcomb, 2006; Newcomb et al., 2010). These procedures rely on establishing the endurance limits of the pavement materials. The endurance limit is the pavement response (i.e., stress or strain) to loading below which damage (i.e., bottom-up fatigue cracking or rutting) does not accumulate. When the pavement

thickness is selected such that the responses are below the respective endurance limits, structural distress does not occur, and a maximum thickness has effectively been achieved. There are many examples of long-life pavements that were designed, intentionally or through overdesign, to have pavement responses below the respective endurance limits. The nationwide perpetual pavements awards program, sponsored by the Asphalt Pavement Alliance (APA, 2019), catalogs these pavement sections.

The application of perpetual pavement concepts could help determine a maximum thickness for a given set of design conditions. Figure 1.2 shows the same example designs developed in Figure 1.1 but now also shows a maximum thickness determined through perpetual pavement analysis using the design software PerRoad, version 4.4. One could imagine combining the two series in Figure 1.2 to establish the design curve shown in Figure 1.3, where the thinner sections were determined with the AASHTO 1993 approach until they reached the perpetual thickness of 12.5 inches, at which point the maximum value governs. In this way, the perpetual analysis is simply a check on the conventional design and applied to ensure responsible use of resources.

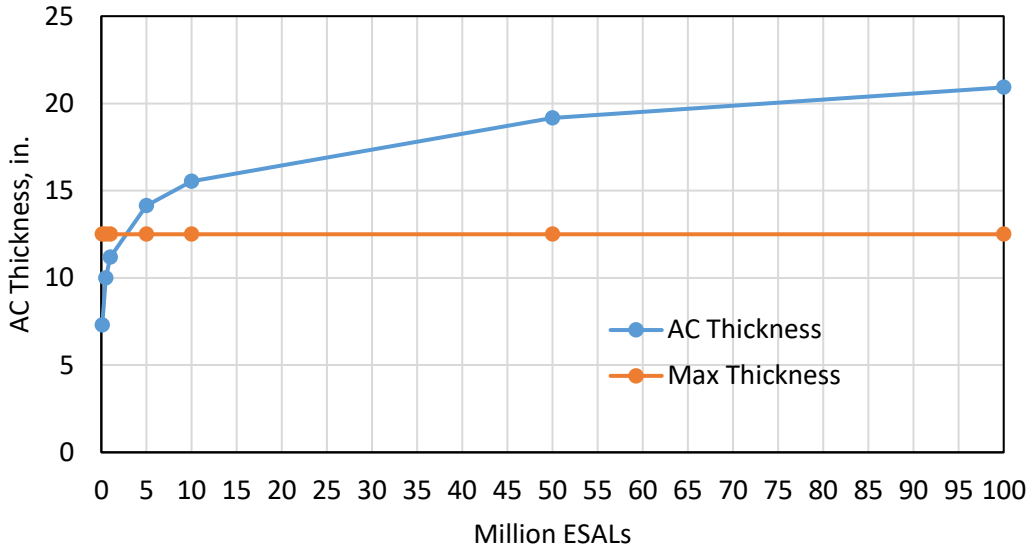

Figure 1.2 AC Thickness Determined from AASHTO 1993 and PerRoad

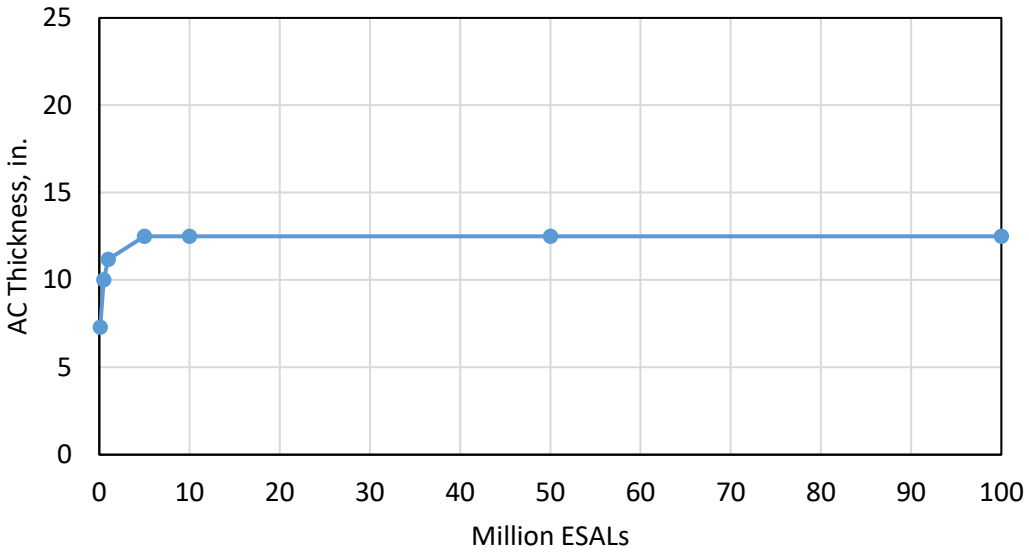

Figure 1.3 AC Design Thickness with Maximum Value at 12.5 inches

This approach of using PerRoad to arrive at maximum thicknesses is more fully explained in another report (Tran et al., 2016) and Table 1.1 shows maximum thicknesses over a range of conditions that included varying subgrade support, varying base modulus, and three climate conditions. This simple table provides designers with a rapid tool for evaluating if their specific designs are approaching or exceeding maximum values, which could then be further evaluated on a case-by-case basis.

Table 1.1 Ranges of Maximum AC Thicknesses for 6-inch Base (Tran et al., 2016)

Subgrade Mr (ksi)	Base Mr (ksi)	Calculated AC Thickness (in.)				Range of Maximum Thicknesses (in.)
		Minneapolis (PG 64-34)	Phoenix (PG 70-22)	Baltimore (PG 64-22)	Average	
5	30	12.5	15.5	14	14.0	12.5-15.5
5	50	12	15	14	13.7	12-15
5	100	12	14	13.5	13.2	12-14
10	30	10.5	14	12	12.2	10.5-14
10	50	10.5	13	12	11.8	10.5-13
10	100	10	12	11	11.0	10-12
20	30	9	12.5	10	10.5	9-12.5
20	50	8.5	12.5	9.5	10.2	8.5-12.5
20	100	8	12	9	9.7	8-12

Successful implementation of any maximum thickness design procedure is important for its routine use by designers. A good example of practical implementation may be found in Chapter 54 of the Illinois DOT Bureau of Design and Environment Manual (IDOT, 2010). Developed by Thompson and Carpenter (2006), this procedure uses the highest mean monthly pavement temperature to determine the corresponding asphalt modulus at this design temperature. A design load is selected (typically 18 or 20 kip) and applied to the pavement at the critical temperature and chosen level of subgrade support. The cross-section is designed to maintain the maximum tensile strain below 70 με Figure 1.4 shows a geographically-based design chart developed from this process for the state of Illinois (IDOT, 2010), where thicknesses range from 14 to 17 inches, increasing for more southerly counties where strain levels will be higher due to increased temperatures. It should be noted that this procedure is used to determine the maximum pavement thickness as a check of the conventional mechanistic-empirical approach in Illinois.

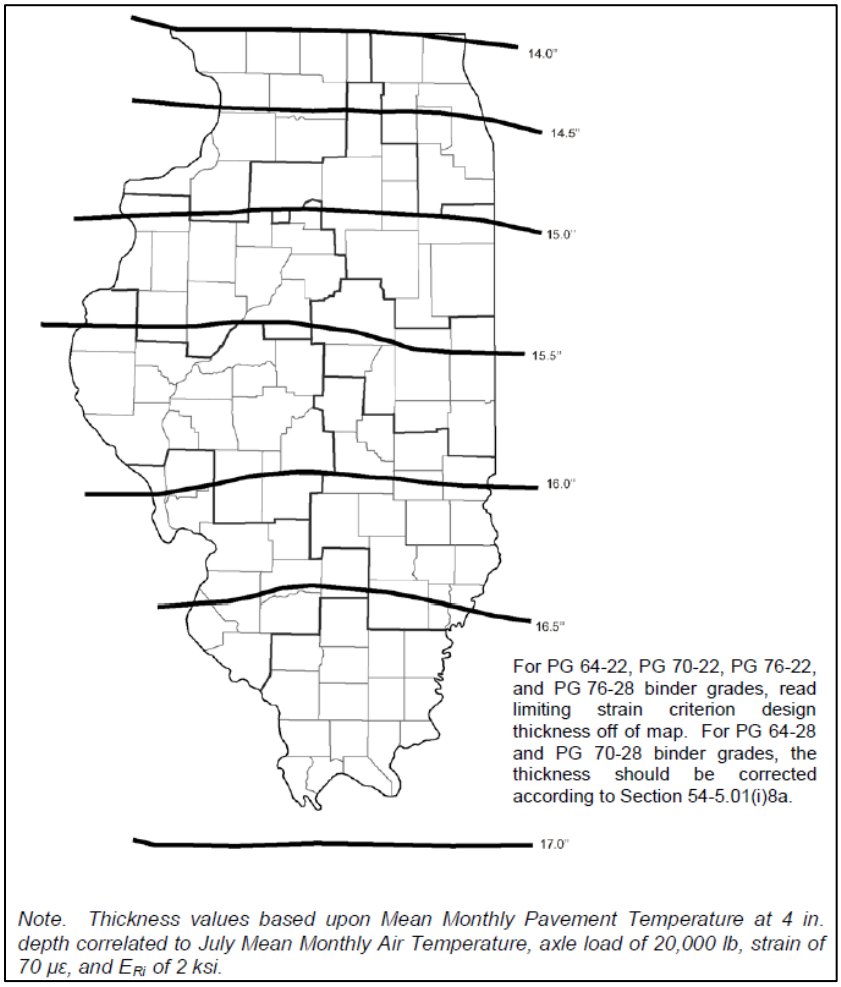

Figure 1.4 Illinois Perpetual Pavement Thickness Design Chart (*IDOT, 2010*)

The Alabama Department of Transportation (ALDOT), like most state agencies in the U.S., currently uses the 1993 AASHTO Design Guide for new pavement and overlay thickness design. ALDOT does not currently have a process or policy on maximum asphalt pavement thickness that, in some

situations, could lead to overdesigned pavement structures. Regardless of the design approach used, there is a need to have a methodology or design check to determine the maximum thickness for any given design.

Project Objectives

Given the needs described above, this project has three primary objectives:

1. Develop a methodology for ALDOT to determine maximum AC thicknesses. The approach should serve as a design check of their existing pavement design policy and procedures.
2. Verify the methodology using existing pavement sections in Alabama.
3. Recommend ranges of maximum thickness for a range of ALDOT design conditions.

Report Organization

The remainder of this report was organized to follow the tasks described in the project proposal workplan as follows: Chapter 2 (Task 1) presents a literature review, followed by development of the preliminary methodology presented in Chapter 3 (Task 2). Chapter 4 (Task 3 & 4) presents validation of the methodology and recommended maximum pavement thicknesses for a range of conditions. Finally, Chapter 5 (Task 5) contains a summary, results, and conclusions.

CHAPTER 2
LITERATURE REVIEW

This literature review synthesizes (1) the significance of incorporating maximum asphalt layer thickness in pavement design, (2) the concept of perpetual pavement design, (3) the approaches and criteria adopted by state highway agencies for perpetual pavement design, (4) and the current practices for determining the maximum asphalt layer thickness. The outcome of this review summarizes how state highway agencies have implemented and utilized the perpetual pavement design concept to design asphalt pavements and to place upper limits on their thicknesses.

Concept of Maximum Asphalt Layer Thickness

Asphalt pavement thickness design, for both new and overlay scenarios, has been evolving since the 1960's from empirical towards mechanistic-empirical design frameworks. Regardless of the design methodology, the fundamental goal of thickness design has been to determine the optimum cross-section to achieve the desired performance under the prevailing conditions (i.e., traffic, climate, and materials). Central to that effort has been calibration of design systems to accurately predict when and how a pavement will deteriorate over time. While calibration can be effective in developing more accurate predictions and therefore optimize cross sections, most design systems do not have a maximum thickness built into the procedure, which can yield unreasonably thick cross-sections. Figure 2.1 shows a simple example, developed with the AASHTO 1993 Design Guide, where AC thickness is plotted against the design traffic quantified by equivalent single axle loads (ESALs). Clearly, the AC thickness increases indefinitely with traffic to overly thick sections that are likely overdesigned and impractical to build. This problem also exists with more modern mechanistic-empirical design approaches such as the Mechanistic-Empirical Pavement Design Guide (AASHTO, 2008). Each design approach is simply a set of mathematical equations that yields recommended design thicknesses given a set of inputs and leaves it to the designer, or written policy, to decide when the section is sufficiently thick.

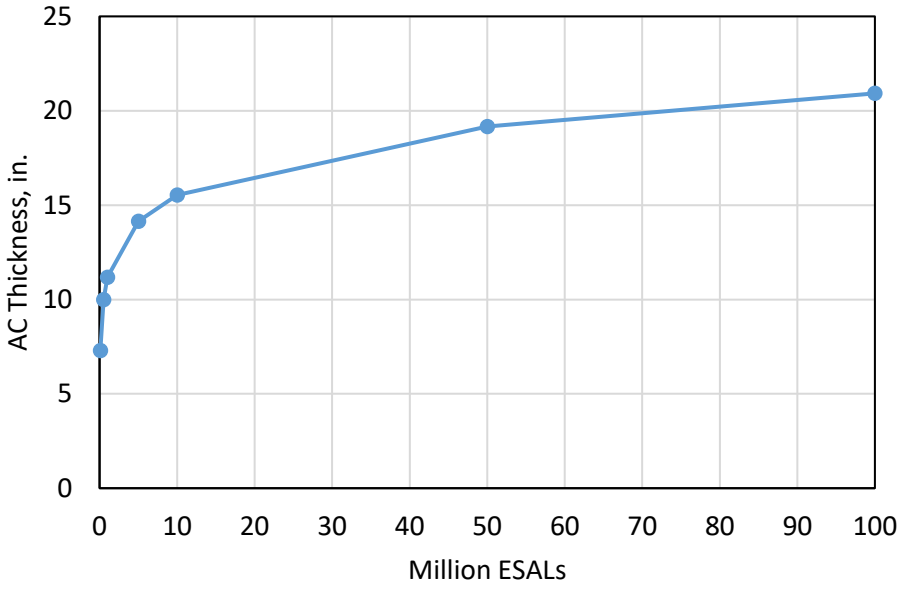

Figure 2.1 Thickness Design Example Using 1993 AASHTO Design Guide

Recent research and advancements in the study of long-life pavements has led to the development of perpetual pavement design procedures (TRB, 2001; Timm and Newcomb, 2006; Newcomb et al., 2010). These procedures rely on establishing the endurance limits of the pavement materials. The endurance limit is the pavement response to loading (i.e., stress or strain) below which damage (i.e., bottom-up fatigue cracking or structural rutting) will not accumulate. When the pavement thickness is selected such that the responses are below the respective endurance limits, structural distress does not occur, and a maximum thickness has effectively been achieved.

There are many examples of long-life pavements that were designed, intentionally or through overdesign, to have pavement responses below the respective endurance limits. The nationwide perpetual pavements awards program, sponsored by the Asphalt Pavement Alliance, catalogs these pavement sections. Application of perpetual pavement concepts could help determine a maximum thickness for a given set of design conditions. Figure 2.2 shows the same example designs developed in Figure 2.1, but now also showing a maximum thickness determined through perpetual pavement analysis using the design software PerRoad, version 4.4. One could imagine combining the two plots in Figure 2.2 to establish the design curve shown in Figure 2.3 where the thinner sections were determined with the AASHTO 1993 approach until they reach the perpetual thickness of 12.5 inches at which point the maximum value governs. In this example, the perpetual analysis is simply a check on the conventional design and applied to ensure responsible use of resources.

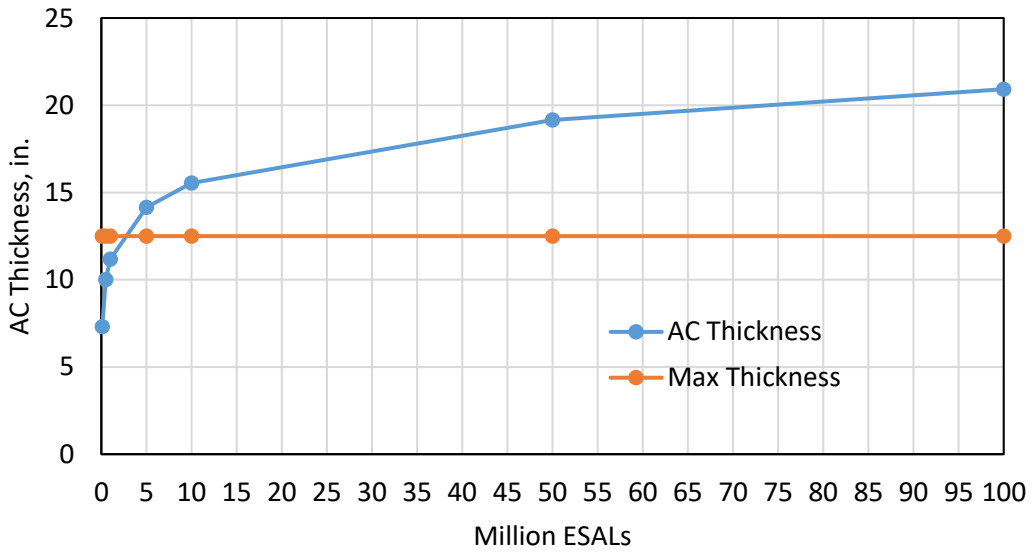

Figure 2.2 AC Thickness Determined from AASHTO 1993 and PerRoad

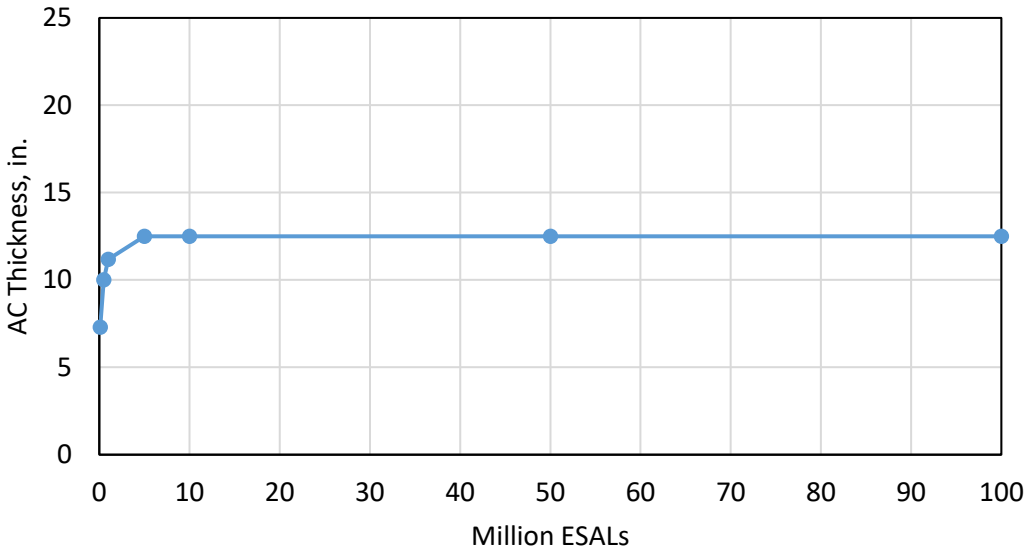

Figure 2.3 AC Design Thickness with Maximum Value at 12.5 inches

Concept of Perpetual Pavement Design

A perpetual pavement is referred to as an asphalt pavement designed and built to last longer than 50 years without requiring major structural rehabilitation or reconstruction (Newcomb et al., 2010). The benefits of perpetual pavement include eliminating costly reconstruction, lowering user delay cost, and reducing the consumption of non-renewable materials and energy (Timm and Newcomb, 2006). For asphalt pavement, the most critical structural distresses are fatigue cracking and structural rutting, which significantly affect its service life. Thus, an ideal perpetual pavement structure should contain a rut-resistant and wear-resistant surface layer, a rut-resistant intermediate layer, and a fatigue resistant base layer. A proper structural design and an appropriate material selection procedure are necessary to obtain a long-lasting asphalt pavement.

Based on the concept of mechanistic-empirical pavement design, fatigue cracking is dependent on the tensile strain at the bottom of asphalt layer, and structural rutting is mainly related to the compressive strain at the top of subgrade. Monismith and McLean (1972) found that asphalt mixtures have a fatigue endurance limit (FEL) likely at 70 microstrain, indicating that the fatigue life of an asphalt mixture could be infinite if the strain level is below the FEL. Thompson and Carpenter (2006) confirmed that asphalt pavement is considered to be perpetual if the critical tensile strain at the bottom of the asphalt layers is less than the FEL. They also reported that 70 microstrain is a conservative value for FEL. If the tensile strain remains around 70-100 microstrain, no accumulation of fatigue damage occurs in an asphalt mixture. Von Quintus (2006) found that the FEL of asphalt pavement is 65 microstrain at a 95 percent confidence level based on the analysis of the long-term pavement performance (LTPP) data. Prowell et al. (2010) developed a standard practice to predict the FEL based on laboratory fatigue test results and reported that the FEL of asphalt mixture varies from 75 to 200 microstrain for a set of six asphalt mixtures where the gradation was held constant while the binder grade and asphalt content varied. It was found that the strain level corresponding to the endurance limit was mix dependent with a greater influence arising from binder properties (i.e., binder grade, modification) than from asphalt content/air voids content (Prowell et al., 2010). Modified binders generally produced higher fatigue endurance limits, all else being equal (Prowell et al., 2010). In general, the existing data support the existence of an endurance limit for asphalt mixture, but the field data from the NCAT Test Track indicates that asphalt pavements could still be perpetual if the measured tensile strain levels exceed the

FEL of asphalt mixtures (Prowell et al. 2010). Table 2.1 compares the field-measured tensile strain and laboratory-determined FEL for six test sections at the NCAT Test Track. Sections N3, N4, and N9 were observed as perpetual pavements without any fatigue cracking while they only had 33%-88% of field-measured strains below their FELs. Willis (2009) and Tran et al. (2015) suggested that a single FEL may not be an appropriate criterion for perpetual pavement design, and the cumulative strain distribution should be considered as a design threshold.

Table 2.1 Field-Measured Tensile Strains and Laboratory-Determined FELs (Tran et al., 2015)

Section ID	Laboratory-Determined FEL (με)	Percent of Field-Measured Strains below FEL	Field Performance
N3-2003	151	33%	Perpetual
N4-2003	146	38%	Perpetual
N8-2006	203	50%	Fatigue Cracking
N9-2006	203	88%	Perpetual
N10-2006	130	8%	Fatigue Cracking
S11-2006	118	3%	Fatigue Cracking

Willis (2009) analyzed the laboratory-determined FEL of asphalt mixtures and the field-measured tensile strain of various pavement sections at the NCAT Test Track. He proposed a concept of fatigue ratio to correlate the laboratory-determined FEL with field-measured tensile strain. The fatigue ratio was calculated by dividing the field-measured tensile strain at the n^{th} percentile by the laboratory-determined FEL at a 95% confidence lower limit. He developed a stochastic perpetual pavement design criteria based on a cumulative probability distribution of tensile strain, which is shown in Table 2.2. Willis (2009) found that the sections with bottom-up fatigue cracks had higher tensile strains than those without cracks when the strain level was above the 55^{th} percentile of strain distribution, which is illustrated in Figure 2.4.

Table 2.2 Original Limiting Strain Distribution Criteria for Perpetual Pavements (Willis, 2009)

Percentile of Strain Distribution	Tensile Strain Limit, με
99%	394
95%	346
90%	310
85%	282
80%	263
75%	247
70%	232
65%	218
60%	205
55%	193

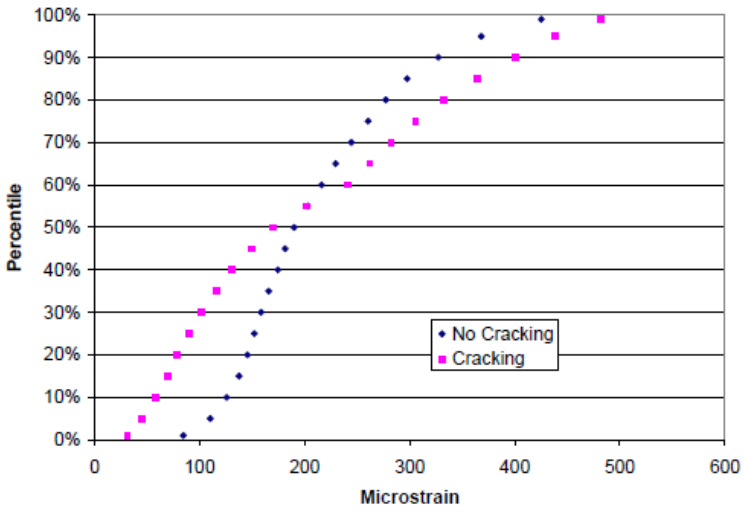

Figure 2.4 Strain Distribution Profiles for Sections with and without Fatigue Cracks (Willis, 2009)

Tran et al. (2015) pointed out that the limiting strain distribution threshold based on the field-measured strains might not be applicable to perpetual pavement design because layered elastic theory predicted different strain levels than field-measured. They used the PerRoad software Version 3.5, which uses layered elastic theory, to predict the strain distributions of 12 test sections at the NCAT Test Track. They refined the limiting strain distribution threshold based on the PerRoad-predicted strains as shown in Table 2.3. Castro et al. (2017) used the PerRoad software to analyze the strain distributions of eight additional perpetual pavement sections located in different climatic regions. They confirmed that all of the selected perpetual pavements met the refined limiting strain distribution criteria shown in Table 2.3. They also found that the limiting tensile strain above the 60th percentile of strain was effective in differentiating the pavements with and without fatigue cracks.

Table 2.3 Refined Limiting Strain Distribution Criteria for Perpetual Pavements (Tran et al., 2015)

Percentile of Strain Distribution	Tensile Strain Limit, με
99%	326
95%	257
90%	221
85%	194
80%	175
75%	158
70%	143
65%	131
60%	120
55%	110

Regarding rutting, Monismith et al. (2004) and Walubita et al. (2008) suggested that vertical compressive strain at the top of subgrade should be less than 200 microstrain to prevent structural rutting. This criterion for vertical compressive strain was widely adopted for perpetual pavement design (Timm and Newcomb, 2006). Castro et al. (2017) analyzed the measured vertical compressive strain data for asphalt pavements and recommended that perpetual pavement have the 50th percentile vertical compressive strain at the top of subgrade set to less than 200 microstrain.

In summary, perpetual pavement design aims to limit the horizontal tensile strain at the bottom of an asphalt layer and the vertical compressive strain at the top of the subgrade to eliminate bottom-up fatigue cracking and rutting distresses, respectively. The limiting strain criteria could be a single value or a distribution-based threshold for perpetual pavement design. Application of these concepts is discussed in the following sections with emphasis on how maximum pavement thicknesses may be computed.

Perpetual Pavement Design Approaches

Currently, the AASHTOWare Pavement ME Design (PMED) methodology adopts the concept of FEL to predict the long-term fatigue cracking performance of asphalt pavements. AASHTOWare PMED considers the FEL as a material property for asphalt layers, which is assumed to be independent of temperature or mixture modulus. In other words, the pavement designer needs to assign a single value for all asphalt mixtures within a single run of the software. The default FEL in AASHTOWare PMED is 100 microstrain. Note that AASHTOWare PMED does not consider any limiting strain criteria for structural rutting.

The Colorado Department of Transportation (CDOT) uses AASHTOWare PMED to design perpetual pavements that will last 50 years without requiring major structural rehabilitation or reconstruction (CDOT 2021). To improve the prediction accuracy, CDOT provides locally calibrated coefficients of performance models in AASHTOWare PMED.

Castro et al. (2018) utilized the JULEA program in AASHTOWare PMED to compute the critical strains of ten test sections at NCAT Test Track and eight perpetual pavements from other locations. In AASHTOWare PMED, the dynamic modulus of asphalt concrete is related to pavement temperature, and the moduli of unbound base and subgrade are dependent on moisture content. Considering that the pavement temperature and moisture profiles vary by time, the computed critical strains of each pavement section should change with analysis time. They collected the computed critical strain distributions of these pavement sections and developed a limiting strain distribution criterion for perpetual pavement design, which is shown in Table 2.4. They also reported that the selected perpetual pavements had their 50th percentile of predicted vertical compressive strains less than 200 microstrain.

Table 2.4 PMED-Based Limiting Strain Distribution Criteria for Perpetual Pavements (Castro et al., 2018)

Percentile of Strain Distribution	Strain Limit, με
95%	129
90%	116
85%	107
80%	101
75%	92
70%	84
65%	81
60%	72
55%	68

PerRoad is another tool for perpetual pavement design, which uses a layered-elastic theory combined with Monte Carlo simulations to estimate critical stresses and strains within an asphalt pavement. PerRoad considers variabilities of material moduli and layer thicknesses as well as the seasonal variation impact on material moduli. PerRoad accommodates horizontal tensile strain distribution criteria for fatigue cracking and single vertical compressive strain criteria for rutting. Table

2.5 summarizes the limiting strain criteria in PerRoad Version 4.3 (Timm et al., 2017). Islam et al. (2020) evaluated the design of four pavement sections using PerRoad and AASHTOWare PMED. They found that AASHTOWare PMED predicted tensile strains at the bottom of the asphalt layer were much less than 70 microstrain, but over 20% of the PerRoad predicted tensile strains exceeded 70 microstrain. In general, PerRoad predicted higher tensile strains at the bottom of an asphalt layer than AASHTOWare PMED for the four pavement sections. For a 50-year design period, AASHTOWare PMED required a relatively lower asphalt layer thickness than PerRoad.

Table 2.5 PerRoad-Based Limiting Strain Distribution Criteria for Perpetual Pavements (Timm et al., 2017)

Criteria	Percentile of Strain Distribution	Strain Limit, με
Horizontal Tensile Strain	95%	257
	85%	194
	75%	158
	65%	131
	55%	110
Vertical Compressive Strain	50%	200

In Texas, perpetual pavement is designed via a mechanistic-empirical process incorporated in the flexible pavement design system FPS 21 (TxDOT 2021). The FPS21 design is also based on a linear-elastic analysis system. The key material properties are the back-calculated moduli from the falling weight deflectometer test. The current limiting strain criteria in FPS21 include a maximum horizontal tensile strain of 70 microstrain at the bottom of the asphalt layer and a maximum vertical compressive strain of 200 microstrain on the top of the subgrade. The pavement designer uses FPS21 to calculate the primary strain responses to traffic loading for the anticipated heavy wheel loads for each season of the year at the critical locations, and then compare these strains against the limiting strain criteria to determine whether the designed structure is a perpetual pavement. Based on the FPS21 analysis and field observation of in-service Texas perpetual pavements, Walubita and Scullion (2010) suggested that the total asphalt layer thickness of a perpetual pavement could be reduced from 22 inches to 14 inches. Figure 2.5 illustrates the proposed change for Texas perpetual pavement structures.

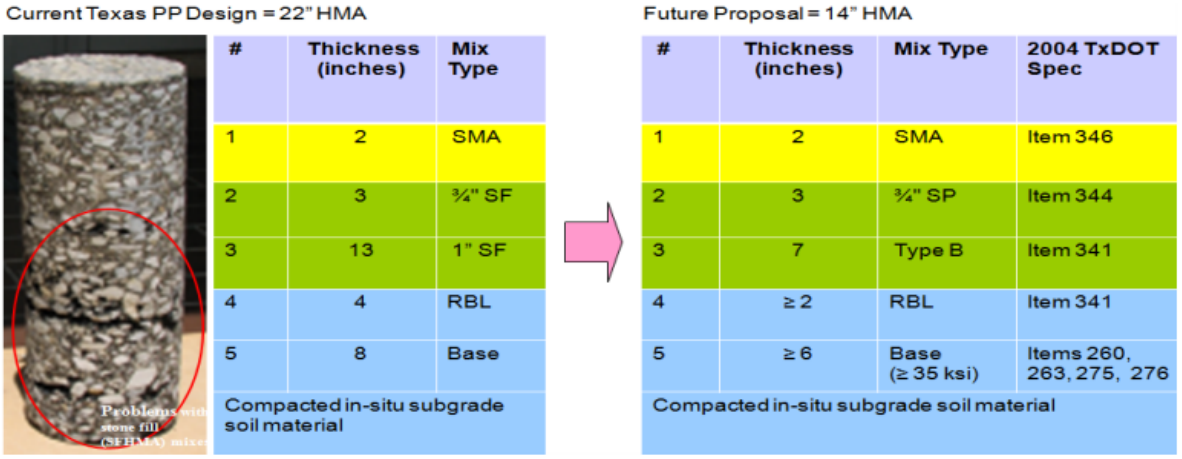

Notes: SMA = stone matrix asphalt; SF = stone-filled asphalt (3/4-in or 1-in NMAS); RBL = rich (asphalt) bottom layer; SP = Superpave (3/4-in NMAS); Type B = 1-in NMAS base/intermediate dense graded mix.

Figure 2.5 Proposed Texas Perpetual Pavement Structures (Walubita and Scullion, 2010)

The Illinois Department of Transportation (IDOT) employs a limiting strain criterion when designing full-depth asphalt pavements (i.e., asphalt concrete directly on subgrade). The design procedure assumes that asphalt layer rutting and thermal cracking are adequately considered in the material selection and mix design process (IDOT 2010). The structural design controls fatigue cracking by limiting the tensile strain at the bottom of the asphalt layer, using a series of design charts to account for varying soil and traffic conditions, as follows:

- The design limiting strain for the asphalt layer is first determined in Figure 2.6 based on the designed traffic factor, which is quantified by the total number of 18-kip ESALs anticipated in the design lane during the design period. Example 1, shown in Figure 2.6a, demonstrates that if the design traffic factor is 5.0 the corresponding design limiting strain will be approximately 75 microstrain. Example 2, in Figure 2.6b, shows that if the design traffic factor is 0.4 the corresponding design limiting strain will be approximately 195 microstrain.
- Using the selected limiting strain selected in Figure 2.6 the nomograms presented in Figure 2.7 can be used to determine the asphalt layer thickness for any given asphalt mixture modulus and subgrade support level. Example 1, shown in Figure 2.7a, indicates that if the pavement structure has a fair subgrade and the asphalt modulus is 600 ksi and the design limiting strain is 75 microstrains, the design asphalt layer thickness will be 11.0 inches. Example 2, in Figure 2.7b, demonstrates that if the pavement structure has a poor subgrade and the asphalt modulus is 600 ksi and the design limiting strain is 195 microstrains, the design asphalt layer thickness will be 6.25 inches.

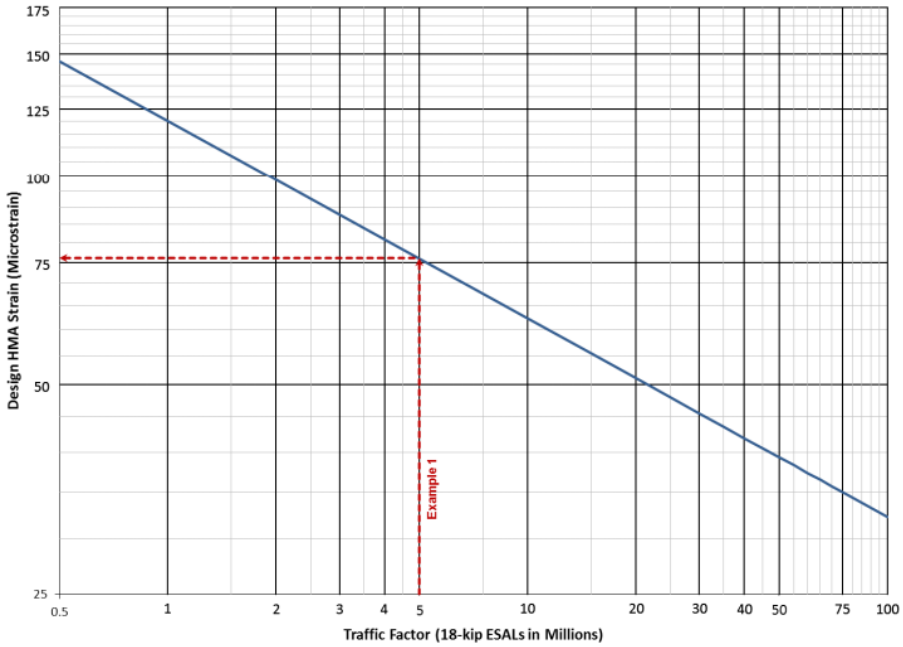

a. Traffic Factor ≥ 0.5

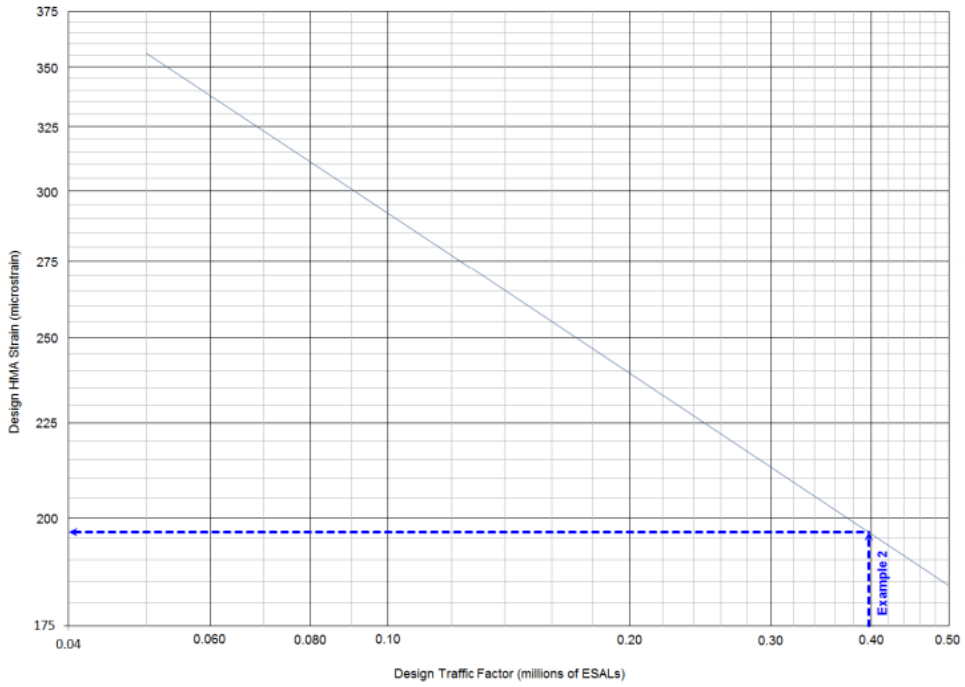

b. Traffic Factor < 0.5

Figure 2.6 Relationship Between Designed Limiting Strain of Asphalt Layer and Traffic Factor (IDOT, 2010)

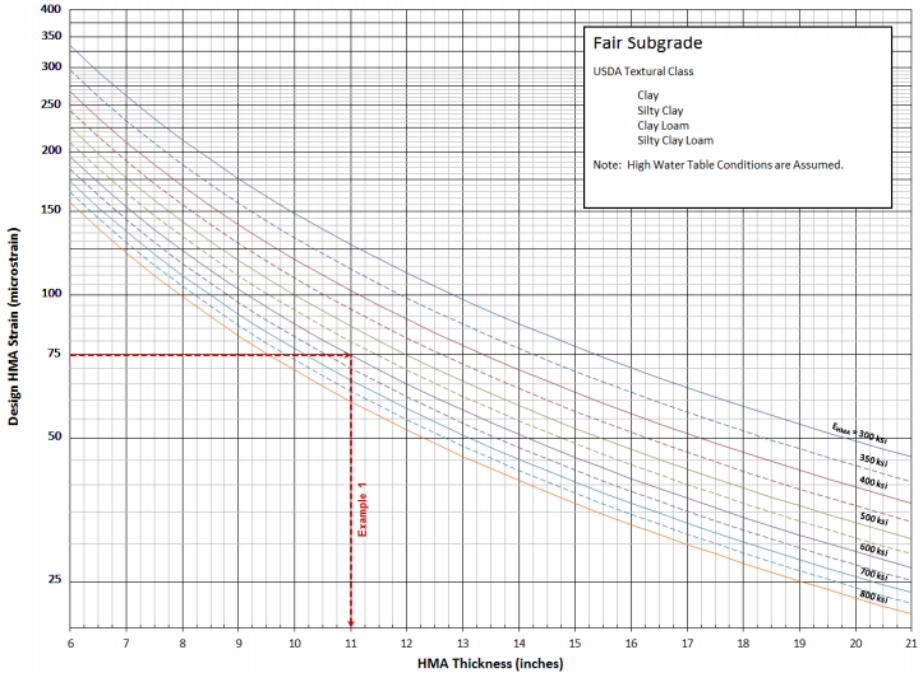

a. Fair Subgrade

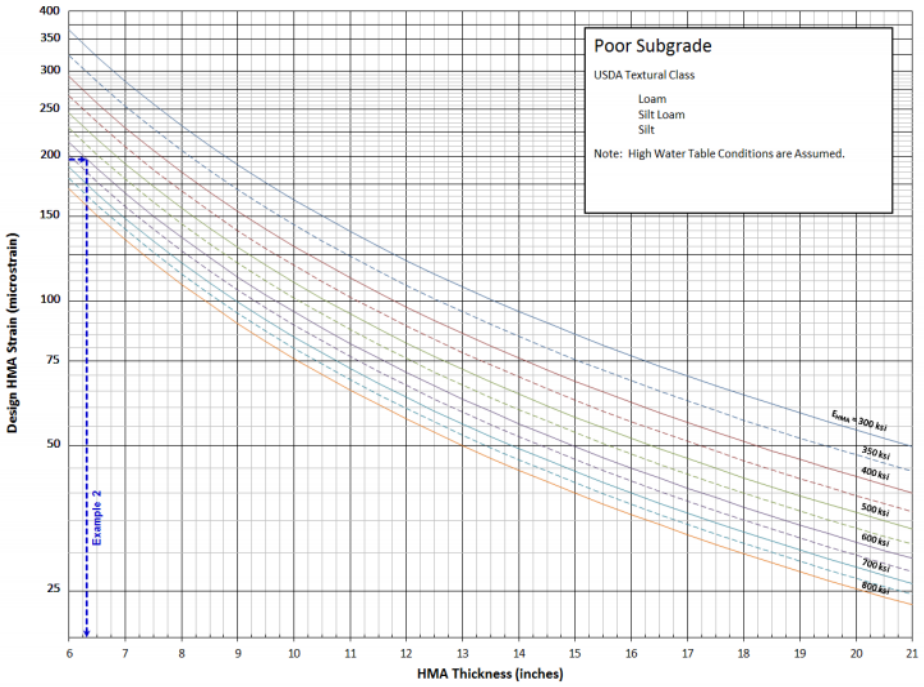

b. Poor Subgrade

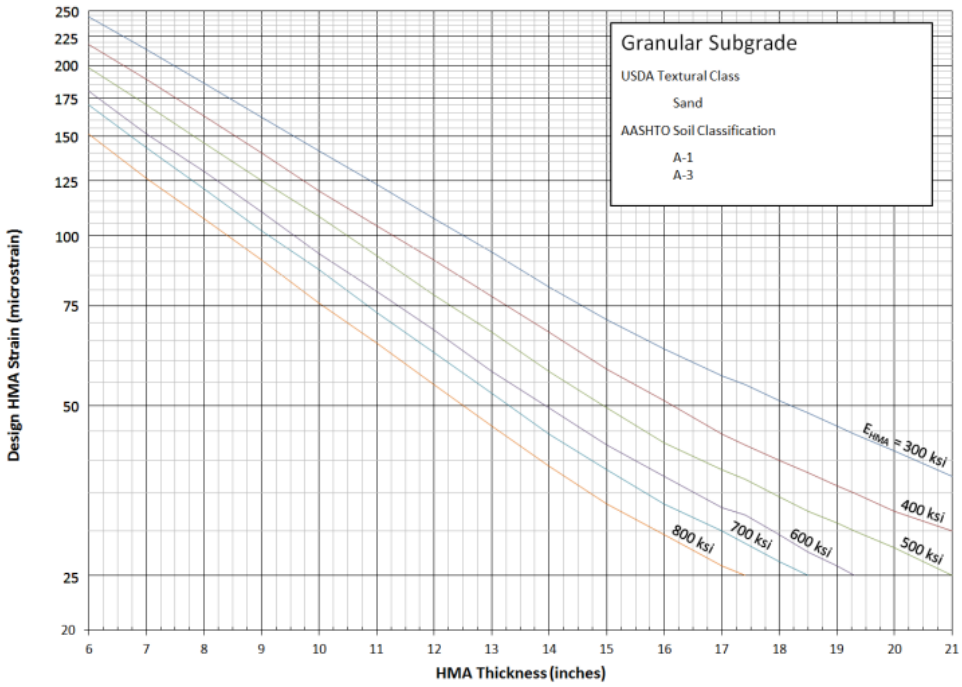

c. Granular Subgrade

Figure 2.7 Illinois DOT Design Charts for Asphalt Layer Thickness (IDOT, 2010)

Determining Maximum Asphalt Layer Thickness

Based on the limiting strain criteria, IDOT provides a contour map for checking the maximum pavement thickness of a full-depth asphalt pavement (IDOT 2010). As shown in Figure 2.8, the state of Illinois is divided into seven regions that have maximum thicknesses ranging from 14 to 17 inches. These thickness values were calculated based on the mean monthly pavement temperature with an axle load of 20 kips, a limiting tensile strain of 70 microstrain, and a subgrade modulus of 2 ksi.

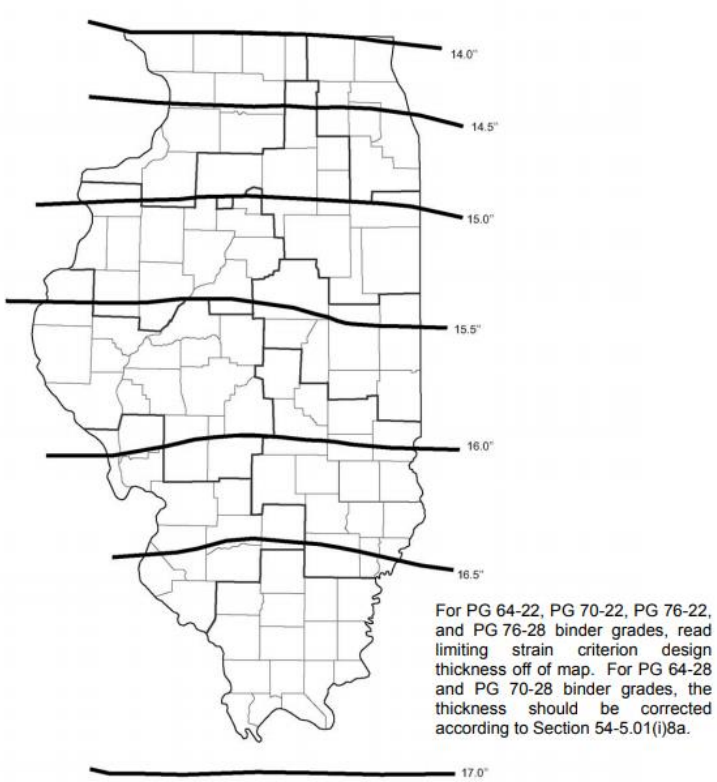

Figure 2.8 Maximum Asphalt Layer Thickness for Full-Depth Asphalt Pavement in Illinois (IDOT 2010)

The Pennsylvania Department of Transportation (PennDOT) uses the AASHTO 1993 method to design the asphalt pavement structure (PennDOT 2019). The determination of the asphalt pavement design is restricted by the minimum and maximum thickness of each pavement layer shown in Table 2.6. For a full-depth asphalt pavement, the maximum thickness of surface layer is 4.5 inches, and the maximum thickness of asphalt treated base is 12 inches. However, it is not clear how the PennDOT determines the maximum thickness of each pavement layer.

Table 2.6 Minimum and Maximum Thickness of Each Pavement Layer in Pennsylvania (PennDOT 2019)

COURSES	MAXIMUM THICKNESS	MINIMUM THICKNESS		
	ALL HIGHWAY CLASSIFICATIONS	MFC A & B	MFC C & D	MFC E
Surface	4 in	N/A	3.5 in* – 4 in	3.5 in* – 4 in
CABC, CABC-DG	16 in	N/A	8 in	6 in
Subbase	As Required	N/A	6 in	6 in
Surface	4 in	N/A	3.5 in* – 4 in	3.5 in* – 4 in
Agg./Cement Base Courses	12 in	N/A	5 in	5 in
Subbase	As Required	N/A	6 in	6 in
Surface	4.5 in	4 in	3.5 in* – 4 in	1 in** – 2 in
Superpave Base Course	15 in	3 in	3 in	4 in
Subbase	As Required	8 in	6 in	6 in
Surface	4.5 in	N/A	3.5 in* – 4 in	1 in** – 2 in
Agg./Bituminous Base Course	12 in	N/A	5 in	5 in
Subbase	As Required	N/A	6 in	6 in
Surface	4 in	4 in	3.5 in* – 4 in	3.5 in* – 4 in
Plain Cement Concrete Base Course	12 in	7 in	5 in	5 in
Subbase	As Required	8 in	6 in	6 in

*3.5 inches may only be used if 1 inch SP 9.5 mm FG Wearing Course is used with 2.5 inches SP 19.0 mm Binder Course.

**1 inch may only be used if 1 inch SP 9.5 mm FG Wearing Course is used.

Tran et al. (2015) conducted a case study to determine the maximum asphalt layer thickness based on the PerRoad analysis. The case study was conducted for full-depth asphalt pavement structures at different locations with various climate conditions across the country. The PerRoad simulations were done with one traffic level consisting of 100% single axles weighing 20-22 kips, and different base and subgrade moduli that had seasonal variation. In the study, the maximum thickness of asphalt layer was determined based on the following two criteria:

- The cumulative distribution of the calculated horizontal tensile strains at the bottom of asphalt layer was lower than the limiting strain distribution shown in Table 2.3.
- The 50th percentile of vertical compressive strains at the top of subgrade were below 200 microstrain.

Tables 7 through 9 list the determined maximum asphalt layer thickness over a range of conditions that included varying subgrade support, varying base modulus, and three climate conditions. These tables provide designers a rapid tool for evaluating if their specific designs are approaching or exceeding maximum values that could then be further evaluated on a case-by-case basis.

Table 2.7 Ranges of Maximum AC Thicknesses for 6-inch Base (Tran et al., 2015)

Subgrade Mr (ksi)	Base Mr (ksi)	Calculated AC Thickness (in.)				Range of Maximum Thicknesses (in.)
		Minneapolis (PG 64-34)	Phoenix (PG 70-22)	Baltimore (PG 64-22)	Average	
5	30	12.5	15.5	14	14.0	12.5-15.5
5	50	12	15	14	13.7	12-15
5	100	12	14	13.5	13.2	12-14
10	30	10.5	14	12	12.2	10.5-14
10	50	10.5	13	12	11.8	10.5-13
10	100	10	12	11	11.0	10-12
20	30	9	12.5	10	10.5	9-12.5
20	50	8.5	12.5	9.5	10.2	8.5-12.5
20	100	8	12	9	9.7	8-12

Table 2.8 Ranges of Maximum AC Thicknesses for 8-inch Base (Tran et al., 2015)

Subgrade Mr (ksi)	Base Mr (ksi)	Calculated AC Thickness (in.)				Range of Maximum Thicknesses (in.)
		Minneapolis (PG 64-34)	Phoenix (PG 70-22)	Baltimore (PG 64-22)	Average	
5	30	12.5	15	14	13.8	12.5-15
5	50	11.5	14.5	13.5	13.2	11.5-14.5
5	100	11	13	12.5	12.2	11-13
10	30	10.5	13	11.5	11.7	10.5-13
10	50	10	12	11.5	11.2	10-12
10	100	9	11	10.5	10.2	9-11
20	30	9	12.5	10.5	10.7	9-12.5
20	50	8.5	12	10	10.2	8.5-12
20	100	7.5	10.5	9	9.0	7.5-10.5

Table 2.9 Ranges of Maximum AC Thicknesses for 10-inch Base (Tran et al., 2015)

Subgrade Mr (ksi)	Base Mr (ksi)	Calculated AC Thickness (in.)				Range of Maximum Thicknesses (in.)
		Minneapolis (PG 64-34)	Phoenix (PG 70-22)	Baltimore (PG 64-22)	Average	
5	30	12	14.5	13.5	13.3	12-14.5
5	50	11	13.5	12.5	12.3	11-13.5
5	100	10	12	11.5	11.2	10-12
10	30	10	12	11	11.0	10-12
10	50	9	11	10	10.0	9-11
10	100	8	10	9	9.0	8-10
20	30	8.5	11	10.5	10.0	8.5-11
20	50	7.5	10	9.5	9.0	7.5-10
20	100	6.5	9	8.5	8.0	6.5-9

Summary

This chapter reviewed the concepts of maximum asphalt layer thickness and perpetual pavement design and discussed the approaches to designing perpetual pavement and determining maximum asphalt layer thickness. The key findings are summarized as follows.

- The perpetual pavement design aims to eliminate bottom-up fatigue cracking and structural rutting distresses by limiting the horizontal tensile strain at the bottom of asphalt layer and the vertical compressive strain at the top of subgrade.
- For perpetual pavement design, the limiting strain criterion could be a single value or a distribution-based threshold. Both PerRoad and AASHTOWare PMED are capable of designing perpetual pavements.
- Based on the limiting strain criteria, Illinois Department of Transportation (IDOT 2010) provided a contour map for checking the maximum pavement thickness of a full-depth asphalt pavement, and Tran et al. (2015) suggested tables of the maximum asphalt layer thickness values based on subgrade and base moduli.

CHAPTER 3
METHODOLOGY FORMULATION – PRELIMINARY PERPETUAL PAVEMENT ANALYSIS

Introduction

The primary objective of the preliminary investigation was to analyze existing Alabama Department of Transportation (ALDOT) relatively thick pavement sections and determine their design thicknesses against the threshold strain limits developed by Tran et al. (2015) using three sets of modulus inputs. A total of 13 Interstate pavement sections in Alabama were considered in this analysis. The considered pavement sections have relatively thick asphalt layers ranging from 8.3 to 18.0 inches, as detailed in Table 3.21. It should be noted that these thicknesses are in or exceed the range of expected thicknesses for perpetual pavements (Newcomb et al., 2000) and had no reported deep structural distresses such as bottom-up fatigue cracking or structural rutting. Therefore, they made good candidates for evaluating existing perpetual pavement design criteria.

Table 3.21 Pavement Sections Considered for the Preliminary Analysis

Section ID	Route	County	Milepost	No. of FWD test locations	AADT	Truck %	Existing Layer Thickness (in.)	
							AC	Base
1	I-22 W	Walker	47.2 - 40.3	67	16,839	27	17.0 - 18.0	6.0
2	I-65 N	Mobile	0.0 - 8.3	79	108,650	8	10.5	10.0
3	I-65 S	Mobile	8.3 - 0.0	81	108,650	8	10.4	10.0
4	I-65 N	Conecuh	83.1 - 92.5	96	27,384	28	13.0	10.0
5	I-65 S	Conecuh	92.5 - 83.1	93	27,384	28	13.0	10.0
6	I-85 N	Macon	31.1 - 35.8	49	38,120	24	14.3	8.0
7	I-85 S	Macon	35.8 - 31.1	48	38,120	24	14.3	8.0
8	I-459 N	Jefferson	5.5 - 11.1	57	76,893	20	8.4	6.0
9	I-459 S	Jefferson	11.1 - 5.5	57	76,893	-	8.3	6.0
10	I-65 N	Chilton	198.0 - 205.3	75	42,770	23	12.5 - 14.6	11.0
11	I-65 S	Chilton	205.3 - 198.0	75	42,770	23	13.5 - 14.7	12.0
12	I-65 N	Chilton	211.4 - 216.5	53	45,900	23	13.7 - 17.0	10.0
13	I-65 S	Chilton	216.5 - 211.4	52	45,900	23	14.0 - 14.7	10.0

These sections were built many years ago, so no laboratory-measured modulus data were available. However, ALDOT has been collecting Falling Weight Deflectometer (FWD) deflection data for these sections. The FWD deflection data were used to backcalculate layer moduli of each layer, which were then entered into the AASHTOware Pavement ME™ software to predict seasonal variation in the modulus values of each layer over a design period of 50 years. The obtained modulus values from the Pavement ME software were then used in PerRoad version 4.4 to compute strains at critical locations in these pavement sections. Additional simulations were conducted using default material property values in PerRoad, followed by input values currently used by ALDOT in pavement design practice, since some

of the backcalculated moduli and resulting predictions from Pavement ME were unreasonably high. The overall work plan for the preliminary investigation of exiting ALDOT sections is presented in Figure 3.22.

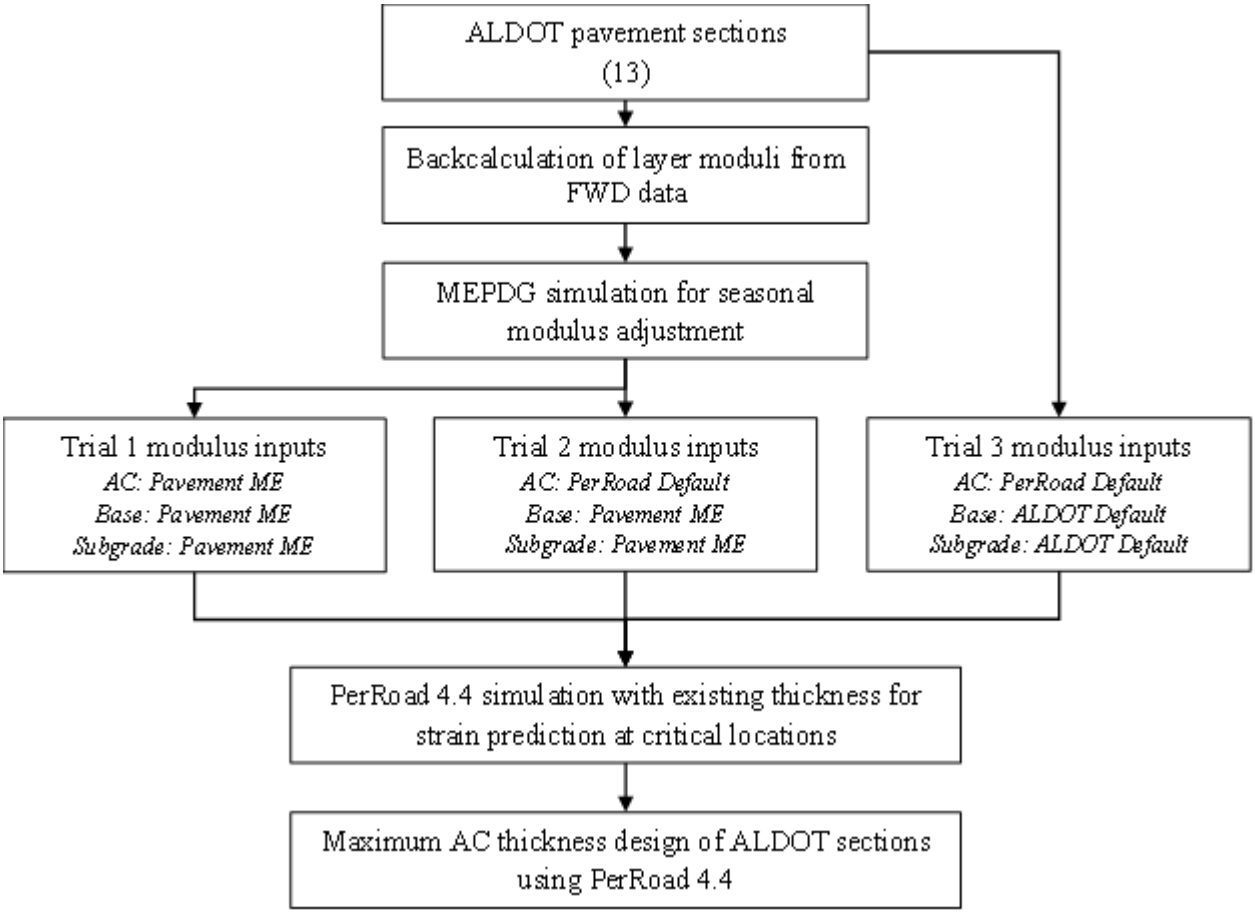

Figure 3.22 Work Plan for the Preliminary Investigation of ALDOT Pavement Sections

Layer Moduli Backcalculation

As mentioned above, FWD data were collected by ALDOT at multiple test stations for each pavement section. For example, Figure 3.2 presents FWD deflection data for five test locations on the I-22 W section in Walker County.

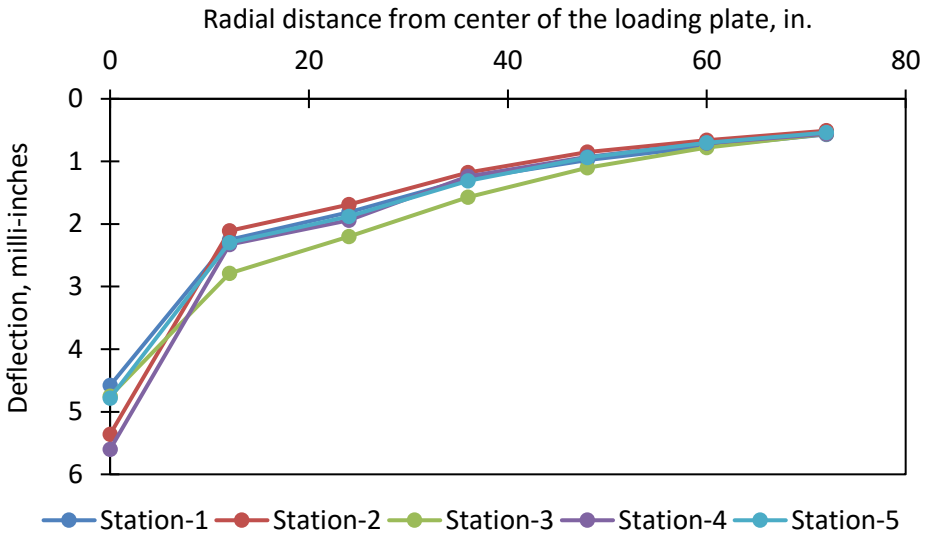

Figure 3.23 FWD Deflection Data of Five Test Stations on the I-22W Walker County Section

A three-layer backcalculation analysis of the 13 pavement sections was conducted using Dynatest's ELMOD backcalculation program. ELMOD yielded very high subgrade moduli values and sometimes corresponding lower moduli values for the granular base material, as shown in Figure 3.24. This apparent compensating layer effect makes the foundation layer values somewhat unreliable from a modeling standpoint, so a more straightforward approach was taken, as described below.

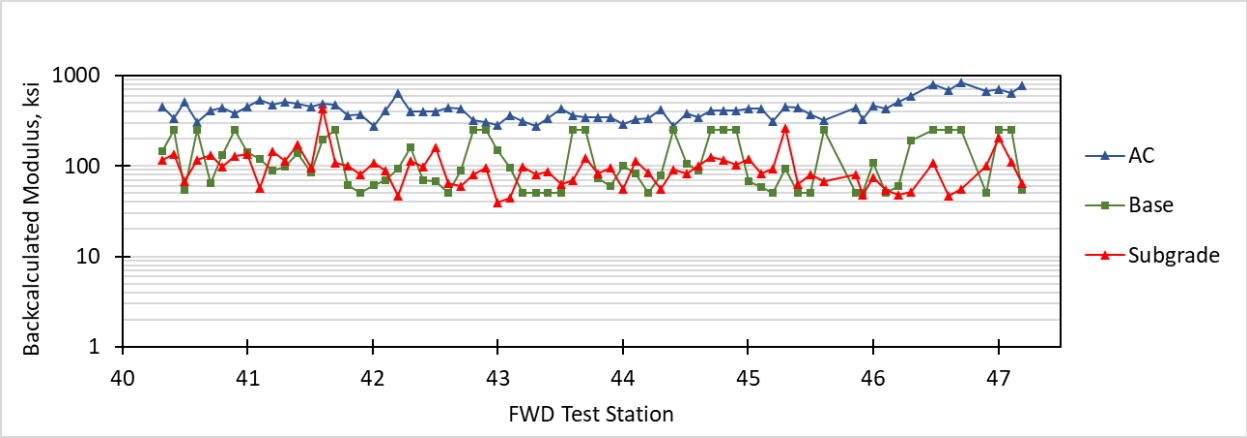

Figure 3.24 Backcalculated Layer Modulus of Pavement Section 1 Modeled as Three-Layer System using ELMOD Software

Due to the backcalculated data exemplified in Figure 3.24, the AASHTO 1993 two-layer backcalculation procedure was used for this study. The traditional AASHTO 1993 backcalculation procedure treats the AC and granular base layers as a single layer with a composite modulus (E_p) using Equation 3.1. The subgrade is treated as the second layer with a resilient modulus (M_R) backcalculated using Equation 3.2. Because this study was aimed at isolating the AC layer properties from the rest of

the pavement to better perform mechanistic simulations, this investigation treated the AC layer as the first layer with a modulus of E_p. The granular base and subgrade layers were assumed to have the same modulus value of M_R and were combined as a single layer for backcalculation purposes. Note that this is not in accordance with standard ALDOT practice when using deflection data to backcalculate layer properties for overlay design.

$$d_0 = 1.5pa\left\{\frac{1}{M_R\sqrt{1+\left(\frac{D}{a}\sqrt[3]{\frac{E_p}{M_R}}\right)^2}}+\frac{\left[1-\frac{1}{\sqrt{1+\left(\frac{D}{a}\right)^2}}\right]}{E_p}\right\} \quad (3.1)$$

$$M_R = \frac{0.24 \times P}{r \times d_r} \quad (3.2)$$

Where,

d_0 = Deflection at the center of the plate at 68°F, in.
d_r = Deflection at offset, r, from center of load plate, in.
r = Offset from center of load plate, in.
p = FWD load plate pressure, psi
a = FWD load plate radius, in.
D = Total thickness above subgrade, in.
M_R = Subgrade resilient modulus, psi
E_p = Effective modulus of all layers above the subgrade, psi

In general, deflection of the outermost sensor that captures the response of only subgrade material due to load dispersion is used to calculate subgrade M_R. As both granular base and subgrade layers were considered a single layer in this study, selecting a sensor location that captures both base and subgrade responses was significant. According to Irwin (1983), the FWD angle of load dispersion is at 34° to the horizontal, as shown in Figure 3.26. Therefore, an angle of load dispersion of 34° was used to determine the sensor location for each pavement section using layer thickness data. Note that sensor location for base and subgrade moduli is dependent on AC and base layer thicknesses and angle of load dispersion. For most pavement sections considered in the study, sensors at a radial distance of 36 and 48 inches from the center of the loading plate were appropriate to capture the response of base and subgrade layers. Surface deflections at the determined sensors were then used in Equation 3.2 to backcalculate moduli values for the base and subgrade layers (M_R) at all test stations for the 13 pavement sections. Finally, it should be noted that if the M_R values in this investigation were to have been used in the 1993 AASHTO Design Guide overlay design procedure, they would have needed to be multiplied by a correction factor. The current ALDOT practice is to use 0.33. However, since these data were used for perpetual pavement analysis in the PerRoad software, where correction factors are not recommended, none were applied.

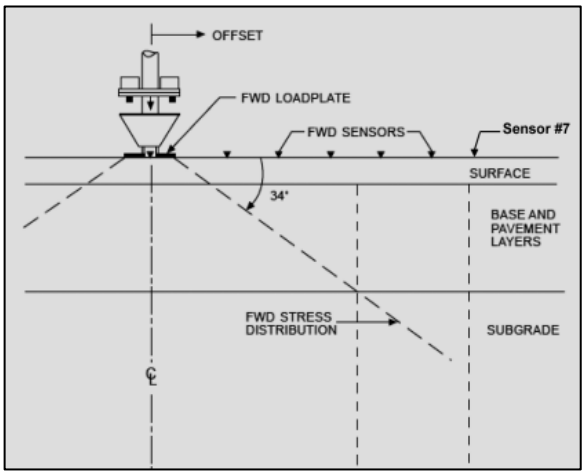

Figure 3.26 FWD load Distribution in Flexible Pavements (Irwin, 1983)

AC layer modulus (E_p) values were calculated using the surface deflection at the center of the loading plate. ALDOT reported the mid-depth temperature of the AC layer. The ALDOT temperature measurement procedure involved drilling a hole to the mid-depth of the AC layer, and the hole was filled with mineral oil a day before the FWD testing. Temperature readings were taken at an unspecified location from the mineral oil on the day of the FWD testing. The reported AC layer temperatures and AC thicknesses were used to determine temperature adjustment factors using Figure 3.25 (AASHTO, 1993). For thicknesses and AC mix temperatures outside the ranges presented in Figure 3.25, Equation 3.3 developed by ALDOT was used. The accuracy of the Equation 3.3 to replicate adjustment factors shown in Figure 3.25 was verified by the NCAT team. The FWD central deflections were then multiplied with the temperature adjustment factors to normalize the surface deflection to 68°F. The temperature corrected central deflection and M_R values from the previous exercise were used in Equation 1 to calculate the AC layer modulus at 68°F.

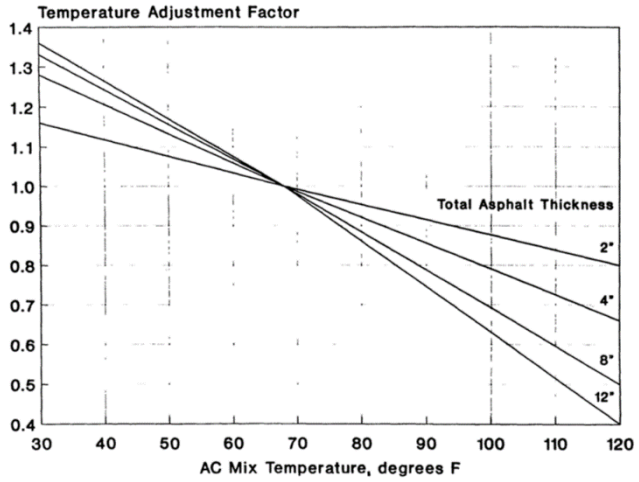

Figure 3.25 Adjustment to Central Deflection for AC Mix Temperature (AASHTO 1993)

$$CF = \begin{cases} 1.007873 + 1.073935logH - 0.45538(logH)^2 + T\begin{pmatrix} -0.00011578 \\ -0.0157931logH \\ +0.00669678(logH)^2 \end{pmatrix}, & T < 68^oF \\ 1.100733 + 0.494469logH - 0.12944(logH)^2 + T\begin{pmatrix} -0.00148136 \\ -0.0072716logH \\ +0.00190348(logH)^2 \end{pmatrix}, & T \geq 68^oF \end{cases} \quad (3.3)$$

Where:

CF =Temperature correction factor
H = AC layer thickness, in.
T = Pavement temperature, °F

The backcalculated layer moduli of pavement section 1 (Westbound I-22 in Walker County) at each FWD test location are presented in Figure 3.27. Backcalculated modulus results of other pavement sections at each FWD test location considered in the study are presented in Appendix A. Table 3.2 shows the average layer moduli calculated using the AASHTO 1993 method for the sections considered in the study. The average modulus of each pavement section represents the arithmetic mean of backcalculated moduli determined for all test stations within each pavement section.

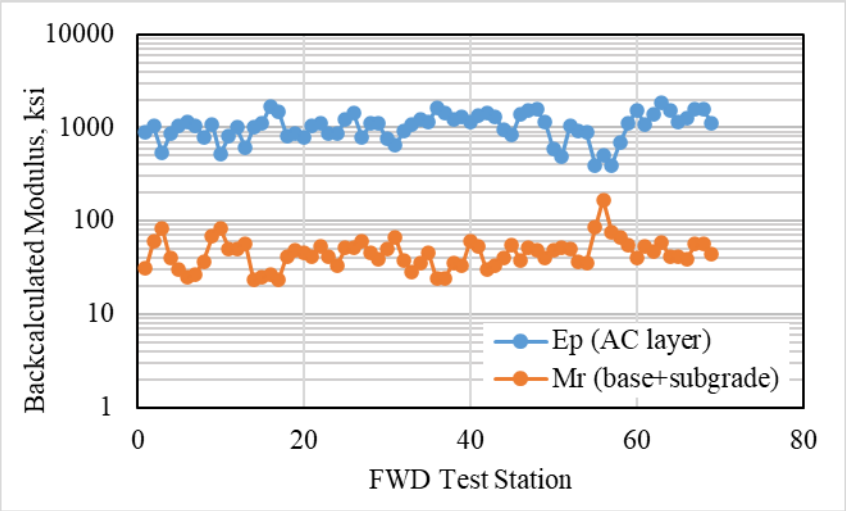

Figure 3.27 Backcalculated Layer Modulus of Pavement Section 1 (I-22 W Walker 47.2 to 40.3) Modeled as Two-Layer System using the AASHTO 1993 Method

Table 3.22 Average Layer Moduli Backcalculated using AASHTO 1993 Backcalculation Method

Route-Direction	County	Average backcalculated layer moduli (ksi)		
		AC layer	Granular Base	Subgrade
I-22 W	Walker	1068.6	47.3	47.3
I-65 N	Mobile	795.9	37.5	37.5
I-65 S	Mobile	1005.6	35.4	35.4
I-65 N	Conecuh	3169.7	52.8	52.8
I-65 S	Conecuh	2475.7	52.4	52.4
I-85 N	Macon	1232.1	42.0	42.0
I-85 S	Macon	1004.1	41.0	41.0
I-459 N	Jefferson	1540.0	42.4	42.4
I-459 S	Jefferson	1417.1	37.8	37.8
I-65 N	Chilton	1052.1	29.9	29.9
I-65 S	Chilton	1009.3	28.8	28.8
I-65 N	Chilton	1051.1	27.9	27.9
I-65 S	Chilton	819.8	26.0	26.0

Adjusting Backcalculated Moduli Data for Seasonal Variations

The backcalculated moduli results in

Table 3.22 represent modulus data of each layer at a single environmental condition (at 68^{o}F for the AC layer and at one moisture condition on the FWD testing day for the base and subgrade layers). However, it is important to adjust the modulus at a single environmental condition to possible environmental conditions that could occur over the design life of the pavement section. The Mechanistic-Empirical Pavement Design Guide (MEPDG) models the pavement structure using the Enhanced Integrated Climate Model (EICM) to determine temperature, moisture and suction variation within the pavement structure throughout the design life at various pavement depths in representative sublayers. The calculated temperature, moisture and suction variations are used to predict the seasonal modulus of each sublayer throughout the design life of the pavement. Therefore, the MEPDG framework integrated into the Pavement ME software was used to model the 13 pavement sections considered for the study to predict the seasonal modulus variation of each layer. Each section was modeled as a three layer system with thickness input from Table 3.21. This step of the analysis was also important to build a dataset and knowledge base off of Alabama pavements as ALDOT considers implementing the MEPDG and the Pavement ME software in the future.

Pavement ME modeling helped capture the seasonal (temporal) variability of the layer moduli. However, it is essential to capture both seasonal (temporal) and within-section variability (material and thickness) in a given pavement section to represent the possible variability of layer moduli. It should be noted that each pavement section considered in this study had multiple FWD test stations. Material and thickness variability of layer moduli were addressed indirectly by modeling each test station as an individual pavement section in the Pavement ME software and then compiling the data to represent

average and standard deviation modulus and thickness values. The Pavement ME input data used for this study are presented in the following section.

Pavement ME Inputs

AC Layer

The Mechanistic-Empirical Pavement Design (MEPDG) approach requires dynamic moduli of the asphalt mixtures as inputs at multiple temperatures and frequencies to develop a master curve within the Pavement ME software. It was practically impossible to generate the AC layer modulus data with the available FWD deflection data at multiple temperatures and frequencies. However, various approaches were recommended in the literature to convert FWD backcalculated AC modulus data to a master curve (NCHRP 1-37A, 2014; Kim et al., 2021; Solatifar et al., 2017). These approaches require a baseline master curve predicted using the Witczak E* model (NCHRP 1-37A, 2004) from the volumetrics of the field cored samples. The approaches recommended by NCHRP 1-37A (2004) and Kim et al. (2021) were not supported by validation with laboratory measured dynamic modulus test data of field cored specimens. Solatifar et al.'s (2017) method was validated with laboratory dynamic modulus test data on field core samples from 10 field test sections. Therefore, the procedure recommended by Solatifar et al. (2017) was used in the study to convert AC backcalculated modulus (E_p) to a master curve.

To convert E_p to a master curve, a baseline master curve was needed. However, no field cores were available to predict modulus from volumetrics using Witczak E* prediction model (NCHRP 1-37A, 2004). A typical ALDOT surface mix was used in section N1 of the 2015 NCAT Test Track cycle. Dynamic modulus data of the N1 surface mix was available for the research team, as shown in

Table **3.23**. The vertically shifted master curves were used to determine the dynamic modulus of each test station at multiple temperatures and frequencies for Level-1 input in the Pavement ME software.

Table 3.23 Dynamic Modulus Data for N1 Surface Mix from the 2015 NCAT Test Track Cycle

Temp (°C)	Freq (Hz)	Modulus (ksi)
4	0.1	1329.7
4	1.0	1718.5
4	10.0	2155.8
20	0.1	451.2
20	1.0	735.5
20	10.0	1111.4
40	0.1	94.3
40	1.0	185.8
40	10.0	360.5

Granular Base and Subgrade Layers

As mentioned in Section 2, the granular base and subgrade modulus was assumed to be the same for backcalculation purposes. The calculated M_R value of each test station of a particular pavement section was used as a Level-1 design input in the Pavement ME software for both the granular base and subgrade layers. The input M_R values were adjusted for monthly seasonal variations using models built within the software based on predicted moisture levels from the EICM.

Climate and Other Inputs

The closest LTPP climate locations for each of the 13 pavement sections were selected to simulate appropriate climatic conditions for the pavement sections. The climate locations chosen for the Pavement ME simulations are described in Table 3.24. Level-3 input values were used for traffic and other properties not described in this document.

Table 3.24 Climate Locations used for the Pavement ME Simulations

Section ID	Route	County	Milepost	Pavement ME Selected Climate Location			
				Location	Latitude	Longitude	MERRA Cell ID
1	I-22 W	Walker	47.2 - 40.3	Jasper, AL	33.85636	-87.30161	137237
2	I-65 N	Mobile	0.0 - 8.3	Mobile, AL	30.60822	-88.24612	133204
3	I-65 S	Mobile	8.3 - 0.0	Mobile, AL	30.60822	-88.24612	133204
4	I-65 N	Conecuh	83.1 - 92.5	Evergreen, AL	31.39617	-87.02340	134358
5	I-65 S	Conecuh	92.5 - 83.1	Evergreen, AL	31.39617	-87.02340	134358
6	I-85 N	Macon	31.1 - 35.8	Franklin, AL	32.44523	-85.79860	135512
7	I-85 S	Macon	35.8 - 31.1	Franklin, AL	32.44523	-85.79860	135512
8	I-459 N	Jefferson	5.5 - 11.1	Hoover, AL	33.35625	-86.85326	136662
9	I-459 S	Jefferson	11.1 - 5.5	Hoover, AL	33.35625	-86.85326	136662
10	I-65 N	Chilton	198.0 - 205.3	Clanton, AL	32.80571	-86.58220	136086
11	I-65 S	Chilton	205.3 - 198.0	Clanton, AL	32.80571	-86.58220	136085
12	I-65 N	Chilton	211.4 - 216.5	Clanton, AL	32.80571	-86.58220	136085
13	I-65 S	Chilton	216.5 - 211.4	Clanton, AL	32.80571	-86.58220	136086

Pavement ME Seasonal Adjustments

As mentioned previously, the MEPDG design framework and Pavement ME software predicts the pavement structure's temperature, moisture, and suction profiles to predict each sublayer's modulus over the design life at one-month intervals. The methods used to adjust environmental variation changes from AC to granular layers as described in the following subsections.

AC Layer

The Pavement ME software divided the AC layer into multiple sub-layers and predicted the modulus of each sublayer at five quintiles, representing the entire temperature range, in each month. The predicted hourly temperature of each sublayer from EICM modeling was used to divide the whole month into five quintiles based on the monthly temperature distribution. The quintile temperatures were used to

determine the modulus of sublayers using the master curve built within the software. Figure 3.28 presents Pavement ME-generated AC modulus for different sublayers and quintiles in the first month of design life for pavement section 10 (I65-N Chilton from milepost 198.0 to 205.3). The average AC layer modulus for each month of the design life was calculated using the thickness-weighted average of all sublayer third quintile values (as the third quintile presents the 50th percentile) as shown in Equation 3.4.

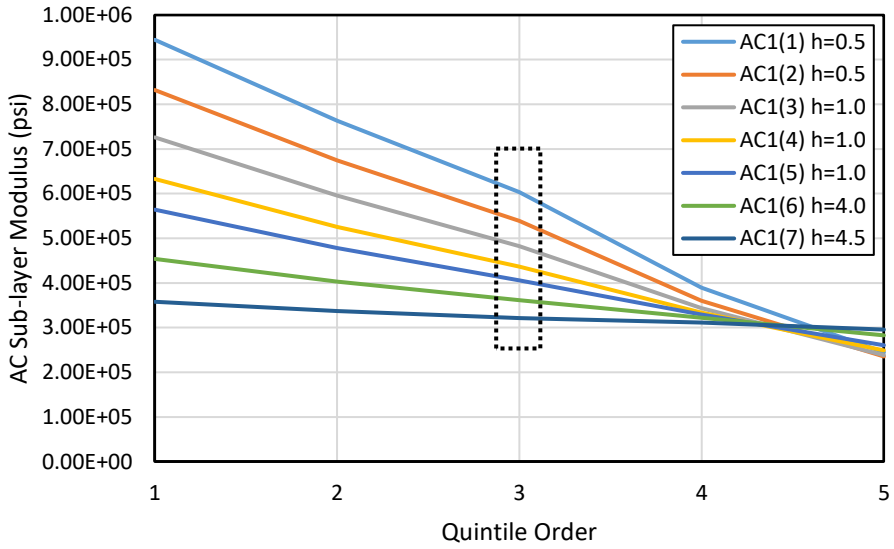

Figure 3.28 AC sub-layer Modulus per Quintile

$$Average\ Layer\ Modulus = \frac{\sum(3^{rd}\ Quintile\ Sublayer\ Modulus \times h_i)}{\sum h_i} \quad (3.4)$$

Where, h_i= Individual Sub-layer thickness (inch)

As discussed earlier, each FWD test location was modeled as an individual section in the Pavement ME software. The process of checking outliers was performed by visual inspection. For example, as shown in Figure 3.29-a, two stations with significantly lower modulus values than the rest were observed. The modulus data corresponding to those two stations were removed for further analysis. The change due to removing outliers by visual inspection is represented in Figure 3.29-b. The data shows a more substantial influence of seasonality in the AC layer moduli than in the base and subgrade layer moduli.

After screening out the outliers, the remaining layer moduli were sorted and grouped by different months of the year. Finally, the average and standard deviation of AC, base, and subgrade layer modulus for a corresponding month over the simulation years were calculated. Figure 3.30 shows the average AC, base, and subgrade modulus variation over the simulation period at different months of the year. It was observed that the AC layer modulus was sensitive to the monthly temperature cycles over the years. In contrast, the base and subgrade layer modulus had the least sensitivity to the temperature cycling, as expected.

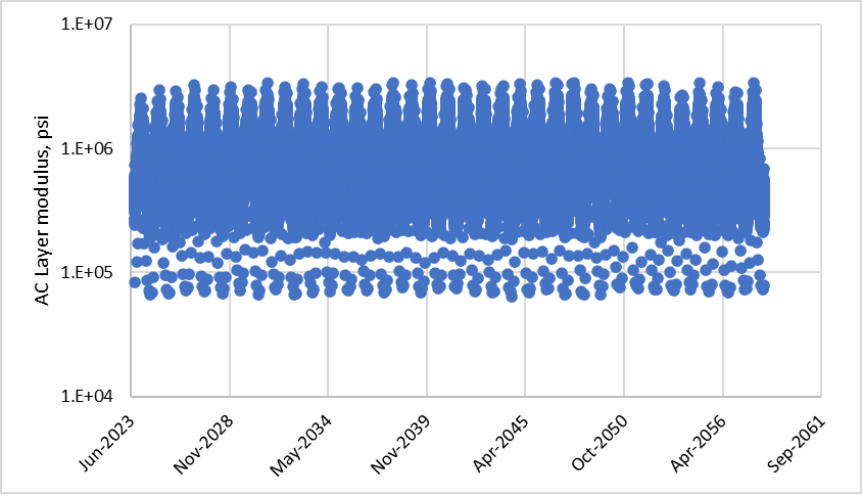

(a)

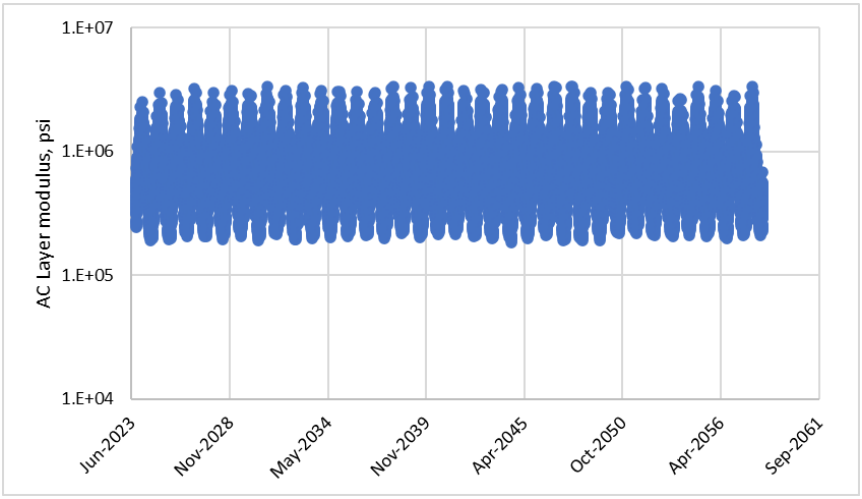

(b)

Figure 3.29 Pavement ME-Generated AC Moduli (a) Before Visual Screening of Outlier Moduli, (b) After Screening of Outlier Moduli

The months within a season were grouped based on the magnitude of the AC layer moduli. Based on the average AC moduli magnitude, there were five seasons as follows: Season 1 (Jan, Feb, Dec), Season 2 (Mar, Nov), Season 3 (Apr, Oct), Season 4 (May, Sept) and Season 5 (Jun, Jul, Aug). The average and COV of AC layer modulus within each season were calculated as an input for the PerRoad version 4.4 materials properties, presented in Table 3.25. Based on the research team's experience with typical asphalt mixtures used in Alabama, the Pavement ME software produced seasonal AC modulus values that were unusually high, especially for sections 8 and 9 on I-65 in Conecuh County. The overestimated AC modulus from Pavement ME software led the research team to investigate using the default AC layer modulus built within the PerRoad 4.4 software for other modulus trials in the study.

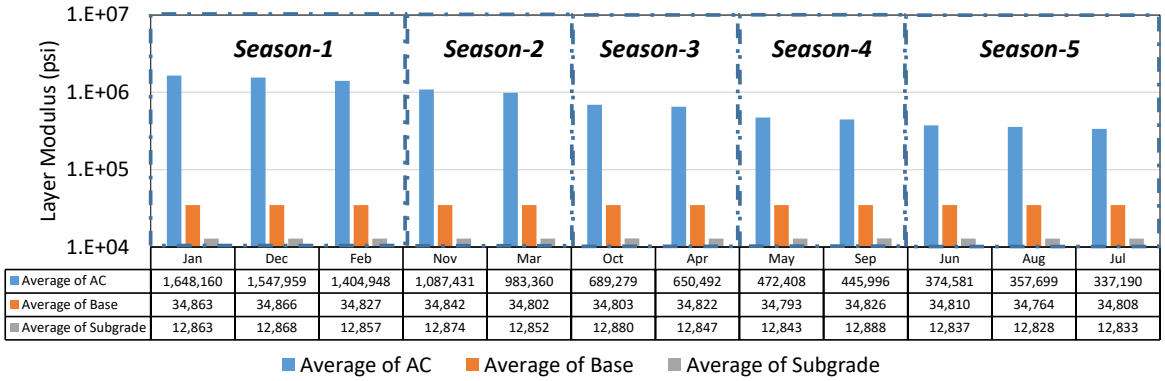

	Jan	Dec	Feb	Nov	Mar	Oct	Apr	May	Sep	Jun	Aug	Jul
Average of AC	1,648,160	1,547,959	1,404,948	1,087,431	983,360	689,279	650,492	472,408	445,996	374,581	357,699	337,190
Average of Base	34,863	34,866	34,827	34,842	34,802	34,803	34,822	34,793	34,826	34,810	34,764	34,808
Average of Subgrade	12,863	12,868	12,857	12,874	12,852	12,880	12,847	12,843	12,888	12,837	12,828	12,833

Figure 3.30 Average Layer Modulus for AC, Base, and Subgrade at Different Months Over the Simulation Period for Section 12

Table 3.25 Seasonal Average AC Layer Modulus Obtained from Pavement ME

Section ID	AC layer Modulus, psi					COV, %
	Season-1	*Season-2*	*Season-3*	*Season-4*	*Season-5*	
1	1,642,803	1,085,111	679,501	463,634	355,439	30
2	1,205,651	987,620	759,723	582,542	500,789	39
3	1,512,697	1,237,631	942,656	722,883	620,981	36
4	4,239,504*	2,867,449	1,890,580	1,298,851	1,033,233	30
5	3,341,199	2,253,188	1,480,747	1,019,015	812,568	29
6	1,966,223	1,420,070	942,780	634,482	476,173	35
7	1,587,189	1,135,519	753,926	507,878	381,232	29
8	2,078,722	1,551,078	950,906	622,796	484,844	47
9	2,165,466	1,674,021	1,141,042	774,615	585,936	50
10	1,602,626	1,081,787	700,285	480,919	373,375	26
11	1,519,313	1,020,191	659,196	452,199	350,865	28
12	1,533,689	1,035,396	669,886	459,202	356,490	38
13	1,307,093	975,339	666,425	469,604	371,480	29

*4,000,000 psi was used as PerRoad 4.4 input (As this is the maximum limit in the software)

Granular Base and Subgrade Layers

The resilient modulus of an unbound layer is affected by stress state, moisture variations, and freeze/thaw effects. Granular materials are considered linear elastic for a level 2 and 3 resilient modulus input. Level-2 design inputs were assigned to granular layers in this study. Therefore, no stress state adjustments were made. For seasonal variation, the MEPDG framework and Pavement ME software adjusts the input resilient modulus (M_{Ropt}) of unbound materials using an environmental adjustment factor (F_{env}), as shown in Equation 3.5.

$$M_R = F_{env}.M_{Ropt} \quad (3.5)$$

During the design life of the pavement, three possible conditions could occur for granular material: frozen (F_F), thawed/recovering (F_R), and unfrozen/fully recovered (F_U). The EICM outputs (hourly moisture and temperature profiles) are used to assign appropriate material conditions for a given analysis location (node) in the pavement structure at a given analysis period (hourly). The Pavement ME software divides granular layers into multiple sublayers similar to the AC layer. It should be noted that frozen, thawed, and unfrozen materials can coexist within the same sublayer, but it should also be emphasized that these conditions are not prevalent in Alabama and were not modeled by the software.

The environmental adjustment factor of each sublayer during an analysis interval (1 month) is a composite factor representing a weighted average of the factors (F_F, F_R and F_U) that existed in the sublayer during the analysis period. Typically, F_{env} values are more significant than one for cold temperature regions because of the presence of frozen material compared to hot climate regions. The F_{env} values are lower than one for hot climate regions because of unfrozen material presence. A more detailed description of the environmental adjustment factor for granular material is presented in the MEPDG Design Guide (NCHRP 1-37A, 2004).

The Pavement ME software output includes monthly environmental adjusted base and subgrade sublayers moduli. These data were utilized to calculate the thickness-weighted average seasonal modulus and COV of both base and subgrade. In compliance with the AC layer, five seasons were considered for granular layers: Season 1 (Jan, Feb, Dec), Season 2 (Mar, Nov), Season 3 (Apr, Oct), Season 4 (May, Sept) and Season 5 (Jun, Jul, Aug). The seasonal modulus and COV obtained from the Pavement ME simulation for base and subgrade are presented in Table 3.26 and

Table **3.27**. Interestingly, the values generated in Tables 6 and 7 resulted from entering identical values for the base and subgrade layers for each section and season, respectively. The Pavement ME software took these values, and applied adjustment factors to arrive at the values listed in Tables 3.6 and 3.7.

Table 3.26 Seasonal Average Base Layer Modulus Obtained from Pavement ME

Section ID	Base layer Modulus, psi					COV, %
	Season-1	*Season-2*	*Season-3*	*Season-4*	*Season-5*	
1	55,410	55,370	55,404	55,384	55,337	33
2	49,384	49,366	49,345	49,338	49,429	17
3	47,452	47,434	47,419	47,443	47,429	20
4	68,193	68,126	68,131	68,150	68,292	24
5	69,171	69,128	69,132	69,142	69,099	23
6	55,018	54,998	54,988	54,972	54,915	30
7	53,699	53,679	53,670	53,654	53,598	22
8	53,210	52,943	53,147	52,894	52,760	30
9	46,372	46,340	46,326	46,305	46,293	31
10	36,887	36,884	36,877	36,876	36,829	21
11	36,221	36,218	36,212	36,210	36,165	22
12	34,852	34,822	34,812	34,809	34,794	32
13	33,136	33,134	33,128	33,126	33,085	31

Table 3.27 Seasonal Average Subgrade Layer Modulus Obtained from Pavement ME

Section ID	Subgrade layer Modulus, psi					COV, %
	Season-1	*Season-2*	*Season-3*	*Season-4*	*Season-5*	
1	20,811	20,811	20,811	20,813	20,782	32
2	19,135	19,135	19,137	19,138	18,984	17
3	16,370	16,372	16,372	16,373	16,348	19
4	24,434	24,434	24,436	24,442	24,376	24
5	24,331	24,331	24,333	24,336	24,297	31
6	19,363	19,363	19,364	19,366	19,336	29
7	18,886	18,886	18,887	18,887	18,860	21
8	19,022	19,051	19,400	19,539	19,450	29
9	16,703	16,704	16,705	16,706	16,648	31
10	13,491	13,491	13,491	13,491	13,473	20
11	13,262	13,263	13,263	13,263	13,243	21
12	12,863	12,863	12,864	12,865	12,833	31
13	12,815	12,816	12,816	12,818	12,760	31

PerRoad Inputs

The objective of the analysis was to evaluate the 13 ALDOT pavement sections with three different modulus datasets using PerRoad version 4.4. The pavement sections were modeled as a three-layer system. The input values used to analyze and design the pavement sections considered in this study are described in this section. PerRoad utilizes layered elastic theory coupled with Monte Carlo simulation to estimate the strain distribution at critical locations in the pavement structure. To achieve the desired precision, 5000 Monte Carlo cycles were used to compute the horizontal tensile strain at the bottom of AC, the vertical compressive strain at the top of the base, and the vertical compressive strain at the top of the subgrade. These are the known critical locations for perpetual pavement design and analysis. Key inputs for the PerRoad 4.4 software are:

- Seasonal pavement layer moduli
- Thickness of bound and unbound materials
- Load spectrum for traffic
- Design criteria (limiting strain at critical locations)

Layer Moduli

Three modulus dataset trials were used for AC, base and subgrade layers. The seasonally adjusted modulus from the Pavement ME simulations were used for Trial 1. The Trial 1 modulus inputs used for AC, base and subgrade were presented in Table 3.25, Table 3.26 and

Table **3.27**. The Trial 1 AC modulus values appeared to be overestimated compared to general understanding and expectancy of asphalt mixtures used in Alabama. Consequently, predicted strain distributions from Trial 1 modulus values were seemingly much too low. Therefore, to eliminate the issue of overestimation, in Trial 2, the default layer modulus for PG 64-22 built in the PerRoad 4.4 software was used. PerRoad 4.4 required seasonal average air temperatures and seasonal AC modulus estimation. The historical mean air temperature data from National Oceanic and Atmospheric Administration (NOAA) station located in Montgomery, AL were used for seasonal air temperatures. Montgomery is the geographical center of Alabama, and all other sections are located nearby. To avoid the complication in estimating AC layer modulus, the NCAT team decided to follow the same seasonal distribution and AC modulus for all the stations within the study. Based on 130,550 historical temperature data points, the quintile values were extracted as indicated in Figure 3.31. Five quintile air temperatures were used for Trial 2 as mean air temperatures corresponding to the five seasons considered. PerRoad 4.4 estimates AC layer modulus using mean seasonal pavement temperatures (MMPT) at the upper one-third depth of the AC layer, as shown in Equation 3.7. Equation 3.6 was used to determine MMPT from mean seasonal air temperature (MMAT) and AC layer thickness. Table 3.28 presents PerRoad 4.4 default layer modulus calculated using Equation 3.7 for the AC layer with PG 64-22. The seasonally adjusted modulus from the MEPDG simulations was used for base and subgrade (Table 3.26 and

Table **3.27**) in Trial 2.

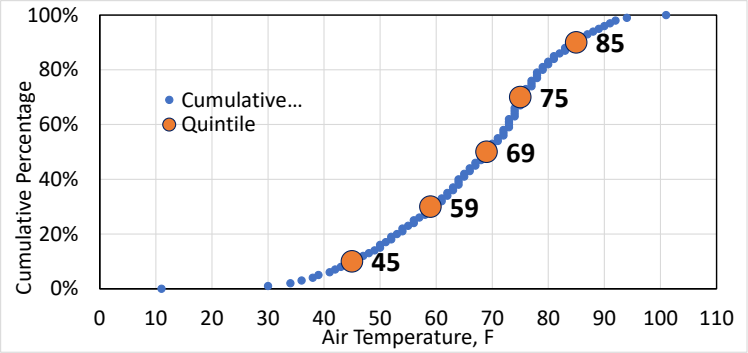

Figure 3.31 Historical Mean Air Temperature Recorded at Montgomery, AL Station

$$MMPT = MMAT\left[1 + \frac{1}{z+4}\right] - \left[\frac{34}{z+4}\right] + 6 \quad (3.6)$$

$$E_{HMA} = 7351157e^{-0.038MMPT} \quad (3.7)$$

Where:

z = 1/3 of AC depth in pavement structure, in.
E_{HMA} = AC layer modulus, psi
MMPT = mean seasonal pavement temperature, F
MMAT = mean seasonal air temperature, F

Based on the preliminary strain calculations, it was concluded that using the PerRoad Default AC moduli for PG 64-22 at different seasonal temperatures at Trial 2 somewhat eliminates the overestimation of material strength that occurred in Trial 1. However, based on the NCAT's experience with the soil strength of Alabama, the base and subgrade modulus from the Pavement ME output was also overestimated. Thus, in Trial 3, the base and subgrade layer moduli were fixed at 25,000 psi and 8,000 psi, respectively, when the default AC modulus for PG 64-22 was used. Moduli values of 25,000 psi and 8,000 psi were used as typical ALDOT design moduli inputs for base and subgrade.

Table 3.28 PerRoad 4.4 Default PG 64-22 AC Modulus for Sections in the Study

Section ID	PerRoad 4.4 default AC modulus, psi				
	Season-1	***Season-2***	***Season-3***	***Season-4***	***Season-5***
1	1,015,172	565,445	372,268	289,690	190,721
2	1,001,175	547,881	356,180	275,081	178,831
3	1,000,876	547,510	355,842	274,775	178,584
4	1,006,720	554,803	362,496	280,803	183,470
5	1,006,720	554,803	362,496	280,803	183,470
6	1,009,219	557,938	365,367	283,410	185,592
7	1,012,626	562,227	369,305	286,992	188,514
8	995,398	540,723	349,682	269,211	174,097
9	995,096	540,351	349,345	268,907	173,853
10	1,005,690	553,514	361,317	279,734	182,602
11	1,007,711	556,044	363,632	281,834	184,309
12	1,009,036	557,707	365,155	283,218	185,435
13	1,009,311	558,053	365,472	283,506	185,669

Table 3.29 Modulus Input Used for the PerRoad 4.4 Simulation

Trial	Pavement Layer		
	AC	**Base**	**Subgrade**
1	Pavement ME Output (Table 3.25)	Pavement ME Output (Table 3.26)	Pavement ME Output (Table **3.27Table 3.25**)
2	PerRoad Default (Table 3.28)	Pavement ME Output (Table 3.26)	Pavement ME Output (Table **3.27Table 3.25**)
3	PerRoad Default (Table 3.28)	25,000 psi	8,000 psi

Thickness and Poisson Ratio

The average thickness and coefficient of variance (COV) of structural layers of pavement were estimated from the dataset provided by ALDOT. The thickness distribution was assumed to be a normal distribution for all layers with the estimated mean and COV from the thickness database provided by ALDOT. It should be noted that for most of the pavement sections considered, the thickness data were had COVs of zero. It was presumed that the thickness values were estimated by ALDOT for the pavement sections in these cases. The Poisson's ratios were chosen as 0.35, 0.4 and 0.45 for AC, base and subgrade, respectively.

Traffic Load Spectrum

The PerRoad 4.4 software uses traffic load spectra to account for the traffic variability on the strain distribution at critical locations. The default rural interstate load spectra in the software were used for this study. The default axle weight distribution within PerRoad 4.4 was used for this study and presented in Figure 3.32. Some of the key load spectra inputs used for the study are shown in **Error! Reference source not found.**

Table 3.30 Traffic Loading Conditions for the PerRoad Strain Calculations

Two-Way AADT	1000	
% Trucks	10	
% Trucks in Design Lane	90%	
Axle Groups/day	136	
% Truck Growth	4	
Directional Distribution	50%	
Percentages of Axle Types	Single	50.43%
	Tandem	48.81%
	Tridem	0.76%

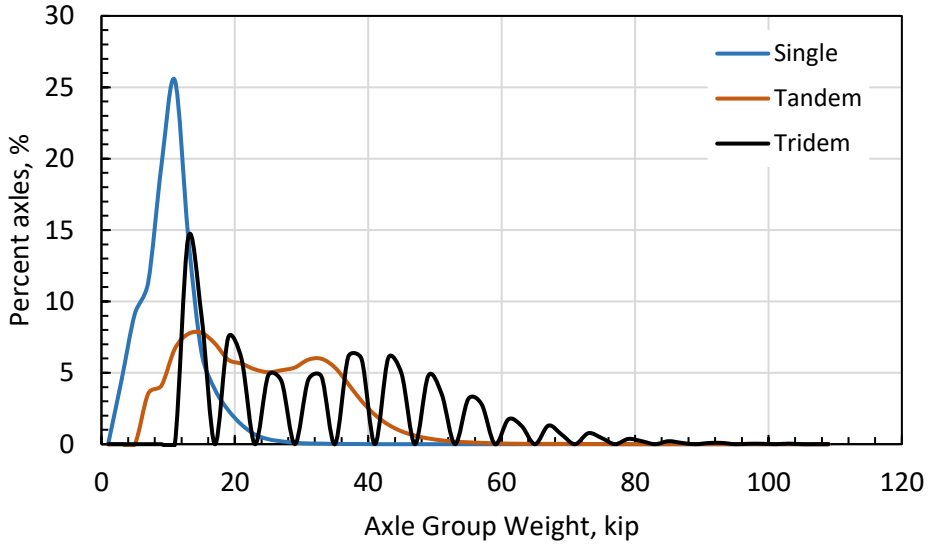

Figure 3.32 Default Axle Weight Distribution in PerRoad 4.4 Software

Design Criteria

To determine the maximum AC layer thickness, the limiting strain criteria were set according to the previous work done at NCAT on perpetual road experience and agency expectations (Tran et al., 2015). The summary of the performance criteria used are tabulated in Table 3.31 and 12.

Table 3.31 Performance Criteria used for the Perpetual Pavement Analysis

Layer	Location	Mode	Threshold/Criteria
AC	Bottom of AC	Horizontal Tensile Strain Distribution	Tran et al., 2015 (see Table 3.32)
Base	Top of Base	Vertical Compressive Strain	200 microstrain at 50th Percentile
Subgrade	Top of Subgrade	Vertical Compressive Strain	200 microstrain at 50th Percentile

Table 3.32 Design Limiting Criteria for Horizontal Strain at the Bottom of AC (Tran et al., 2015)

Percentile	Limiting predicted tensile microstrain criteria
55	110
60	120
65	131
70	143
75	158
80	175
85	194
90	221
95	257
99	326

PerRoad Simulation Results

Existing Thickness

Figure 3.33 presents the tensile strain at the bottom of AC of three pavement sections ranging from thickest (17.5") to thinnest (8.4") AC layer thickness in the study with three modulus input trials. The tensile strain distribution at the bottom of the AC layer fell well below the threshold strain distribution considered for Trial 1 which was expected given the thicknesses and very high modulus values. Similarly, as shown in Figure 3.34, the compressive strain on top of the subgrade was far smaller than the critical failure strain of 200 microstrain at the 50^{th} percentile. This could be due to the thicker AC layer than needed for a perpetual pavement and/or higher moduli values used in Trial 1 (obtained from Pavement ME software). It should be noted that section 4, with 13 inches of AC, had an unrealistically higher modulus in season 1 (4,239,504 psi). Trial 2 modulus inputs yielded higher tensile and compressive strains at the critical locations due to lower AC modulus than Trial 1. The change in tensile and compressive strains is much higher in sections with thinner AC layers for Trial 2 inputs.

Even with reduced AC modulus data, strains yielded from the Trial 2 analysis were very low compared to the design criteria, as shown in Figure 3.33 and Figure 3.34. The base layer modulus values used in Trial 2 were in the range of 33 to 69 ksi and subgrade modulus values were in the range of 12 to 24 ksi. Based on the experience with Alabama materials, the NCAT team concluded that unbound layer modulus values used for Trials 1 and 2 were significantly higher than the in-situ field condition (ALDOT design default values). Therefore, to make a more realistic estimate of material moduli, the investigation continued using Trial 3 modulus inputs with a base modulus of 25 ksi and subgrade modulus of 8 ksi, which relates more to the values ALDOT currently uses for pavement design. From Figure 3.33 and Figure 3.34, it was observed that moving from Pavement ME produced moduli input to typical ALDOT design moduli input resulted in the increased horizontal tensile strains at the bottom of the AC. This implies that modulus values predicted using the backcalculation procedure and Pavement ME seasonal adjustments considered in this study over predicted moduli of the pavement layers. The effect of input modulus was evident in thin AC (section 8) sections compared to thick AC (section 1) sections. Similar

observations were made for the remaining ten pavement sections, presented in Appendix A. Among the 13 pavement sections, sections 8 and 9 with AC thicknesses of 8.3" and 8.4" produced horizontal strains close to the limiting strain criteria and the vertical strain exceeded the limiting strain of 200 microstrain using Trial 3 modulus inputs.

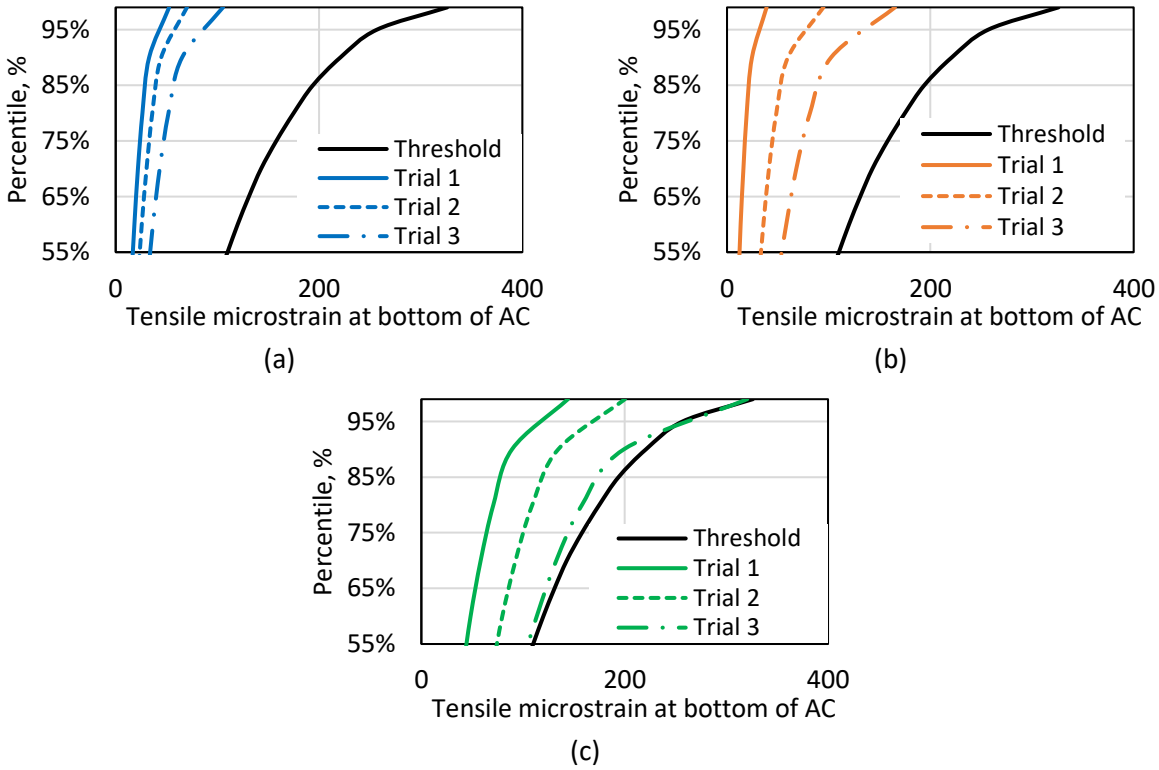

Figure 3.33 PerRoad Simulated Tensile Strain Distribution at the Bottom of the AC layer with Different Modulus Input Trials for (a) Section 1 (17.5"AC), (b) Section 4 (13"AC) and (c) Section 8 (8.4"AC)

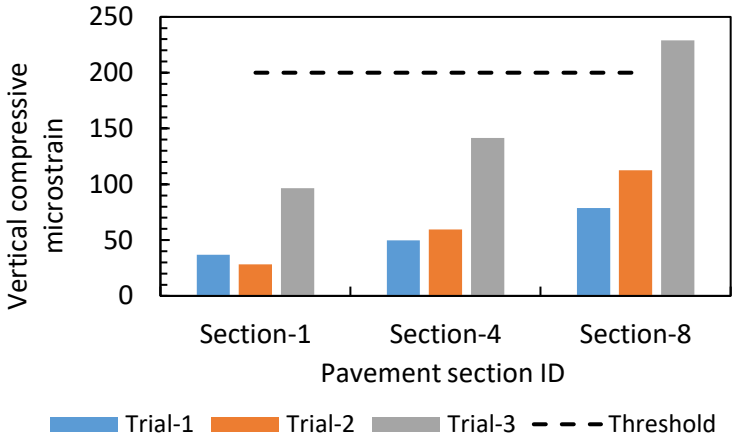

Figure 3.34 PerRoad Simulated 50th Percentile Compressive Strain using Different Modulus Input Trials for Section 1 (17.5"AC), Section 4 (13"AC) and Section 8 (8.4"AC) on Top of the Subgrade

In summary, the three modulus input trials produced tensile strain levels below the respective strain limits confirming that these tensile strain limits considered (Tran et al., 2015) are appropriate for AL pavements. The Pavement ME simulated modulus input (Trial 1) produced unrealistically low strain levels compared to the limiting strain criteria for all the 13 sections considered. Pavement ME yielded seasonal AC modulus values were 2 to 3 times higher compared to the PerRoad 4.4 default AC modulus for PG 64-22 (Trial 2) for most of the sections and 4 to 5 times higher for sections 8 and 9 on I65 in Conecuh County. For Trial 2, default AC modulus for PG 64-22 mixtures were used along with Pavement ME produced base and subgrade modulus. Trial 2 modulus inputs had strain levels that were also unrealistically low compared to the limiting strain criteria. Base and subgrade modulus values used in Trial 2 were on the higher side; therefore, ALDOT design default modulus values were used for Trial 3. The Trial 3 modulus inputs produced lower strain levels for 11 out of 13 pavement sections considered. Pavement sections 8 and 9 (on I65 north and south bounds in Conecuh County) with AC thicknesses of 8.3 and 8.4 inches produced strains that exceeded the limiting strain criteria at both critical locations (horizontal strain at the bottom of the AC and vertical strain at the top of subgrade) with Trial 3 modulus inputs. The remaining 11 pavement sections with thick AC layers produced lower strain levels but more than expected strain levels in perpetual pavements. Therefore, Trial 3 modulus inputs were considered the best approach among the three examined trials using existing perpetual pavement design criteria.

Maximum AC Thickness

Based on the results of the previous section, most of the sections considered in this study have thicker AC thicknesses than needed for a perpetual pavement using currently accepted design criteria in PerRoad. Therefore, using three trial modulus inputs, another effort was made to design the maximum AC layer thickness needed for each pavement section. Like the analysis presented above, the two critical locations were selected for the design to avoid bottom-up fatigue cracking and structural rutting. Design criteria given in the previous section for horizontal tensile strain distribution at the bottom of the AC layer and 50^{th} percentile compressive strain on top of the subgrade layer were considered the design criteria. AC layer thicknesses for each pavement section were iterated until a minimum thickness that satisfied the design criteria at critical locations was achieved, called the maximum AC thickness. The analysis was conducted using three input modulus trials previously described in the study.
Table **3.33** presents the existing and designed maximum AC thicknesses for different pavement sections. This was done to the nearest 0.5 inches, rounded up.

The Trial 1 modulus inputs resulted in very thin maximum AC thicknesses in the range of 3.0 to 6.5 inches which is neither practical nor reasonable for interstate pavements. As mentioned before, the modulus values yielded from the Pavement ME software were very high for all three layers. The lower maximum AC thicknesses were due to higher modulus values used for this trial. This was especially true for sections 4 and 5, with very high AC (3,300-4,000 ksi), base (around 68 ksi), and subgrade (about 24 ksi) modulus values. The reduction in the AC layer modulus for Trial 2 resulted in more reasonable maximum AC thicknesses of 6.0 to 8.0 inches. However, it would still be considered too thin for perpetual interstate pavements. However, the modulus used for base and subgrade was still high for Alabama materials. The Trial 3 modulus inputs with ALDOT default values resulted in expected

maximum AC thicknesses in the range of 8.5 to 10.0 inches which are in better agreement with well-established perpetual pavement thickness ranges.

Table 3.33 Maximum AC Thicknesses with Different Modulus Input Trials

Section ID	Route	County	Milepost	Existing Thickness, in.		Maximum AC Thickness, in.		
				Asphalt Layer	Granular Layer	Trial-1	Trial-2	Trial-3
1	I-22 W	Walker	47.2 - 40.3	17.0 - 18.0	6.0	4.5	6.5	9.5
2	I-65 N	Mobile	0.0 - 8.3	10.5	10.0	5.5	7.0	8.5
3	I-65 S	Mobile	8.3 - 0.0	10.4	10.0	4.0	7.0	8.5
4	I-65 N	Conecuh	83.1 - 92.5	13	10.0	3.5	6.0	8.5
5	I-65 S	Conecuh	92.5 - 83.1	13	10.0	3.0	6.0	8.5
6	I-85 N	Macon	31.1 - 35.8	14.3	8.0	4.0	6.5	8.5
7	I-85 S	Macon	35.8 - 31.1	14.3	8.0	4.5	6.5	9.0
8	I-459 N	Jefferson	5.5 - 11.1	8.4	6.0	5.0	6.5	10.0
9	I-459 S	Jefferson	11.1 - 5.5	8.3	6.0	4.0	7.5	10.0
10	I-65 N	Chilton	198.0 - 205.3	12.5 - 14.6	11.0	5.0	7.5	8.5
11	I-65 S	Chilton	205.3 - 198.0	13.5 - 14.7	12.0	5.0	7.5	8.5
12	I-65 N	Chilton	211.4 - 216.5	13.7 - 17.0	10.0	6.5	7.5	8.5
13	I-65 S	Chilton	216.5 - 211.4	14.0 - 14.7	10.0	6.5	8.0	8.5

Results Summary

This chapter presented an analysis of the design thicknesses of the 13 pavement sections provided by ALDOT with three different modulus datasets using PerRoad version 4.4. None of these sections were reported to have deep structural distresses and were considered good candidates for perpetual analysis. This analysis was divided into two parts. The first part was performing PerRoad 4.4 analysis with existing pavement section thicknesses, and the second part was designing the maximum AC thickness needed using three different modulus datasets. Based on the results presented in this chapter, the following observations were made:

- A three-layer backcalculation analysis resulted in higher subgrade modulus values than the base layer and was discarded from further analysis. Two-layer backcalculation was then attempted and carried through the entire analysis procedure.
- The seasonally adjusted modulus values from the Pavement ME software were very high compared to the NCAT team's expectation of the materials used in Alabama. The AC layer modulus values for Season 1 were in the range of 1,200 to 4,200 ksi, base layer moduli were in the range of 33 to 69 ksi, and subgrade moduli were in the range of 12 to 24 ksi. Therefore, different moduli were derived from PerRoad defaults and using currently accepted ALDOT input values for pavement thickness design.
- For all three modulus trials used, the predicted horizontal tensile strain distribution at the bottom of the AC and the mean vertical compressive strain on top of the subgrade using existing layer thicknesses were very low compared to the design criteria considered in the study, except for sections 8 and 9 with 8.3 and 8.4 inches of AC layer. This suggested that the AC layers in

these sections are thicker than what is needed for a perpetual pavement using the current design criteria.

- The Trial 1 modulus inputs resulted in thinner AC layers in the range of 3.0 to 6.5 inches due to higher modulus values from the Pavement ME software. This range was deemed impractical and unreasonable for interstate pavements.
- The Trial 2 modulus inputs resulted in more reasonable AC thicknesses in the range of 6.0 to 8.0 inches but still on the relatively thinner side for perpetual interstate pavements. However, modulus values used for the design were higher (base: 33-69 ksi; subgrade:12-24 ksi).
- The Trial 3 modulus inputs (ALDOT default) resulted in the most reasonable AC thicknesses in the range of 8.5 to 10.0 inches.

CHAPTER 4
METHODOLOGY VALIDATION

The primary goal of this task was to validate and make necessary changes to the methodology developed as part of Task 2. This included examining the validity of using existing field limiting tensile strain criteria for designing perpetual pavements in Alabama. Based on pavement design principles, bottom-up fatigue cracking depends on the tensile strain at the bottom of the asphalt layer, and subgrade rutting is mainly related to the compressive strain at the top of the subgrade. For the methodology developed in Task 2, the limiting strain criteria were set according to the previous work done at NCAT on perpetual pavement experience and agency expectations (Tran et al., 2015). The field limiting tensile strain criteria developed were based on long-term performance observed at the NCAT Test Track, an accelerated loading testing facility. As per Tran et al. (2015), the NCAT Test Track truck fleet had 14.29% steering, 71.42% single, and 14.29% tandem axles with loading as follows:

- Steer axles: 8-10 kips (20%) and 10-12 kips (80%)
- Single axles: 20-22 kips (100%)
- Tandem axles: 38-40 kips (80%) and 40-42 kips (20%)

The axle load spectrum applied at the NCAT Test Track is much more severe than the national average axle load spectrum for the rural interstate functional class developed by Timm and Newcomb (2010). In fact, it is much more severe than most open-access roadway load spectra since it focuses all the loadings at the legal limit. As per **Error! Reference source not found.**, single and tandem axle loads fall at about the 100^{th} and 98^{th} percentile compared to loading on a representative interstate pavement. The strain distribution limit proposed by Tran et al. (2015) was validated by Castro et al. (2017) using perpetual pavement sections recognized by the Asphalt Pavement Alliance. In the 2017 validation, legal axle load limits were utilized in PerRoad simulations, as they closely represent the truck traffic loads at the NCAT Test Track, and the traffic data for the perpetual pavement sections were unavailable. The NCAT Test Track axle load spectra and legal load limits do not represent the typical axle load spectrum on open access highways. Therefore, there is a need to evaluate the applicability of the field limiting tensile strain criteria developed from the NCAT Test Track's performance to open access highways such as interstate and state highways in Alabama.

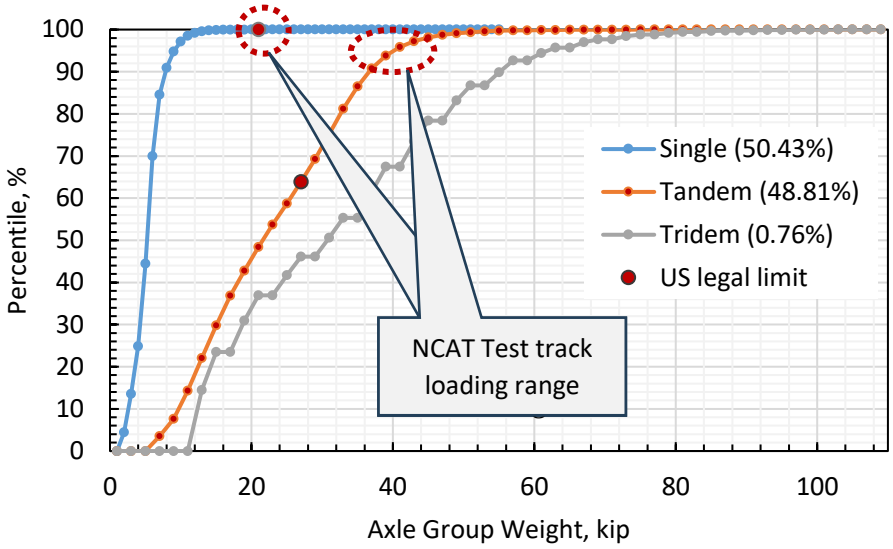

Figure 4.35 Default Axle Load Spectra of Rural Interstate developed by Timm and Newcomb (2010)

Validation of Formulated Methodology

Pavement Sections Used for Validation

ALDOT provided pavement thickness and performance data based on the cores extracted from a total of 33 pavement sections, including the original 13 sections from Task 2 and 20 new pavement sections. Performance information from 31 sections out of 33 pavement sections (excluding two pavement sections from Task 2 in Macon County) that included both interstate and state routes was used to examine the validity of existing limiting strain criteria for ALDOT's open access highways. ALDOT evaluated these pavement sections for resurfacing purposes between 2017 and 2022. Along with surface distress surveys, the evaluation included pavement thickness and crack depth determination using multiple cores from these sections. The average asphalt concrete (AC) layer thickness reported for the pavement sections ranged from 8.3 to 18.0 inches, as detailed in Table 4.34.

The crack depth information from the core log data was used to distinguish sections with structural bottom-up cracking from the sections that did not have any bottom-up cracking. A pavement section was categorized as bottom-up cracked for this study if one or more full-depth cracks were identified in the core log information of that particular pavement section. Figure 4.36 shows an example of core pictures taken from I-22W in Walker County and I-65N in Mobile County, Alabama. A total of 27 cores were taken from Section 1, and none showed a full-depth crack (cracks limited to the surface layers); therefore, this section is considered not bottom-up cracked. On the other hand, two cores from Section 2 showed full-depth cracks; thus, Section 2 was categorized as bottom-up cracked. Eight sections showed no bottom-up cracking, while 23 showed signs of bottom-up cracking (Table 4.34).

Table 4.34 also presents the original construction year of the 31 sections. Seven sections that did not show evidence of bottom-up cracking were constructed at least 38 years by the time cores were taken for inspection, making them good candidates for evaluating existing perpetual pavement design criteria. Even though Section 1 was constructed in 2006, the expectation is that it will not be prone to bottom-up cracking in the future as this section had a relatively thick AC layer of 18 inches. Therefore,

this section was considered a perpetual section with respect to bottom-up cracking. The service life of sections that showed evidence of bottom-up cracking ranged from 15 to 54 years by the time cores were taken for evaluation purposes.

(a) (b)

Figure 4.36 Core Pictures from ALDOT Material Reports with Two Core Examples from (a) Section 1 (Not Bottom-up Crack) and (b) Section 2 (Bottom-up Cracked)

Table 4.34 Selected Pavement Sections from Alabama

Section ID	Route	County	Milepost	Original Construction Year	Average Thickness, in.		Functional Classification	Bottom-Up Cracking
					AC	Agg. Base		
1	I-22 W	Walker	47.2 - 40.3	2006	18.0	6.0	Rural interstate	No
2	I-65 N	Mobile	0.0 - 8.3	1968	10.5	10.0	Urban interstate	Yes
3	I-65 S	Mobile	8.3 - 0.0	1968	10.4	10.0	Urban interstate	Yes
4	I-65 N	Conecuh	83.1 - 92.5	1969	13.0	10.0	Rural interstate	Yes
5	I-65 S	Conecuh	92.5 - 83.1	1969	13.0	10.0	Rural interstate	Yes
6	I-459 N	Jefferson	5.5 - 11.1	1984	8.4	6.0	Urban interstate	Yes
7	I-459 S	Jefferson	11.1 - 5.5	1984	8.3	6.0	Urban interstate	Yes
8	I-65 N	Chilton	198.0 - 205.3	1964	14.3	11.0	Rural interstate	No
9	I-65 S	Chilton	205.3 - 198.0	1964	13.8	12.0	Rural interstate	No
10	I-65 N	Chilton	211.4 - 216.5	1964	14.2	10.0	Rural interstate	No
11	I-65 S	Chilton	216.5 - 211.4	1964	14.4	10.0	Rural interstate	No
12	I-65 N	Lowndes	139.0 to 150.6	1969	8.8	9.5	Rural interstate	Yes
13	I-65 S	Lowndes	150.6 to 139.0	1969	9.3	9.5	Rural interstate	Yes
14	I-65 N	Butler	131.8 to 139.0	1969	9.6	9.5	Rural interstate	Yes
15	I-65 S	Butler	139.0 to 131.8	1969	9.6	9.5	Rural interstate	Yes
16	SR-2 W	Madison	125.0 to 108.6	1980	9.9	6.0	Rural principle arterial	Yes
17	SR-2 E	Jackson	132.0 to 138.1	1980	11.0	6.0	Rural principle arterial	Yes
18	SR-2 E	Jackson	129.0 to 135.0	1980	11.0	6.0	Rural principle arterial	Yes
19	SR-25 N	Etowah	212.9 to 219.4	1992	9.3	6.0	Urban principle arterial	Yes
20	SR-25 S	Etowah	219.0 to 212.9	1992	9.6	6.0	Urban principle arterial	Yes
21	SR-38 E	Tallapoosa	90.0 to 94.5	2003	9.5	6.0	Rural principle arterial	Yes
22	SR-38 W	Tallapoosa	94.5 to 90.0	2003	10.3	6.0	Rural principle arterial	Yes
23	SR-13 N	Franklin	295.9 to 299.9	<1970	9.0	6.0	Rural principle arterial	Yes
24	SR-13 S	Franklin	299.9 to 295.9	<1970	9.9	6.0	Rural principle arterial	Yes
25	SR-13 N	Clarke	78.2 to 81.9	1976	8.3	8.0	Rural principle arterial	Yes
26	SR-13 S	Clarke	81.9 to 78.2	1976	8.3	8.0	Rural principle arterial	Yes
27	SR-13 N	Washington	52.0 to 48.5	1990	9.9	8.0	Rural principle arterial	Yes
28	SR-13 S	Washington	48.5 to 52.0	1990	11.4	8.0	Rural principle arterial	Yes
29	SR-2 W	Jackson	138 to 132	1980	11.0	6.0	Rural principle arterial	No
30	SR-1 N	Marshall	280 to 287	<1970	13.0	6.0	Rural principle arterial	No
31	SR-1 S	Marshall	287 to 280	<1970	14.3	6.0	Rural principle arterial	No

PerRoad Inputs

PerRoad 4.4 was used to analyze and simulate strain response at the bottom of the AC layer of the 31 sections used for the validation. PerRoad 4.4 is a pavement design tool built on the concept of multilayered elastic analysis utilizing a stochastic approach through Monte Carlo simulation. The program considers layer elastic moduli, thickness, and traffic axle load distribution as inputs, along with the expected variability of moduli and thicknesses, respectively. The program utilizes Monte Carlo simulation to randomly generate structural and loading parameters within the expected variability range and solve for mechanistic responses in the pavement structure to estimate strain distributions at user-defined critical locations. The study's objective was to evaluate the limiting horizontal strain at the bottom of the AC layer and thus was selected as the analysis location within the pavement structure. 5,000 Monte Carlo cycles were used to compute the horizontal tensile strain at the bottom of the AC layer. Structural and traffic loading inputs used for PerRoad 4.4 simulation are described below.

Structural Inputs

The average layer thickness information of each pavement section provided in Table 4.34 was used to model the pavement structures in PerRoad 4.4. A coefficient of variance of 5% and 8% were used to account for the potential construction variability of layer thickness in the stochastic analysis. Based on the developed methodology from Task 2, the default AC layer moduli for PG 64-22 built into the software were used. PerRoad 4.4 uses seasonal average air temperatures to estimate seasonal AC layer moduli using mean seasonal pavement temperatures (MMPT) at the upper one-third depth of the AC layer, as shown in Equation 4.1. Equation 4.2 was used to determine MMPT from mean seasonal air temperature (MMAT) and AC layer thickness.

$$E_{HMA(PG\ 64-22)} = 7351157e^{-0.038MMPT} \quad (4.1)$$

$$MMPT = MMAT\left[1 + \frac{1}{z+4}\right] - \left[\frac{34}{z+4}\right] + 6 \quad (4.2)$$

Where:

z	= 1/3 of AC depth in pavement structure, in.
E_{HMA}	= AC layer modulus, psi
MMPT	= mean seasonal pavement temperature, F
MMAT	= mean seasonal air temperature, F

Modulus values of 25,000 and 8,000 psi for aggregate base and subgrade, respectively, were used as defined in the developed methodology. No seasonal changes to the granular layer modulus were considered. Coefficients of variance of 40% and 50% were used to represent potential variability of the unbound layer modulus values.

Climate Zones

In Task 2, temperature data from a single climate station in Montgomery, AL, was used to represent the whole state. However, the selected pavement sections for the study were spread across Alabama. Since temperature significantly affects the AC modulus and consequently tensile strain levels, it is important to understand the seasonal air temperatures across Alabama. Therefore, the historical mean air temperature data from each county of Alabama between the years 2010 and 2022 were analyzed from the MERRA database to examine the variations in seasonal air temperature (Rienecker et al., 2011). From the historical climate information, it was observed that the average annual hourly air temperature (AAHT) could be used to divide the state into three climatic regions (Figure 4.37) as follows:

- Zone-1: AAHT > 70°F (two counties)
- Zone-2: 66°F ≤ AAHT ≤ 70°F (36 counties)
- Zone-3: AAHT < 66°F (29 counties)

Figure 4.37 also shows the location of each of the pavement sections considered for the validation exercise.

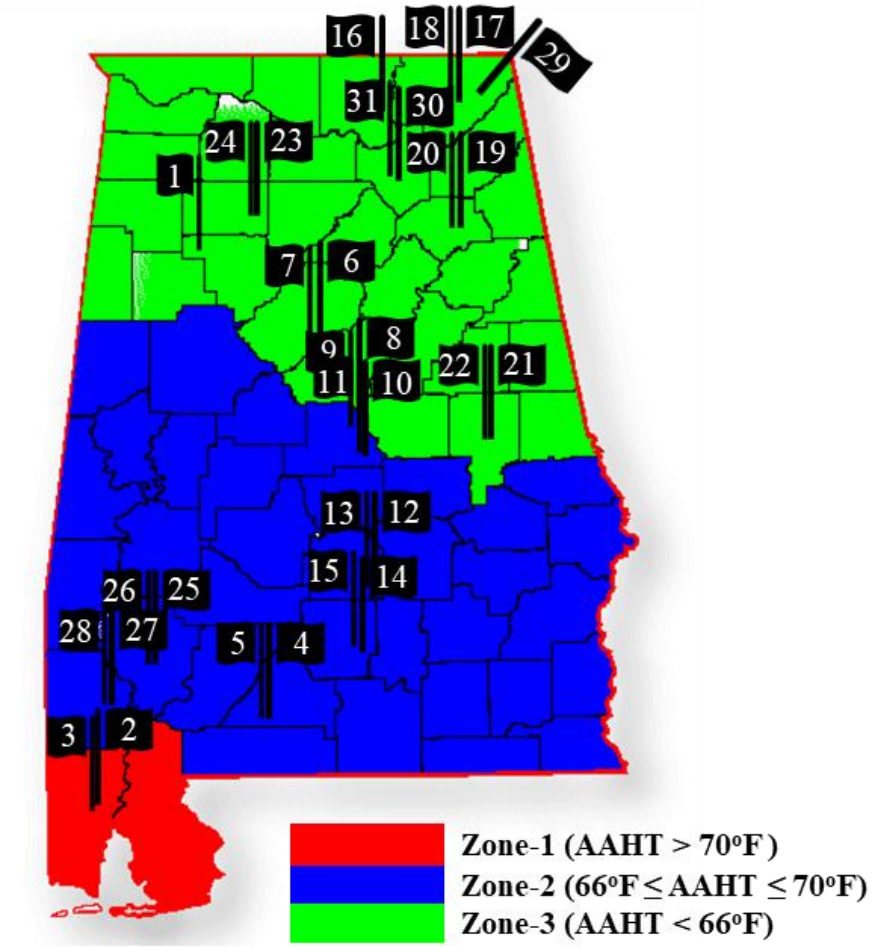

Figure 4.37 Three Climate Zones of Alabama and Positioning of Pavement Sections Considered in the Study

Quintile temperatures were extracted for all three climatic zones, as indicated in Figure 4.384 and Table 4.2, based on the historical temperature data points. Five quintile air temperatures were used for the PerRoad 4.4 analysis (shown in Table 4.35) to represent five mean seasonal air temperatures (MMAT) in each climatic zone in Equation 4.2. These temperatures, in turn, were used in Equation 4.1 to generate the five seasonal AC moduli in each climate zone, which is also listed in Table 4.2.

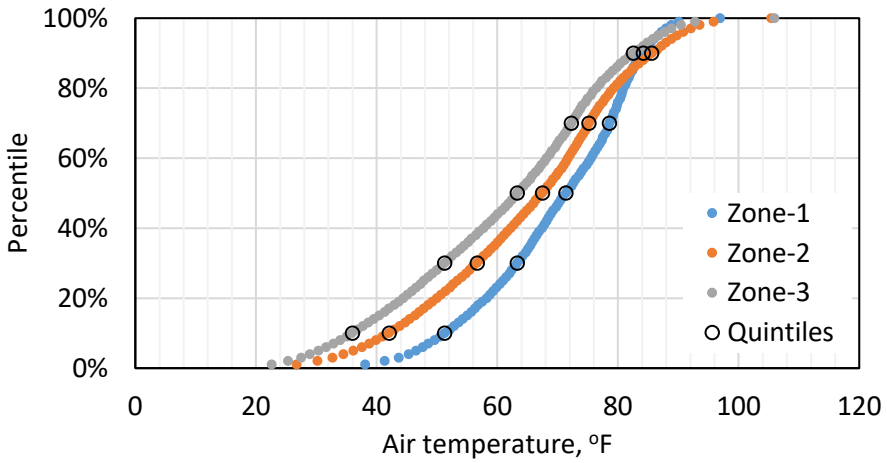

Figure 4.38 Historical Mean Air Temperature Distribution in Three Climatic Zones of Alabama

Table 4.35 Quintile Air Temperatures used for PerRoad Analysis to Represent Five Mean Seasonal Temperatures

Climatic Zone	Quintile				
	10%	30%	50%	70%	90%
	Air Temperatures, F				
Zone-1	51.3	63.3	71.4	78.6	84.2
Zone-2	42.1	56.7	67.5	75.2	85.6
Zone-3	36.0	51.3	63.3	72.3	82.6
	AC Moduli, ksi				
Zone-1	744,353	436,306	304,228	220,804	172,086
Zone-2	1,124,282	590,006	366,200	260,638	164,654
Zone-3	1,470,833	744,353	436,306	292,281	186,422

Traffic Inputs

Timm and Newcomb (2010) developed the national average vehicle class and axle load spectrum for various highway functional classes, which are currently utilized as the default load spectrum in PerRoad 4.4. ALDOT highway functional classification maps were used to determine the functional classification of sections considered for the study (ALDOT, 2023). Two types of axle load spectra were used for the validation study, as follows: (1) default axle load spectra built-in PerRoad 4.4 were used for each pavement section based on their functional classification (as shown in Table 4.34), named “highway axle load spectra” in the rest of the document and (2) Legal axle load limit represented by 100% single axles with 20 to 22-kip loading.

Validation with Field Performance

This section presents the results of the validation effort simulated with both highway axle load spectra and legal axle load limit.

Highway Axle Load Spectra

The 31 pavement sections were simulated using PerRoad 4.4, with input parameters as described in section 2.2 and the highway axle load spectra. The PerRoad results simulated using the highway axle load spectra were used to evaluate the applicability of the exiting limiting horizontal strain criteria in distinguishing sections that experienced bottom-up cracking from those that did not. As the main scope of the validation was on structural cracking, the vertical strain on top of the subgrade was not analyzed.

Sections 1 to 11 from Table 4.34 were analyzed for verification purposes. The predicted tensile strain values for each pavement section were used to generate cumulative strain distributions, as shown in Figure 4.39, along with the limiting strain criteria recommended by Tran et al. (2015). Notably, the predicted strain distributions using highway axle load spectra for the 11 ALDOT sections fell to the left of the previously recommended limiting strain criteria, suggesting that these sections would not experience bottom-up cracking according to the criteria. However, six out of the 11 sections showed bottom-up cracks based on the core log information. This discrepancy could be because the NCAT Test Track truck load spectra used to develop the existing limiting strain criteria were much more severe than the typical axle load spectra on an interstate system. As a result, it was relatively easier (i.e., less thickness needed) to meet the criteria with more moderate load levels. The results from Figure 4.39 indicate that the existing limiting strain criteria proposed by Tran et al. (2015) are unsuitable for designing perpetual pavements using the highway axle load spectra (axle load spectra of an interstate system); doing so would yield much lower pavement thicknesses than needed, resulting maximum thicknesses that are too thin.

Based on the information from Figure 4.39, new limiting strain criteria were recommended for designing perpetual pavements that carry interstate and state route axle load spectra (simulated with highway axle load spectra). The coring information from sections 2 to 7 showed bottom-up cracks in these sections. However, for sections 4 and 5, ALDOT obtained only two cores in each section, and the AC core thicknesses varied from 6 to 16 inches, with an average of 13 inches of AC layer in each direction. Due to the limited number of cores and the 10-inch thickness difference, the data were deemed unreliable, so these two sections were excluded from the remainder of the study. The strain distribution from Section 2 had the lowest strain levels among the sections with bottom-up cracks. Therefore, this section was used to establish the new “Updated Threshold,” as shown in Figure 4.5, following a similar approach as Tran et al. (2015) and listed in

Table **4.36**.

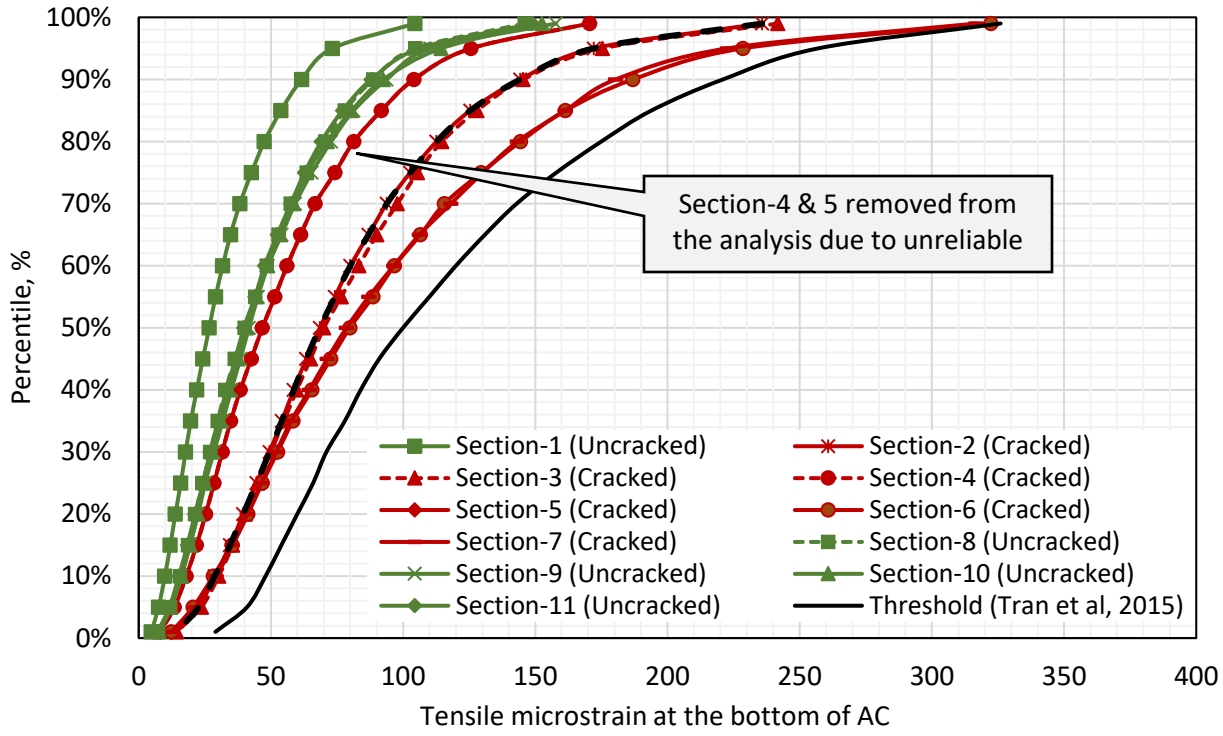

Figure 4.39 Predicted Horizontal Tensile Strain Distributions Simulated with Highway Axle Load Spectra at the Bottom of the AC layer (Sections 1 through 11)

Table 4.36 Existing and Proposed Tensile Strain Distribution Criteria at the Bottom of AC for Perpetual Pavement Design

Percentile of Strain Distribution, %	Tensile microstrain limit proposed by Tran et al. (2)	Proposed Tensile Microstrain Limit from Figure 4.5
1%	29	14
5%	41	23
10%	48	29
15%	54	35
20%	60	40
25%	66	45
30%	71	50
35%	78	54
40%	84	59
45%	91	63
50%	100	69
55%	110	74
60%	120	80
65%	131	87
70%	143	94
75%	158	103
80%	175	113
85%	194	125
90%	221	144
95%	257	172
99%	326	236

Validation of Refined Design Thresholds

Since the proposed limiting strain criteria for interstate loading were based on a limited number of pavement sections, they were validated using predicted horizontal strain distributions and field core information from Sections 12 through 31 in Table 4.34. The following discussions and graphs are divided into two groups to ease the discernment of the data in the plots.

Figure 4.40 shows the expected tensile strain distributions at the bottom of the AC layer of sections 12 to 21. Notably, all the pavement sections from 12 to 21 showed bottom-up cracks based on the core log information. Tensile strain distributions of most sections exceed the proposed limiting strain criteria except for sections 17 and 18. Although sections 17 and 18 showed signs of bottom-up cracking based on the field core information, the proposed limiting strain criteria still categorized these sections as perpetual pavements since their tensile strain distributions fell to the left of the proposed limiting strain criteria. Therefore, the proposed limiting strain failed to effectively categorize the bottom-up cracking performance of sections 17 and 18. However, it was successful in categorizing the performance of 8 out of the 10 sections.

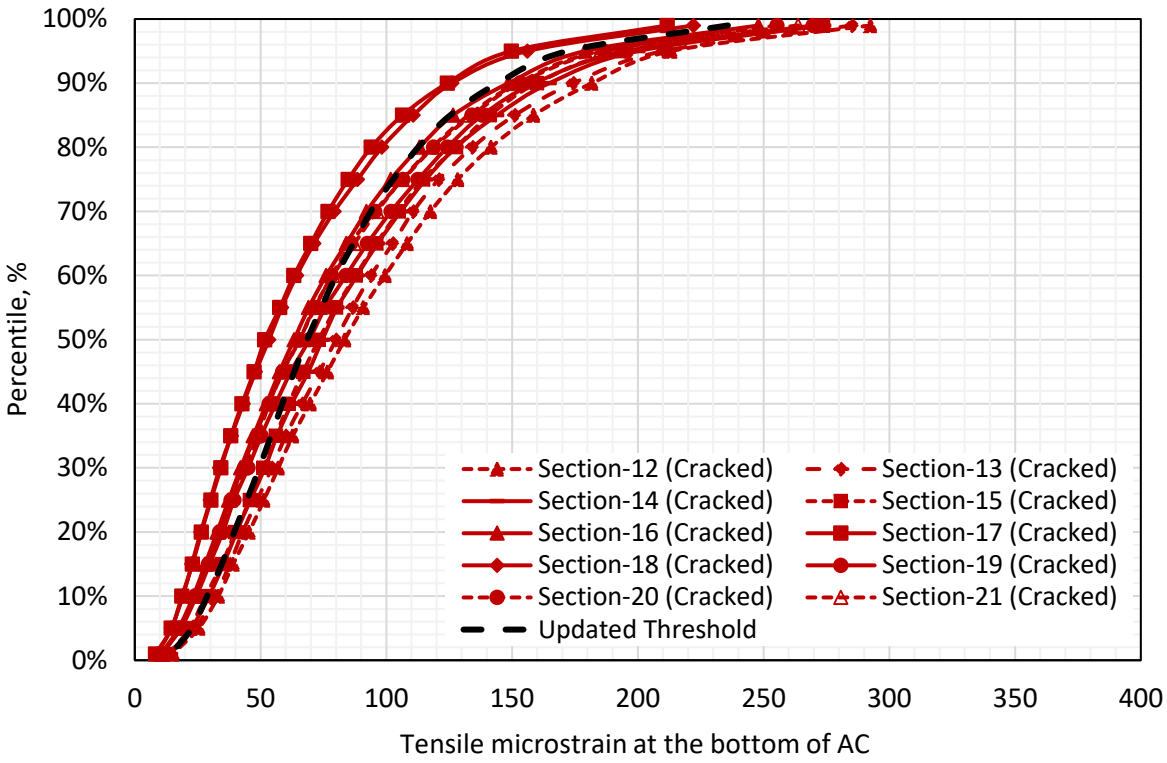

Figure 4.40 Predicted Horizontal Tensile Strain Distributions Simulated with Highway Axle Load Spectra at the Bottom of the AC Layer (Sections 12 through 21)

Figure 4.41 shows the predicted strain distributions of sections 22 to 31. All pavement sections from 22 to 31, except for sections 29, 30, and 31, showed signs of bottom-up cracking based on the field core information. Tensile strain distributions from all the cracked sections exceed the proposed limiting strain criteria except for Section 28. The tensile strain distribution of Section 28 satisfied the proposed limiting strain criteria, categorizing Section 28 as a perpetual pavement. However, field cores from Section 28 showed full-depth cracking. Sections 29, 30, and 31 showed no signs of bottom-up cracking from the field cores, and the simulated strain distributions of these sections were lower than the proposed limiting strain criteria. Therefore, the proposed limiting strain criteria effectively categorized sections with no signs of bottom-up cracking.

In summary, the proposed limiting strain criteria effectively distinguished pavement sections that experienced cracking from those that did not, with only three out of 20 pavement sections not conforming to the criteria. Reasons for these three sections not conforming to the criteria could include inaccurate load spectra or material properties. The reason could be the use of generic, non-site-specific values in the PerRoad simulations. It is possible that using data specific to particular sections would improve the predictive capability of the strain distribution.

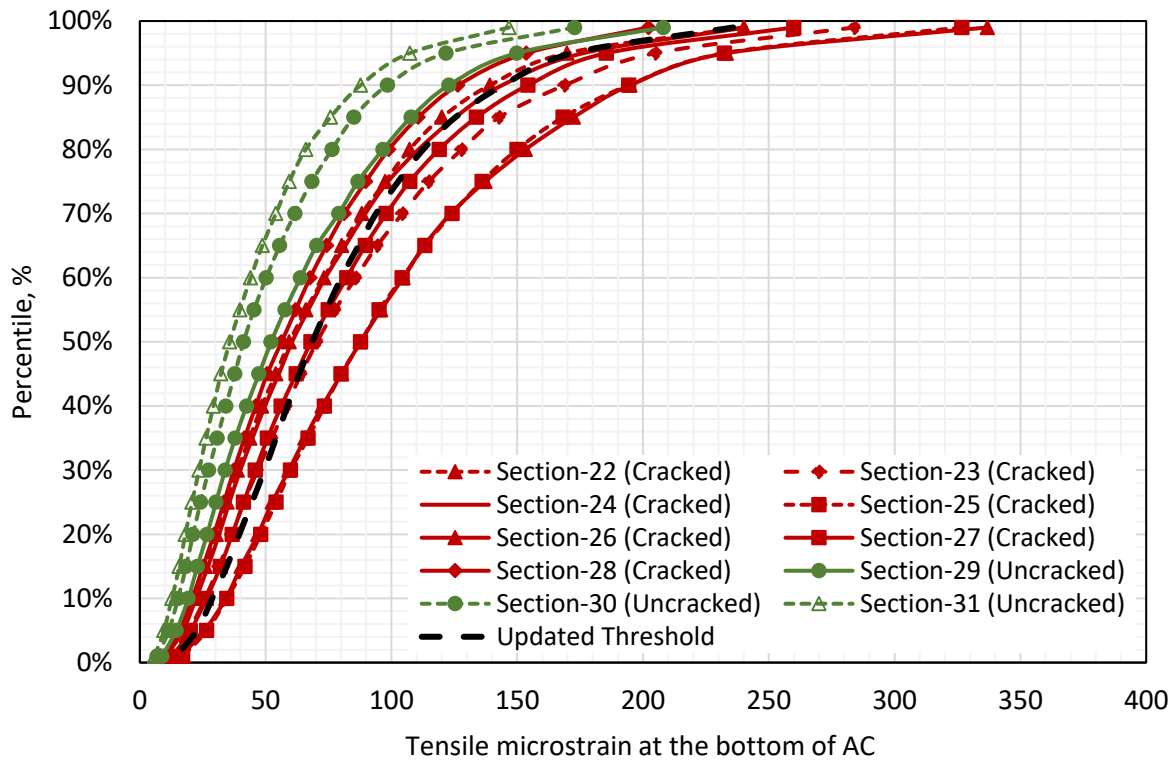

Figure 4.41 Predicted Horizontal Tensile Strain Distributions Simulated with Highway Axle Load Spectra at the Bottom of the AC layer (Sections 22 through 31)

Legal Axle Load Limit

The 31 pavement sections were simulated using PerRoad 4.4 using input parameters as described in section 2.2 and the legal axle load limit. This PerRoad simulation aimed to evaluate the applicability of the existing limiting horizontal strain criteria, which were developed based on legal axle load limits, in distinguishing sections that experienced bottom-up cracking from those that did not crack. All the pavement sections from Table 4.34 were analyzed for verification purposes. The following graphs and discussion are divided into two groups to ease the discernment of the data in the plots.

The predicted tensile strain values for each pavement section were used to generate cumulative strain distributions, as shown in Figure 4.42, along with the limiting strain criteria recommended by Tran et al. (2015). Sections 2 through 7 showed bottom-up cracks in these sections, based on the coring information. Due to reasons mentioned earlier in section 2.3.1, sections 4 and 5 were excluded from the analysis. The predicted strain distributions using legal axle load limit for pavement sections 2, 3, 6, and 7 fell to the right side of the previously recommended limiting strain criteria. Based on coring information, pavement sections 1, 8, 9, 10, and 11 showed no evidence of bottom-up cracking. The predicted tensile strain distribution of these sections simulated using the legal axle load limit fell to the left of the previously recommended limiting strain criteria. Thus, based on Figure 4.42, the existing limiting strain criteria by Tran et al. (2015) was able to distinguish pavement sections that showed evidence of bottom-up cracking when simulated using the legal axle load limit.

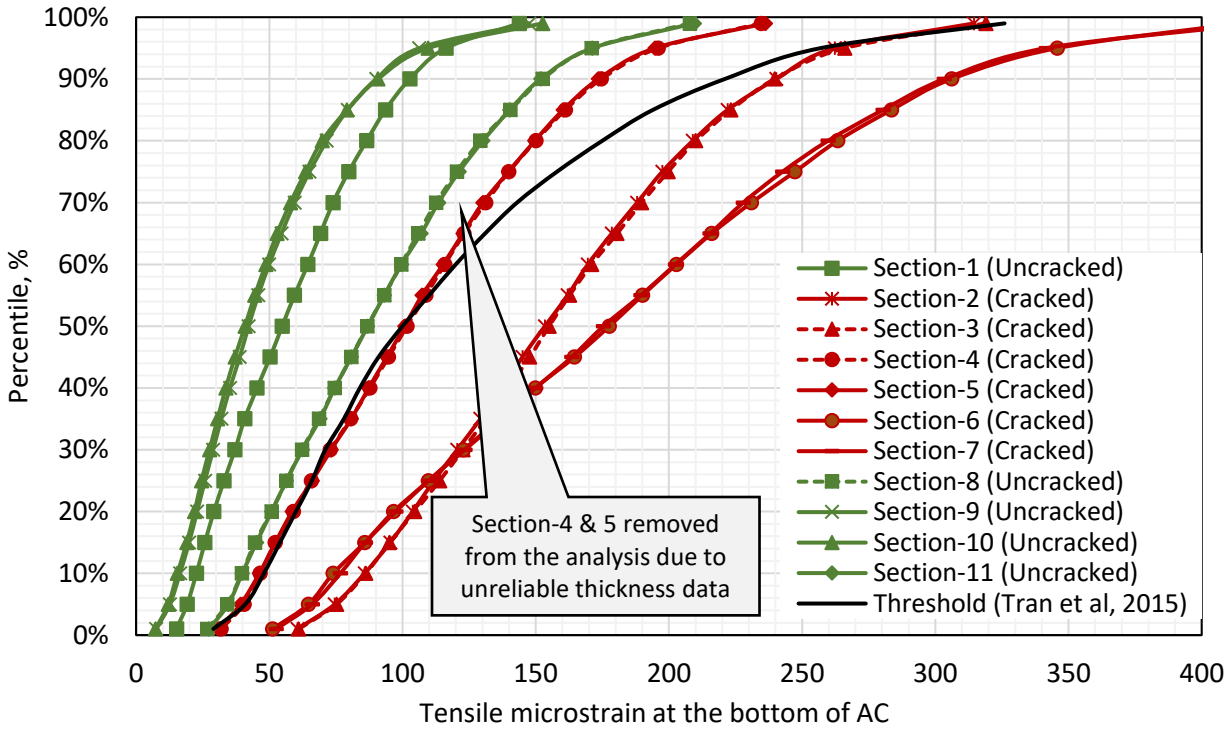

Figure 4.42 Predicted Horizontal Tensile Strain Distributions Simulated with Legal Axle Load Limit at the Bottom of the AC layer (Sections 1 through 11)

Figure 4.43 shows the expected tensile strain distributions at the bottom of the AC layer of sections 12 to 21 simulated using the legal axle load limit. Notably, all the pavement sections from 12 to 21 showed bottom-up cracks based on the core log information (Table 4.34). The tensile strain distributions of all the sections shown in Figure 4.43 exceeded the proposed limiting strain criteria. Thus, the existing limiting strain criteria by Tran et al. (2015) were able to distinguish sections that showed evidence of bottom-up cracking from sections that did not when simulated using the legal axle load limit.

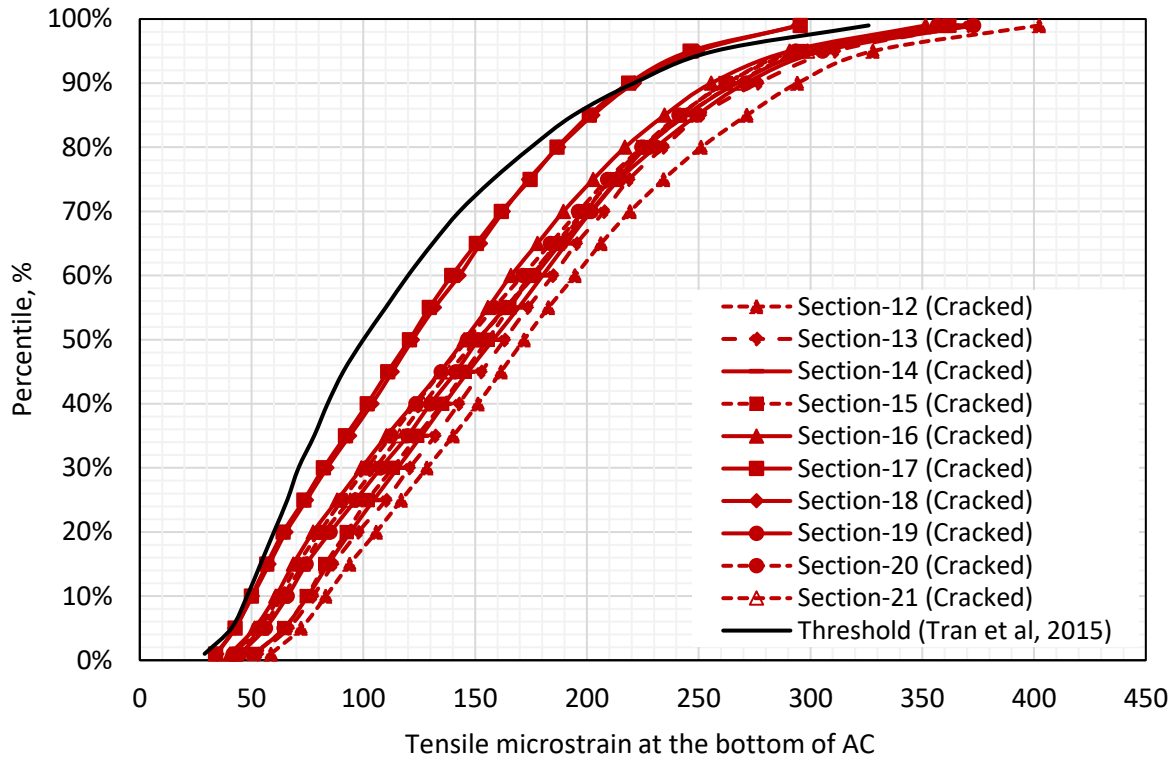

Figure 4.43 Predicted Horizontal Tensile Strain Distributions Simulated with Legal Axle Load Limit at the Bottom of the AC Layer (Sections 12 through 21)

Figure 4.44 presents the expected tensile strain distributions at the bottom of the AC layer of sections 22 to 31 simulated using the legal axle load limit. Notably, all the pavement sections from 22 to 28 showed bottom-up cracks based on the core log information (Table 4.34). Tensile strain distributions of sections 22 to 28 exceed the proposed limiting strain criteria. Section 22 exceeds the existing limiting strain between the 30th and 70th percentiles. Sections 29, 30, and 31 showed no evidence of bottom-up cracking from the coring information. The predicted tensile strain distributions fell to the left side of the criteria by Tran et al. (2015). However, the predicted tensile strain distribution of section 29 exceeds the limiting strain criteria between percentiles 1 and 90. Based on information from Figure 4.42 through Figure 4.44, it can be concluded that existing limiting strain criteria by Tran et al. (2015) was able to distinguish sections that showed evidence of bottom-up cracking from sections that did not when simulated using the legal axle load limit.

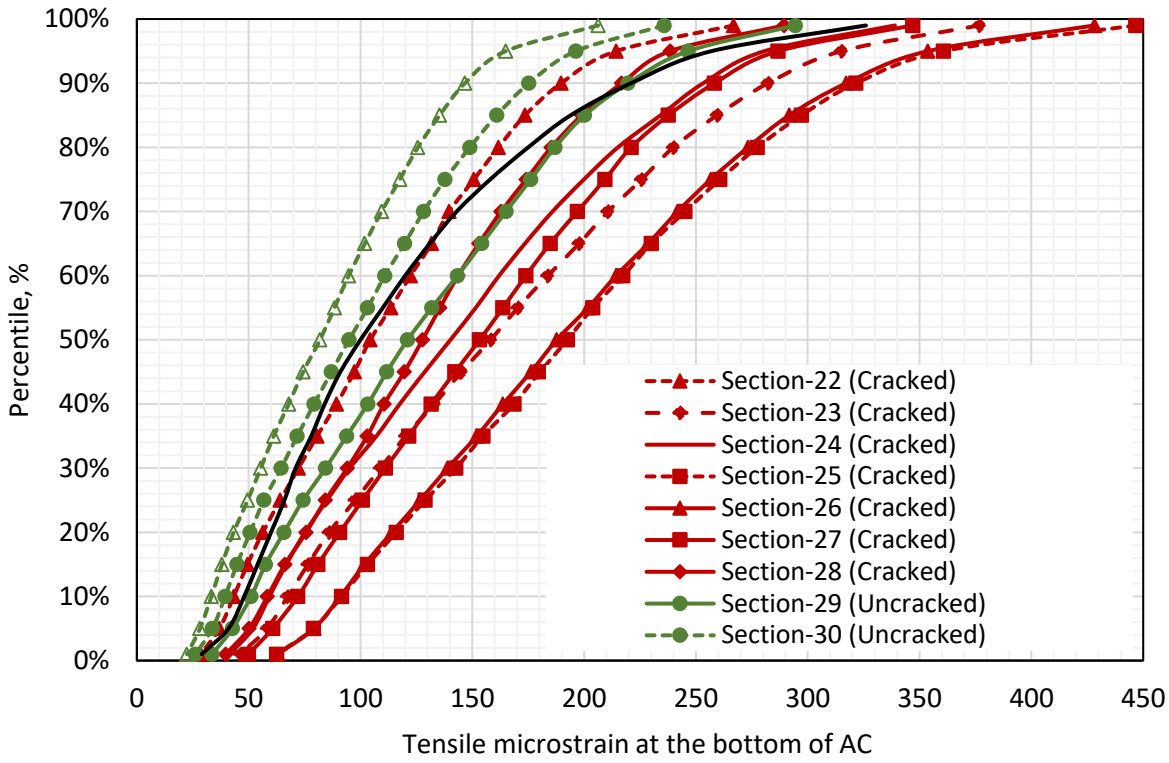

Figure 4.44 Predicted Horizontal Tensile Strain Distributions Simulated with Legal Axle Load Limit at the Bottom of the AC Layer (Sections 22 through 31)

In summary, the following revisions were made to the methodology (developed in Task-2) based on analysis from Task-3:

- From the historical climate information, it was observed that the average annual hourly air temperature (AHAT) could be used to divide the state of Alabama into three climatic zones, as shown in Figure 4.37.
- The results indicate that the existing limiting tensile strain criteria by Tran et al. (2015) are unsuitable for designing perpetual pavements using the highway axle load spectra (Timm and Newcomb, 2010). Using highway axle load spectra along with strain criteria recommended by Tran et al. (2015) will lead to maximum thicknesses that are too thin. Based on these strain distributions, updated limiting strain criteria were proposed and validated for use with highway axle load spectra.
- The results indicate that the existing limiting tensile strain criteria proposed by Tran et al. (2015) remain applicable for determining maximum pavement thickness when using the legal axle load limit to design interstate and state route perpetual pavements.

Design AC Thickness

The revisions to the perpetual pavement design methodology discussed above were used to develop a maximum pavement design thickness catalog for a range of scenarios using the PerRoad 4.4 tool. The following design considerations were made:

- *Load spectra:* Both highway axle load spectra (default rural interstate load spectra built-in PerRoad 4.4) and the legal axle load limit were used for the simulation.
- *Design criteria:* The proposed limiting strain criteria at the bottom of the AC layer were used to control bottom-up fatigue cracking when highway axle load spectra were used. The existing limiting strain criteria by Tran et al. (2015) were used to control bottom-up fatigue cracking when highway axle load spectra were used. The existing design criteria for structural rutting (Tran et al., 2015) were not validated as part of this study, as performance data related to structural rutting was not available from the pavement sections considered. Therefore, only bottom-up fatigue cracking was considered as the mode of failure for the design and used to determine maximum pavement thickness.
- *Climate:* Three climatic zones identified, as shown in Figure 4.37, were used for the design, and quintile air temperature data shown in Figure 4.38 were used to represent average seasonal air temperatures in each climatic zone.
- *Structural inputs:* The pavement structure was designed as a three-layer structure with an AC layer over a granular base over a subgrade.
    - The AC layer moduli, as described in section 2.2.1, were used for PG 64-22 based on the seasonal air temperatures in each of the three climatic zones of Alabama (Figure 4.37). The AC layer thickness for each design was iterated until a minimum thickness that satisfied the limiting strain criteria at the bottom of the AC was achieved. A coefficient of variance of 5% and 30% were used to account for the potential variability of AC layer thickness and moduli in the PerRoad 4.4 simulations.
    - Three base layer thicknesses of 6, 8, and 10 inches were selected for the design. Two base layer moduli of 25 and 50 ksi were selected for the design to represent the modulus of granular aggregate base materials. West et al. (2020) backcalculated base layer moduli of 15 Long-Term Pavement Performance (LTPP) pavement sections with rubblized base and reported a modulus value of 100 ksi as the 50th percentile in the distribution. Therefore, a modulus of 100 ksi was selected for the modulus of rubblized base material in an overlay design scenario. A coefficient of variance of 8% and 40% were used to account for the potential variability of base layer thickness and moduli in the PerRoad 4.4 simulations.
    - Three subgrade moduli of 5, 8, and 15 ksi were selected for the investigation. A coefficient of variance of 50% was used to account for the potential variability of subgrade moduli in the PerRoad 4.4 simulations.

Design AC Thicknesses with Highway Axle Load Spectra

Table 4.37 and Table 4.38 present the maximum pavement design thicknesses of the AC layer for different structural inputs and climatic zones considered using highway axle load spectra. This was done

to the nearest 0.5 inches, rounded up. As shown in Table 4.37, the design AC thickness ranged from 8.5 to 13.0 inches depending on moduli, thickness of granular base, subgrade moduli, and climatic zone. A thicker, stiffer granular base and stiffer subgrade resulted in thinner design AC thicknesses, as expected. The climatic zone used for simulation also had a significant impact on the design AC thickness; moving from South to North (Zone-1 to Zone-3) resulted in a reduction in design thickness of 1.0 inches in a majority of scenarios.

As shown in Table 4.38, the design AC thickness for the rubblized bases ranged from 6.0 to 8.0 inches depending on the thickness of the rubblized base, subgrade moduli, and climatic zone. The climatic zone used for simulation had a significant impact on the design AC thickness; moving from South to North (Zone-1 to Zone-3) resulted in a reduction in design thickness of 1.0 inches for thinner rubblized bases and 0.5 inches for the thicker rubblized bases.

Table 4.37 Design AC Thicknesses with Different Structural and Climatic Inputs for Granular Aggregate Bases (simulated with highway axle load spectra)

Granular base moduli (E_2), ksi	Subgrade moduli (E_3), ksi	Granular base thickness								
		6.0 inch.			8.0 inch.			10.0 inch.		
		Zone-1	*Zone-2*	*Zone-3*	*Zone-1*	*Zone-2*	*Zone-3*	*Zone-1*	*Zone-2*	*Zone-3*
25	5	13.0	12.5	12.0	12.5	12.0	11.5	12.5	11.5	11.0
	8	12.0	11.5	11.0	11.5	11.5	11.0	11.5	11.0	11.0
	15	11.5	11.0	10.5	11.5	11.0	10.5	11.0	10.5	10.5
50	5	11.5	10.5	10.0	10.5	10.0	9.5	10.0	9.5	9.0
	8	10.5	10.0	9.5	10.0	9.5	9.0	10.0	9.0	9.0
	15	10.0	9.5	9.0	9.5	9.0	8.5	9.5	9.0	8.5

Table 4.38 Design AC Thicknesses with Different Structural and Climatic Inputs for Rubblized Bases (simulated with highway axle load spectra)

Rubblized base moduli (E_2), ksi	Subgrade moduli (E_3), ksi	Rubbilized base thickness								
		6.0 inch.			8.0 inch.			10.0 inch.		
		Zone-1	*Zone-2*	*Zone-3*	*Zone-1*	*Zone-2*	*Zone-3*	*Zone-1*	*Zone-2*	*Zone-3*
100	5	8.0	7.5	7.0	7.5	7.0	6.5	7.0	7.0	6.5
	8	7.5	7.0	7.0	7.0	6.5	6.5	7.0	6.5	6.0
	15	7.5	7.0	6.5	7.0	6.5	6.0	6.5	6.5	6.0

Design AC Thicknesses with Legal Axle Load Limit

Table 4.39 and

Table **4.40** present the maximum pavement design thicknesses of the AC layer for different structural inputs and climatic zones considered using the legal axle load limit. This was done to the nearest 0.5 inches, rounded up. As shown in Table 4.39, the design AC thickness ranged from 9.5 to 15.5 inches depending on moduli, thickness of granular base, subgrade moduli, and climatic zone. Like the tables presented above, a thicker, stiffer granular base and stronger subgrade resulted in thinner design AC

thicknesses, as expected. The climatic zone used for simulation also had a significant impact on the design AC thickness; moving from South to North (Zone-1 to Zone-3) resulted in a reduction in design thickness of 1.5 to 2.0 inches.

As shown in

Table **4.40**, the design AC thickness for the rubblized bases ranged from 6.5 to 10.0 inches depending on the thickness of the rubblized base, subgrade moduli, and climatic zone. The climatic zone used for simulation had a significant impact on the design AC thickness; moving from South to North (Zone-1 to Zone-3) resulted in a reduction in design thickness of 1.0 inches.

Table 4.39 Design AC Thicknesses with Different Structural and Climatic Inputs for Granular Aggregate Bases (simulated with legal axle load limit)

Granular base moduli (E_2), ksi	Subgrade moduli (E_3), ksi	Granular base thickness								
		6.0 inch.			8.0 inch.			10.0 inch.		
		Zone-1	*Zone-2*	*Zone-3*	*Zone-1*	*Zone-2*	*Zone-3*	*Zone-1*	*Zone-2*	*Zone-3*
25	**5**	15.5	14.5	13.5	15.0	14.0	13.0	14.5	13.5	12.5
	8	14.5	13.5	12.5	14.5	13.5	12.5	14.0	13.0	12.0
	15	13.5	13.0	11.5	13.5	12.5	11.5	13.5	12.5	11.5
50	**5**	14.0	13.0	12.0	13.0	12.0	11.5	12.5	11.5	11.0
	8	13.0	12.0	11.5	12.0	11.5	11.0	12.0	11.0	10.0
	15	12.0	11.0	10.5	11.5	11.0	10.0	11.0	10.5	9.5

Table 4.40 Design AC Thicknesses with Different Structural and Climatic Inputs for Rubblized Bases (simulated with legal axle load limit)

Rubblized base moduli (E_2), ksi	Subgrade moduli (E_3), ksi	Rubblized base thickness								
		6.0 inch.			8.0 inch.			10.0 inch.		
		Zone-1	*Zone-2*	*Zone-3*	*Zone-1*	*Zone-2*	*Zone-3*	*Zone-1*	*Zone-2*	*Zone-3*
100	**5**	10.0	9.5	9.0	8.5	8.0	7.5	7.5	7.5	7.0
	8	9.5	9.0	8.5	8.5	8.0	7.5	7.5	7.0	6.5
	15	8.5	8.0	7.5	8.0	7.5	7.0	7.5	7.0	6.5

Note that the results presented from the two sets of analyses (i.e., using legal load limits and highway axle load spectra) resulted in similar trends but slightly different magnitudes of maximum thickness. The legal load limit analysis yielded maximum asphalt concrete thicknesses that were, on average, 1.9 inches thicker for the granular base sections and 1.1 inches thicker for the rubblized pavement sections. It was also observed that the differences became smaller when moving from Zone 1 to Zone 2 to Zone 3. The average difference for aggregate base sections in Zone 1 was 2.28 inches, 1.94 inches in Zone 2, and 1.47 inches in Zone 3, respectively. A similar trend was found for the rubblized sections, with Zone 1 at 1.2 inches difference, Zone 2 at 1.1 inches, and Zone 3 at a 1-inch difference, on average. It appears that the legal load limit approach will provide more conservative designs than the

load spectra approach, with the difference diminishing with relatively cooler temperatures and thinner maximum thicknesses.

Bottom-up fatigue cracking was considered the only design mode of failure for the perpetual pavement design discussed above, as the existing design criteria for structural rutting (Tran et al., 2015) were not validated as part of this study. However, in theory, both bottom-up fatigue cracking and structural rutting should be considered as the design mode of failure for the perpetual pavement design. The perpetual pavement design was repeated to control both bottom-up fatigue and structural rutting for the structural inputs and climate zones, as discussed above, with both highway axle load spectra and the legal axle load limit. The results are presented in the Appendix B. The design AC thicknesses using both bottom-up fatigue cracking and structural rutting as design mode failure resulted in unrealistically high AC thicknesses when axle load limits were used for the simulation, both for granular and rubblized bases. Therefore, it is recommended that the existing design criteria for structural rutting (Tran et al., 2015) be validated using field performance data.

Recommended Maximum AC Thickness

As noted above, the two analyses (i.e., legal load limit versus highway load spectra) produced two slightly different sets of maximum asphalt concrete thicknesses. It is recommended to implement the legal load limit approach for the following reasons:

- The legal load limit approach, as documented in Section 2.3.2, was better able to distinguish between sections that did and did not experience bottom-up fatigue cracking.
- The legal load limit approach was not changed from what had been previously documented and recommended by Tran et al. (2015), so the criteria for ALDOT would be consistent with the previous investigation.
- The legal load limit approach provides slightly more conservative maximum asphalt concrete thicknesses compared to the load spectra approach and is well supported by NCAT Test Track sections and ALDOT segments.

One potential deficiency of the legal axle load limit approach is that it does not distinguish between roads having different load spectra since the legal load limit would apply to almost all routes in Alabama. Lower-volume roads, with significantly fewer heavy vehicles, would be designed for maximum thickness with the same criteria, resulting in the same maximum pavement thickness as a high-volume route. Future investigations may need to focus on lower-volume roads to address this deficiency.

Further consideration must be given to the rubblized base sections (Tables 4.5 and 4.7) since these were almost entirely theoretical with only four ALDOT sections used as part of the methodology development and validation. Since some conditions in these tables could lead to excessively thin pavement thicknesses, and are not supported by robust ALDOT field data, it is recommended to only utilize the worst case scenario. Since the load spectra approach is not recommended from this study, that leaves 10 inches of AC over a rubblized base as the worst case situation from Table 4.7.

Summary and Conclusions

The objective of this task was to validate and make necessary revisions to the methodology developed as part of Task 2 of the study. The historical mean air temperature data from each county of Alabama between 2010 and 2022 were analyzed from the MERRA database to assess the variations in seasonal

air temperature. A total of 31 sections from Alabama with known structural and cracking information were considered for this study. The pavement sections were simulated in PerRoad 4.4 to determine the horizontal tensile strain distributions at the bottom of the AC layer. The simulated strain distributions of the 31 pavements were used to evaluate the limiting strain criteria previously proposed by Tran et al. (2015). Based on the results of the study, the following conclusions and recommendations are made:

- From the historical climate information, it was observed that the average annual hourly air temperature (AHAT) could be used to divide the state of Alabama into three climatic zones, as shown in Figure 4.37.
- Eleven pavements were used to evaluate the applicability of the existing limiting strain criteria, simulated with the highway axle load spectra. Even though six of these sections showed bottom-up cracking, as observed from coring, the simulated tensile strain distributions from all 11 pavements were much lower than the existing limiting strain criteria. The results indicate that the existing limiting strain criteria are unsuitable for designing perpetual pavements using the highway axle load spectra. Using these distributions with the existing criteria will lead to maximum thicknesses that are too thin when the highway axle load spectra are used to represent the traffic loading. Based on these strain distributions, updated limiting strain criteria were proposed for use with the highway axle load spectra (as shown in
-
-

- **Table 4.36**). The updated limiting strain distribution was validated using an additional twenty pavement sections. The proposed criteria could properly distinguish 17 of the 20 cracked pavement sections.
- The results of the 31 pavement sections simulated with the legal axle load limit to represent traffic loading indicate that the existing limiting tensile strain criteria by Tran et al. (2015) remain applicable for designing perpetual pavements using the legal axle load limit for the design of interstate and state route perpetual pavements. The existing limiting tensile strain criteria by Tran et al. (2015) were able to distinguish sections that showed evidence of bottom-up cracking

from sections that did not when simulated using the legal axle load limit for 30 of the 31 pavement sections considered.

- It is recommended that ALDOT use the legal load limit approach to determine maximum asphalt concrete thicknesses. The sensitivity analysis conducted for pavements with aggregate bases resulted in maximum thicknesses ranging from 9.5 to 15.5 inches over a range of support and climate conditions. The same approach, when considering asphalt concrete over rubblized base, resulted in some excessively thin asphalt layers not fully supported by ALDOT field data. Therefore, it was recommended to use the worst case condition resulting in a maximum AC thickness of 10 inches over a rubblized concrete pavement.
- The legal load limit approach can be applied to all roadways and provides conservative asphalt concrete maximum thicknesses. Further study is recommended for lower volume roads on the state network to develop criteria more applicable to these routes.

CHAPTER 5
SUMMARY, CONCLUSIONS & RECOMMENDATIONS

The primary objective of this project was to develop a methodology for ALDOT to determine maximum AC thicknesses and make recommendations for maximum AC thickness over a range of design conditions. This report documented a literature review that investigated methods of maximum thickness, the development of a maximum thickness methodology for ALDOT, followed by validation of the developed method. Based on the information presented in previous chapters, the following conclusions and recommendations are made:

- Perpetual pavement concepts provide the means for states to develop and implement reasonable maximum AC thicknesses for flexible pavements.
- Limiting strain criteria have been documented in the engineering literature to facilitate maximum thickness computation.
- ALDOT default moduli for base and subgrade layers, in combination with default asphalt temperature-modulus relationships in PerRoad (version 4.4), provided reasonable maximum pavement thicknesses for the ALDOT sections evaluated. These thicknesses ranged from 8.5 to 10 inches.
- Two methods of characterizing traffic loadings were evaluated in the study: highway load spectra and legal load limit. It was found that pavements should be designed with loading characterization that is reasonably consistent with how the criteria were developed. Failure to do so could result in under- or over-designed maximum thicknesses.
    - The legal load limit approach was better able to distinguish between sections that did and did not experience bottom-up fatigue cracking and is therefore recommended for determining maximum pavement thicknesses.
    - The legal load limit approach provides slightly more conservative maximum asphalt concrete thicknesses than the load spectra approach and is well supported by NCAT Test Track sections and ALDOT segments.
    - One potential deficiency of the legal axle load limit approach is that it does not distinguish between roads having different load spectra since the legal load limit would apply to almost all routes in Alabama. Lower-volume roads, with significantly fewer heavy vehicles, would be designed for maximum thickness with the same criteria, resulting in the same maximum pavement thickness as a high-volume route. Future investigations may need to focus on lower-volume roads to address this deficiency.
- It was found that Alabama can be divided into three climate zones, from north to south, based on average annual hourly air temperature (Figure 4.3) to determine maximum pavement thicknesses over a range of base and subgrade support conditions.
- The recommended maximum AC thicknesses for granular base pavements, using the legal axle load limit approach, in the aforementioned climate zones are shown in Table 5.1.
- The recommended maximum AC thicknesses for rubblized base pavements was 10 inches, representing a worst-case condition.

Table 5.1 Recommended Maximum AC Thicknesses Using Legal Axle Load Approach – Granular Base

Granular base moduli (E_2), ksi	Subgrade moduli (E_3), ksi	Granular base thickness								
		6.0 inch.			8.0 inch.			10.0 inch.		
		Zone-1	*Zone-2*	*Zone-3*	*Zone-1*	*Zone-2*	*Zone-3*	*Zone-1*	*Zone-2*	*Zone-3*
25	**5**	15.5	14.5	13.5	15.0	14.0	13.0	14.5	13.5	12.5
	8	14.5	13.5	12.5	14.5	13.5	12.5	14.0	13.0	12.0
	15	13.5	13.0	11.5	13.5	12.5	11.5	13.5	12.5	11.5
50	**5**	14.0	13.0	12.0	13.0	12.0	11.5	12.5	11.5	11.0
	8	13.0	12.0	11.5	12.0	11.5	11.0	12.0	11.0	10.0
	15	12.0	11.0	10.5	11.5	11.0	10.0	11.0	10.5	9.5

REFERENCES

- Alabama Department of Transportation. (2023). www.dot.state.al.us/maps/HFCMaps.html. Accessed Jul. 26, 2023.
- AASHTO. (1993). *AASHTO Guide for Design of Pavement Structures*. American Association of State and Highway Transportation Officials, Washington D.C.
- AASHTO. (2008). *Mechanistic-Empirical Pavement Design Guide, Interim Edition: A Manual of Practice*. American Association of State and Highway Transportation Officials, Washington, D.C.
- Asphalt Pavement Alliance. (2019). *Perpetual Pavement Award Winners*. http://www.asphaltroads.org/perpetual-pavement/award-winners/, accessed 2019.
- Castro, A., Tran, N., Robbins, M., Timm, D., and Wagner, C. (2017). Further Evaluation of Limiting Strain Criteria for Perpetual Pavement Design. *Transportation Research Record: Journal of the Transportation Research Board*, No. 2640, 41-48.
- Castro, A., Tran, N., Gu, F., Timm, D., and Wagner, C. (2018). Limiting Strain Distribution Criteria for Perpetual Pavement Design Using AASHTOWare Pavement ME Design. *Asphalt Paving Technology*, Volume 87.
- Colorado Department of Transportation. (2021). *M-E Pavement Design Manual*. Accessed at https://www.codot.gov/business/designsupport/materials-and-geotechnical/manuals/2021-m-e-pave-design-manual.
- Applied Research Associates. (2004). *Guide for Mechanistic-Empirical Design of New and Rehabilitated Pavement Structures.* NCHRP Project 1-37A. TRB, National Research Council, Washington, DC.
- Illinois Department of Transportation. (2010). *Illinois Bureau of Design and Environment Manual*. http://dot.state.mn.us/mnroad/nrra/structure-teams/geotechnical/files/manual-pavement-design-illinois.pdf. Accessed September 2, 2021.
- Irwin, L. (1983). *User's guide to Modcomp 2, version 2.1, Local Roads Program*. Cornell Univ., Ithaca, NY.
- Islam, S., Sufian, A., Hossain, M., Miller, R., and Leibrock, C. (2020). Mechanistic-Empirical Design of Perpetual Pavement. *Road Materials and Pavement Design*, Vol. 21, No. 5, 1224-1237.
- Kim, Y., Zeng, Z., and Lee, K. (2021). *Backcalculation of Dynamic Modulus from Falling Weight Deflectometer Data* (No. FHWA/NC/2017-03). North Carolina Department of Transportation. Research and Development Unit.
- Monismith, C. and McLean, D. (1972). Structural Design Considerations. *Journal of Association of Asphalt Paving Technologists*, 41, 12-31.
- Monismith, C., Harvey, J., Bressette, C., Suszko, C., and Martin, J. (2004). *The I-710 Freeway Rehabilitation Project: Mix and Structural Section Design, Construction Considerations and Lessons Learned.* International Symposium on Design and Construction of Long Lasting Asphalt Pavements, pp. 217-262, Auburn, Alabama.
- Newcomb, D., Buncher, M., and Huddleston, I. (2001). *Concepts of Perpetual Pavements*. Transportation Research Circular No. 503. *Perpetual Bituminous Pavements*. Transportation Research Board. pp. 4-11, Washington, D.C.
- Newcomb, D., Willis, R., and Timm, D. (2010). *Perpetual Asphalt Pavements: A Synthesis*. APA101, Asphalt Pavement Alliance, Lanham, MD.
- Pennsylvania Department of Transportation. (2019). *Pavement Policy Manual*. Accessed at https://www.dot.state.pa.us/public/PubsForms/Publications/PUB%20242.pdf.

- Prowell, B., Brown, E., Anderson, R., Daniel, J., Von Quintus, H., Shen, S., Carpenter, S., Bhattacharjee, S., and Maghsoodlo, S. (2010). *Validating the Fatigue Endurance Limit for Hot Mix Asphalt*. NCHRP Report No. 646, Transportation Research Board, Washington, D.C.
- Rienecker M., Suarez, M., Gelaro, R., Todling, R., Bacmeister, J., Liu, E., Bosilovich, M., Schubert, S., Takacs, L., Kim, G., and Bloom, S. (2011). MERRA: NASA's modern-era retrospective analysis for research and applications. *Journal of climate*. 24(14), pp.3624-3648.
- Solatifar, N., Kavussi, A., Abbasghorbani, M., and Sivilevičius, H. (2017). Applying FWD data in developing dynamic modulus master curves of in-service asphalt layers. *Journal of Civil Engineering and Management*, 23(5), 661-671.
- Texas Department of Transportation. (2021). *Pavement Manual.* Accessed at http://onlinemanuals.txdot.gov/txdotmanuals/pdm/manual_notice.htm.
- Thompson, M., and Carpenter, S. (2006). *Considering Hot-Mix-Asphalt Fatigue Endurance Limits in Full-Depth Mechanistic-Empirical Pavement Design*. International Conference on Perpetual Pavements, Columbus, Ohio.
- Timm, D., and Newcomb, D. (2006). Perpetual Pavement Design for Flexible Pavements in the US. *International Journal of Pavement Engineering*, 7:2, 111-119.
- Timm, D., Tran, N., and Rodezno, C. (2017). *Redesign and Updates of the Perpetual Pavement Design Software: PerRoad Version 4.3*. NCAT Research Synopsis 17-06, Auburn, Alabama.
- Tran, N., Robbins, M., Timm, D., Willis, R., and Rodezno, C. (2016). *Refined Limiting Strain Criteria and Approximate Ranges of Maximum Thickness for Designing Long-Life Asphalt Pavements*. NCAT Report 15-05R, Auburn, Alabama.
- Transportation Research Board (TRB). (2001). *Perpetual Bituminous Pavements*. Transportation Research Circular No. 503, Washington, D.C.
- Von Quintus, H. (2006). *Application of the Endurance Limit Premise in Mechanistic-Empirical Based Pavement Design Procedures*. International Conference on Perpetual Pavements, Columbus, Ohio.
- Walubita, L., and Scullion, T. (2010). *Texas Perpetual Pavements – New Design Guidelines*. Texas Department of Transportation Project 0-4822 Report 0-4822-P6, College Station, Texas.
- West R., Gu, F., and Bowers, B. (2020). *Benefits of Rehabilitating Concrete Pavements with Slab Fracturing and Asphalt Overlays*. NCAT Report 20-03. National Center for Asphalt Technology, Auburn, Alabama.

APPENDIX A
Preliminary Perpetual Pavement Analysis
Backcalculated Moduli and Strain Distributions

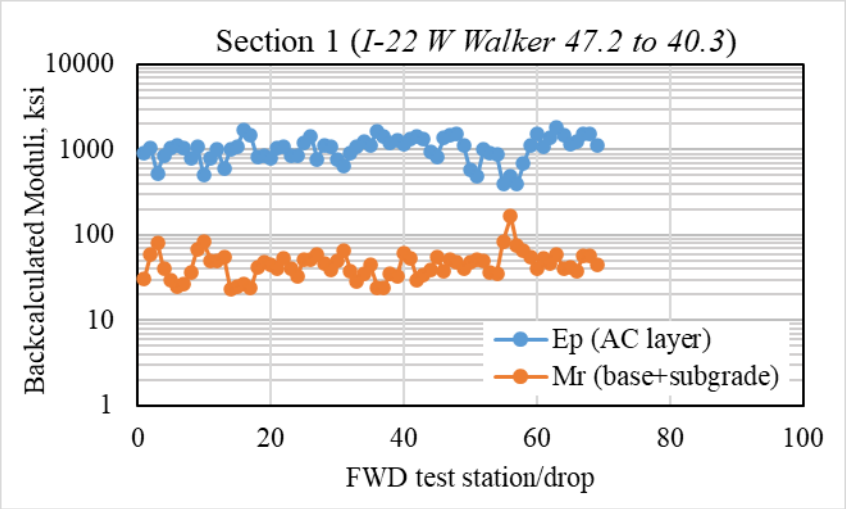

Figure A.1 Backcalculated modulus of Section 1

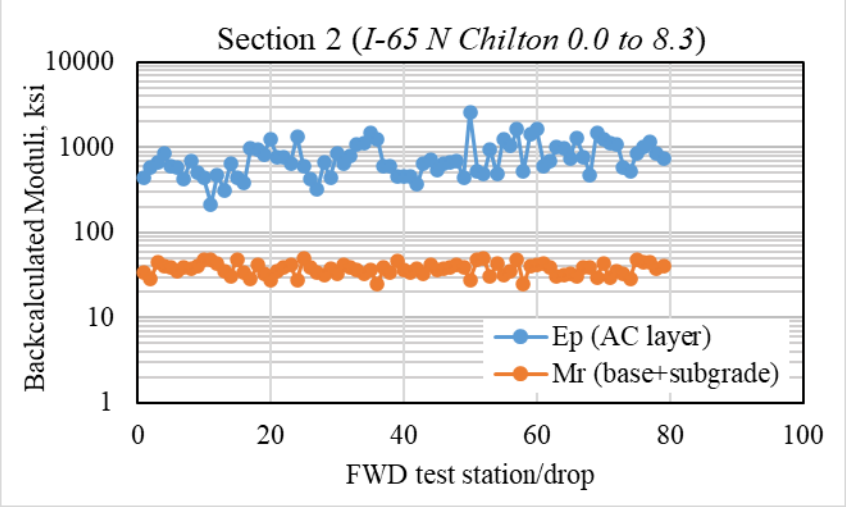

Figure A.2 Backcalculated modulus of Section 2

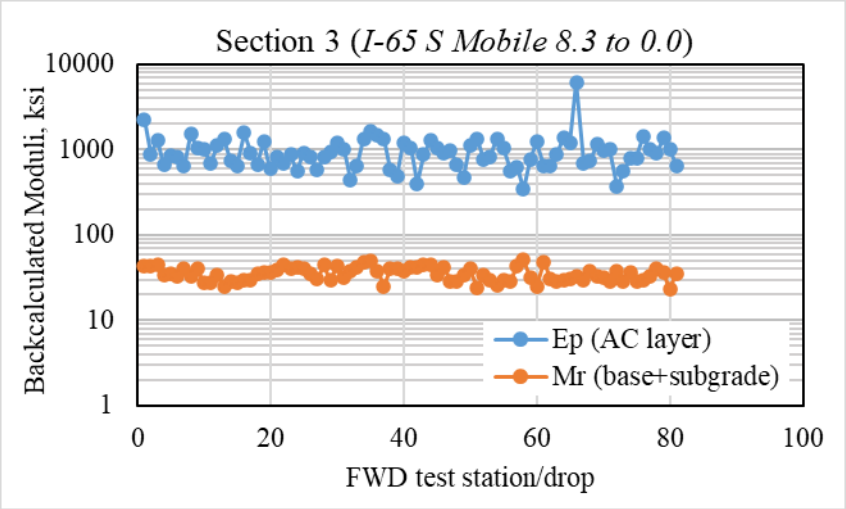

Figure A.3 Backcalculated modulus of Section 3

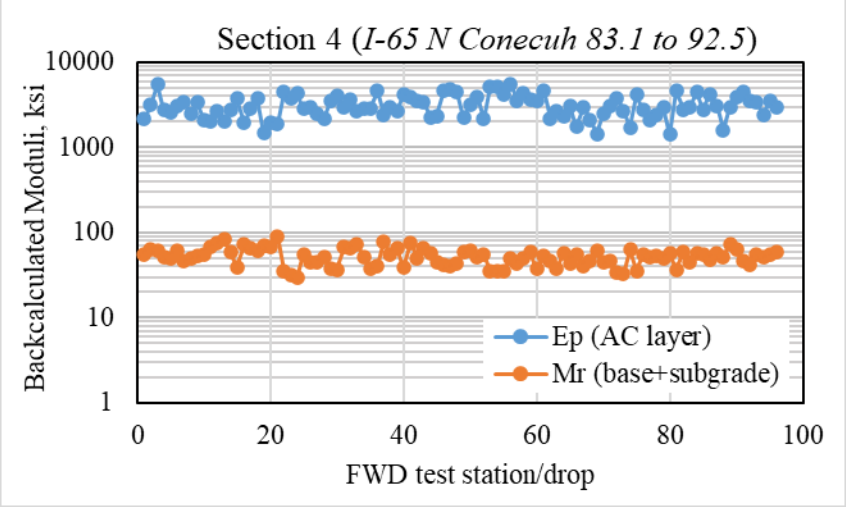

Figure A.4 Backcalculated modulus of Section 4

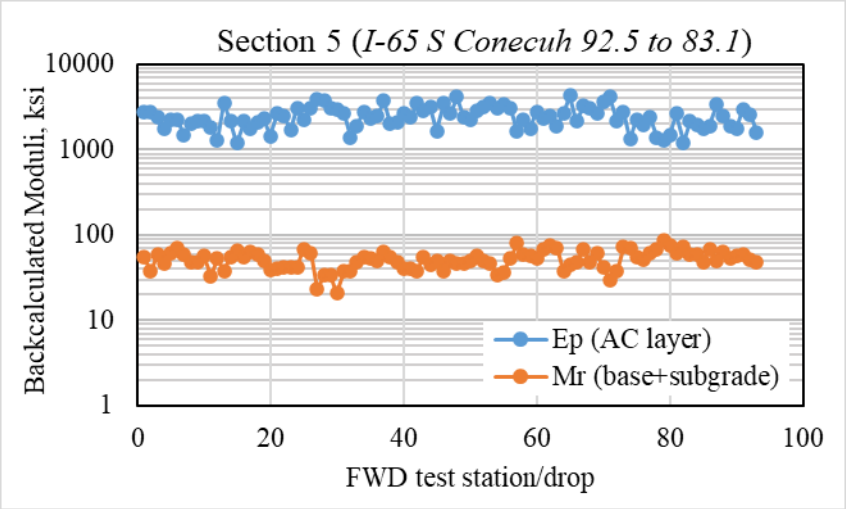

Figure A.5 Backcalculated modulus of Section 5

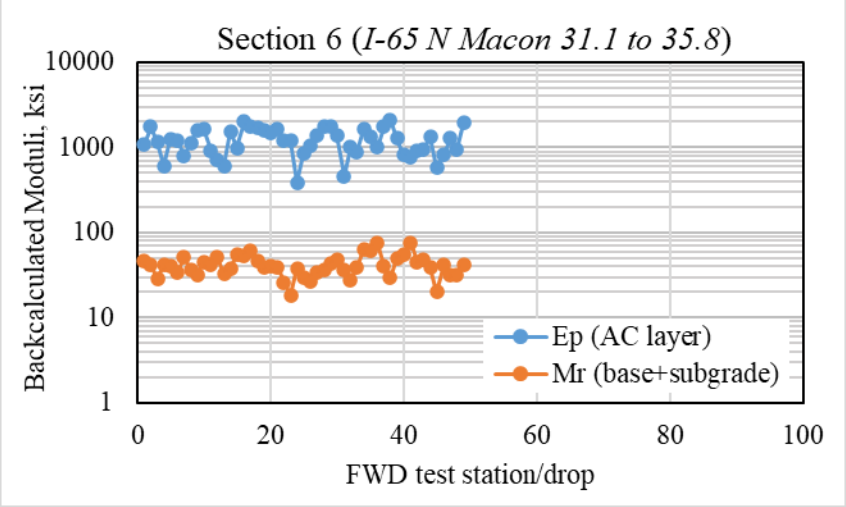

Figure A.6 Backcalculated modulus of Section 6

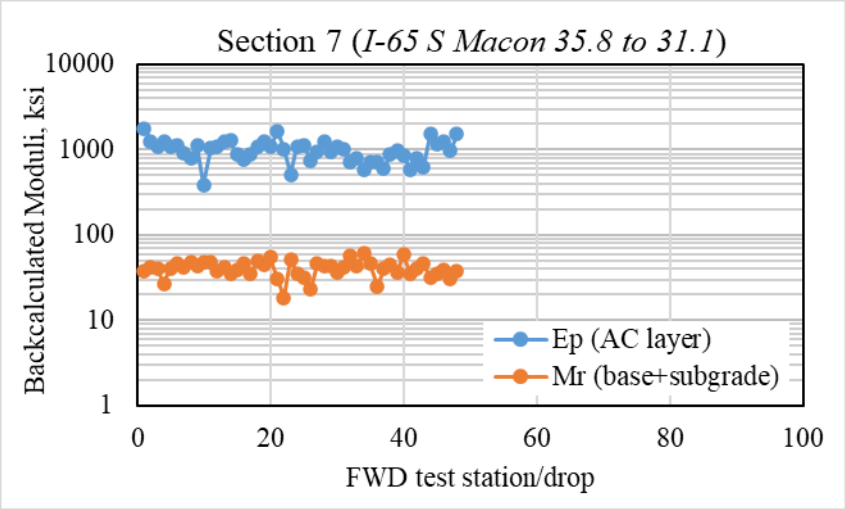

Figure A.7 Backcalculated modulus of Section 7

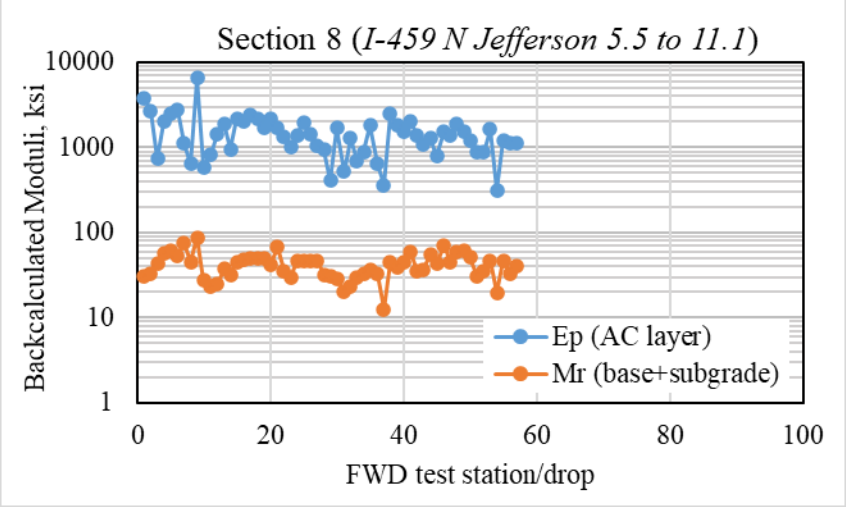

Figure A.8 Backcalculated modulus of Section 8

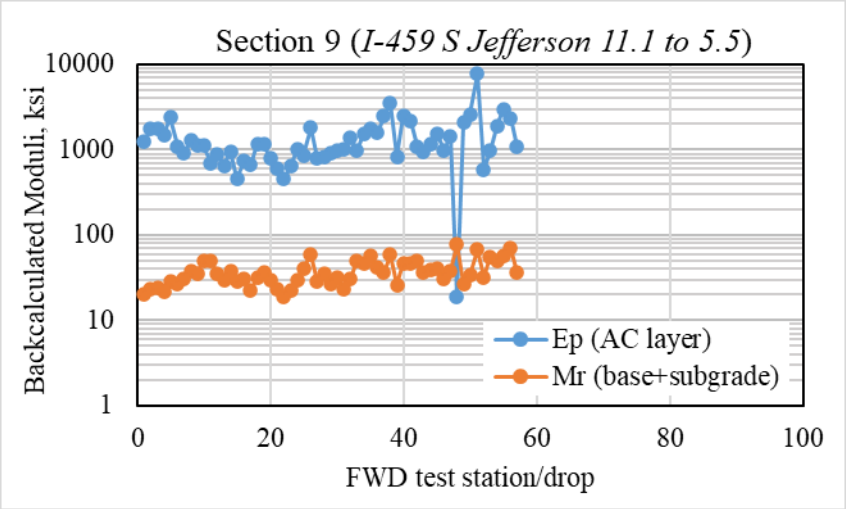

Figure A.9 Backcalculated modulus of Section 9

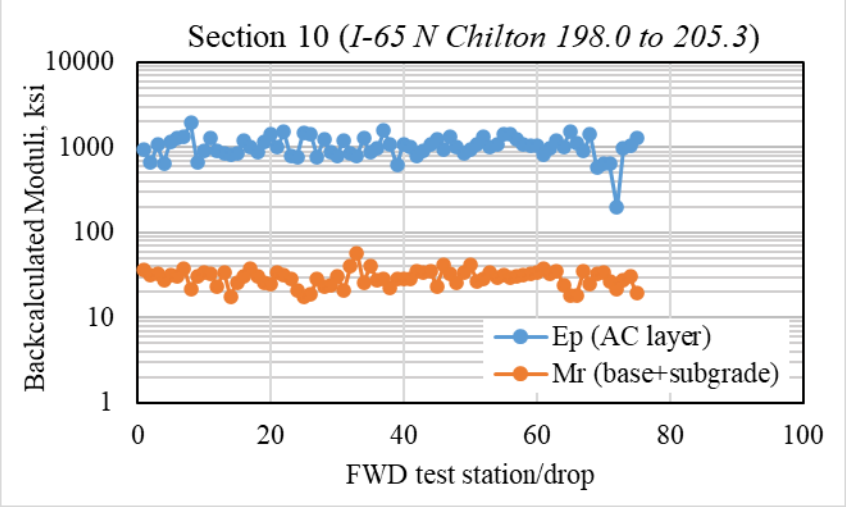

Figure A.10 Backcalculated modulus of Section 10

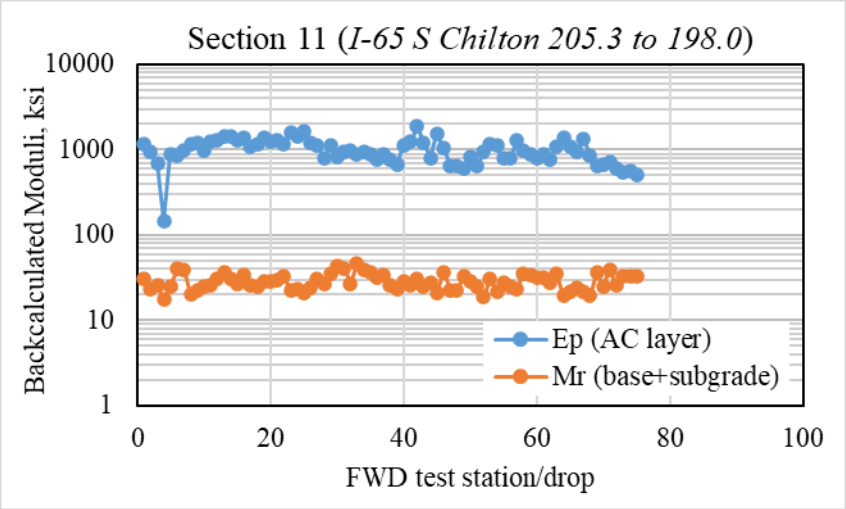

Figure A.11 Backcalculated modulus of Section 11

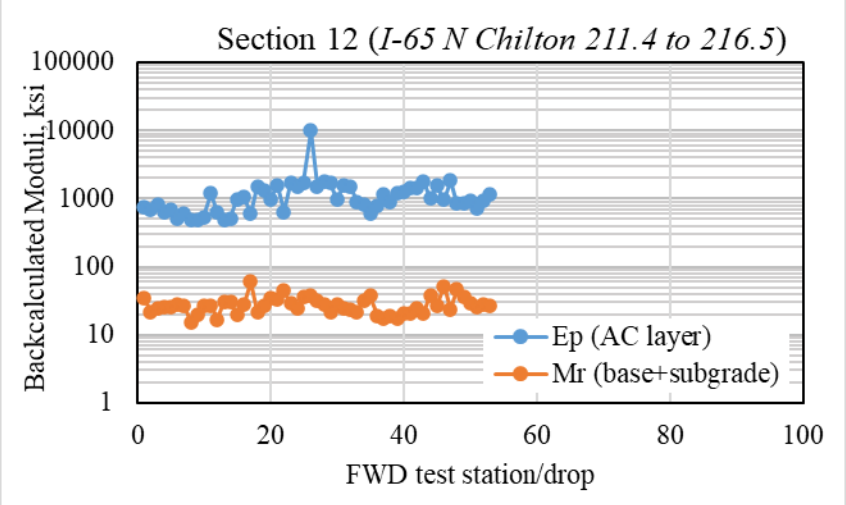

Figure A.12 Backcalculated modulus of Section 12

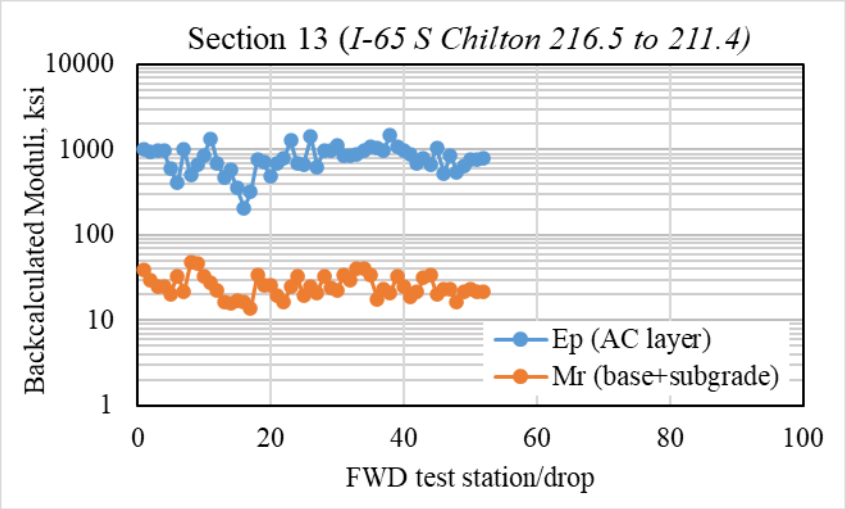

Figure A.13 Backcalculated modulus of Section 13

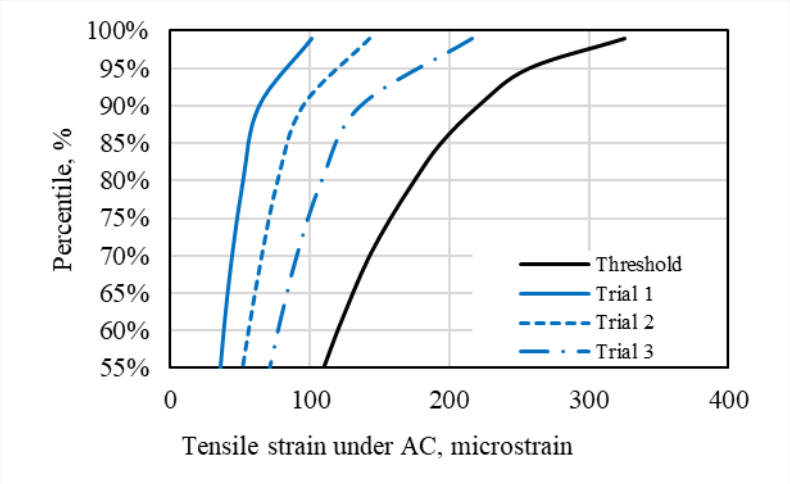

Figure A.14 Tensile strain distribution at the bottom of AC for section 2

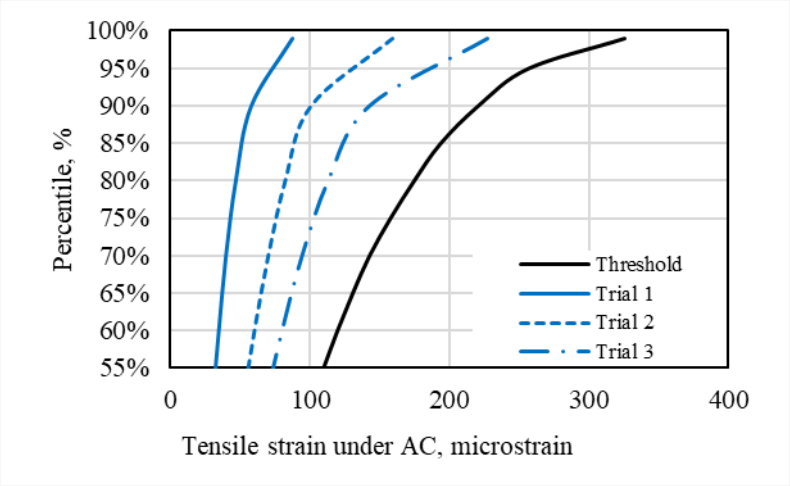

Figure A.15 Tensile strain distribution at the bottom of AC for section 3

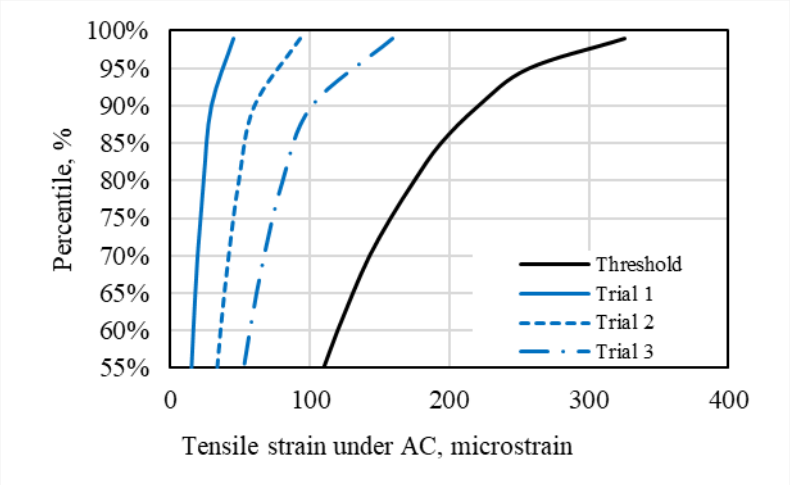

Figure A.16 Tensile strain distribution at the bottom of AC for section 5

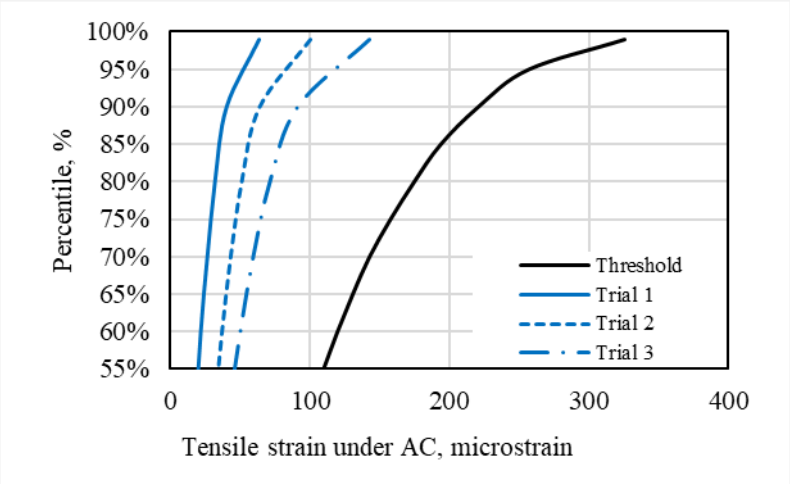

Figure 45 Tensile strain distribution at the bottom of AC for section 6

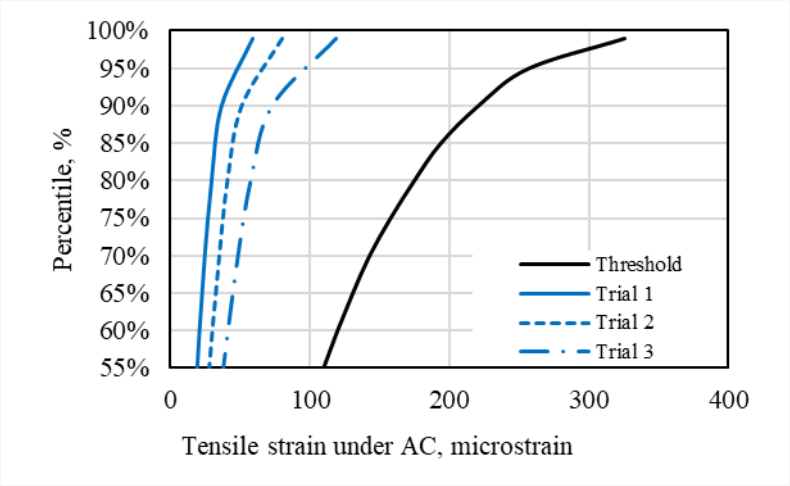

Figure A.18 Tensile strain distribution at the bottom of AC for section 7

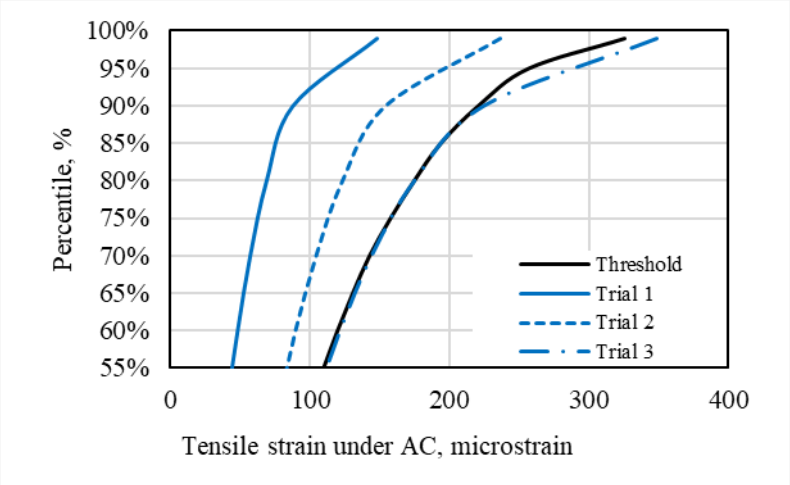

Figure A.19 Tensile strain distribution at the bottom of AC for section 9

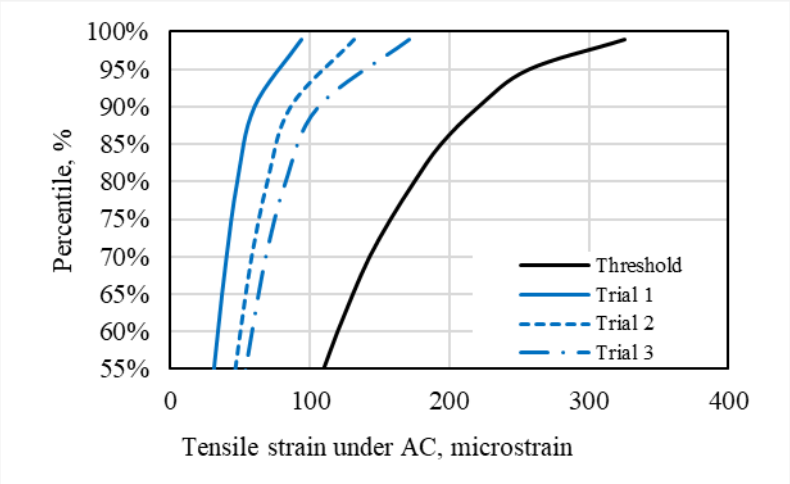

Figure A.20 Tensile strain distribution at the bottom of AC for section 10

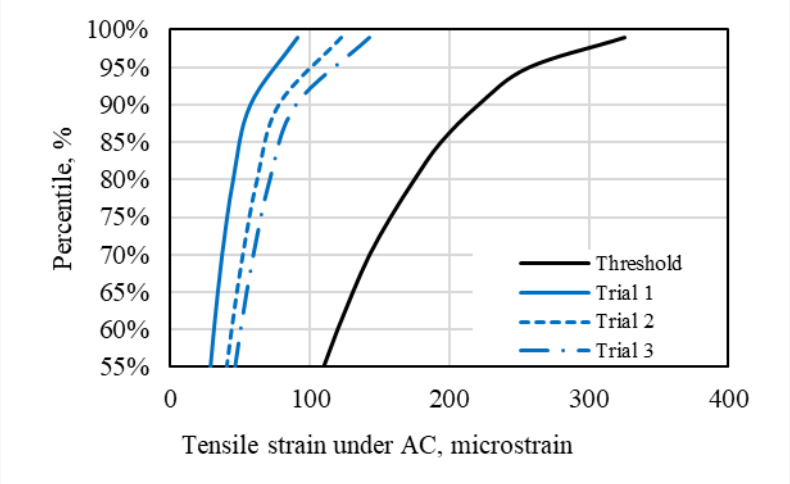

Figure A.21 Tensile strain distribution at the bottom of AC for section 12

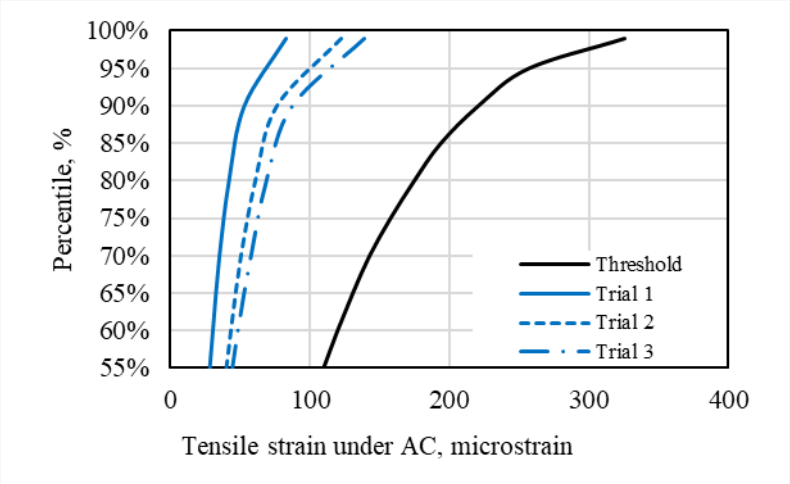

Figure A.22 Tensile strain distribution at the bottom of AC for section 13

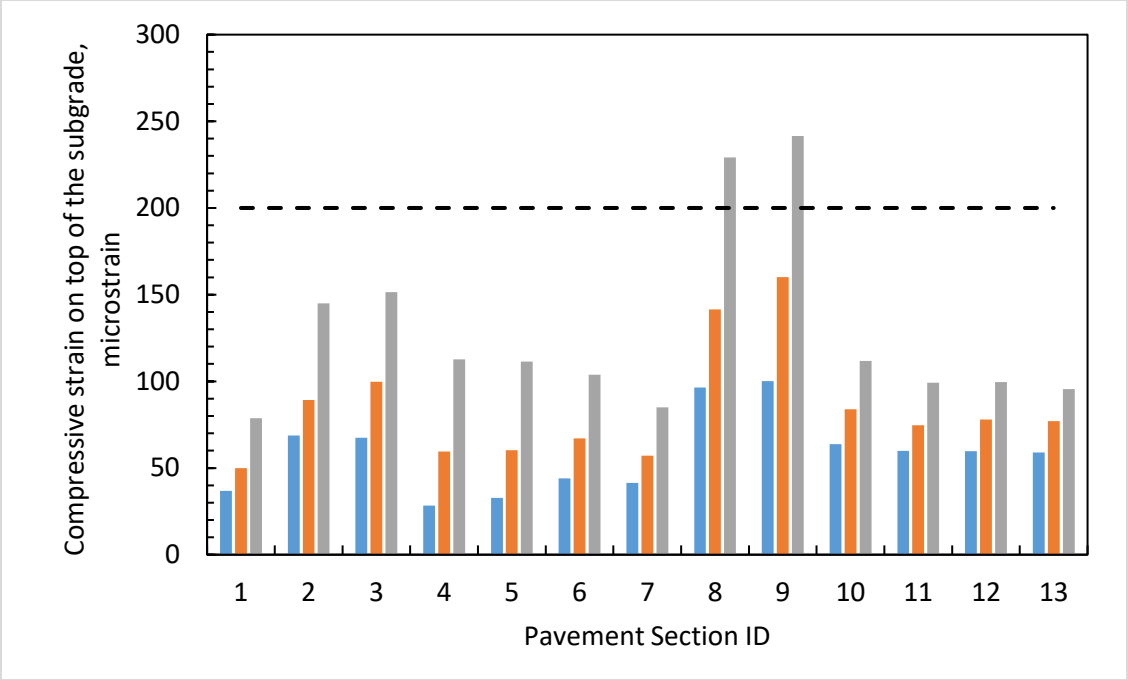

Figure 46 50th percentile compressive strain on top of the subgrade

APPENDIX B
Methodology Validation Design Thicknesses

Table B.1 Design AC thicknesses with different structural and climatic inputs considered for the granular aggregate bases (simulated with highway axle load spectra to control bottom-up fatigue cracking and structural rutting)

Granular base moduli (E_2), ksi	Subgrade moduli (E_3), ksi	Granular base thickness								
		6.0 inch.			8.0 inch.			10.0 inch.		
		Zone-1	*Zone-2*	*Zone-3*	*Zone-1*	*Zone-2*	*Zone-3*	*Zone-1*	*Zone-2*	*Zone-3*
25	**5**	13.0	12.5	12.0	12.5	12.0	11.5	12.5	11.5	11.0
	8	12.0	11.5	11.0	11.5	11.5	11.0	11.5	11.0	11.0
	15	11.5	11.0	10.5	11.5	11.0	10.5	11.0	10.5	10.5
50	**5**	11.5	10.5	10.0	10.5	10.0	9.5	10.0	9.5	9.0
	8	10.5	10.0	9.5	10.0	9.5	9.0	10.0	9.0	9.0
	15	10.0	9.5	9.0	9.5	9.0	8.5	9.5	9.0	8.5

** Indicate scenarios where subgrade rutting governed the design thickness*

Table B.2 Design AC thicknesses with different structural and climatic inputs considered for the rubblized bases (simulated with highway axle load spectra to control bottom-up fatigue cracking and structural rutting)

Rubblized base moduli (E_2), ksi	Subgrade moduli (E_3), ksi	Granular base thickness								
		6.0 inch.			8.0 inch.			10.0 inch.		
		Zone-1	*Zone-2*	*Zone-3*	*Zone-1*	*Zone-2*	*Zone-3*	*Zone-1*	*Zone-2*	*Zone-3*
100	**5**	10.0*	9.5*	9.0*	9.0*	8.5*	8.0*	7.5*	7.0*	7.0*
	8	8.5*	8.0*	7.5*	7.5*	7.0*	7.0*	7.0*	6.5*	6.5
	15	7.5	7.0	6.5	7.0	6.5	6.0	6.5	6.5	6.0

** Indicate scenarios where subgrade rutting governed the design thickness*

Table B.3 Design AC thicknesses with different structural and climatic inputs considered for the granular aggregate bases (simulated with legal axle load limit to control bottom-up fatigue cracking and structural rutting)

Granular base moduli (E_2), ksi	Subgrade moduli (E_3), ksi	Granular base thickness								
		6.0 inch.			8.0 inch.			10.0 inch.		
		Zone-1	*Zone-2*	*Zone-3*	*Zone-1*	*Zone-2*	*Zone-3*	*Zone-1*	*Zone-2*	*Zone-3*
25	**5**	18.0*	17.0*	16.0*	17.5*	16.5*	15.5*	17.0*	16.0*	15.0*
	8	16.0*	15.0*	14.5*	15.5*	14.5*	14.0*	15.0*	14.0*	13.5*
	15	13.5	13.0	11.5	13.5	12.5	11.5	13.5	12.5	11.5
50	**5**	17.5*	16.5*	16.0*	17.0*	16.0*	15.0*	16.0*	15.0*	14.5*
	8	16.0*	15.0*	14.5*	15.0*	14.0*	13.5*	14.0*	13.5*	13.0*
	15	13.5*	12.5*	12.0*	12.5*	11.5*	11.0*	11.5*	11.0*	10.5*

** Indicate scenarios where subgrade rutting governed the design thickness*

Table B.4 Design AC thicknesses with different structural and climatic inputs considered for the rubblized bases (simulated with legal axle load limit to control bottom-up fatigue cracking and structural rutting)

Rubblized base moduli (E_2), ksi	Subgrade moduli (E_3), ksi	Granular base thickness								
		6.0 inch.			8.0 inch.			10.0 inch.		
		Zone-1	*Zone-2*	*Zone-3*	*Zone-1*	*Zone-2*	*Zone-3*	*Zone-1*	*Zone-2*	*Zone-3*
100	**5**	16.5*	15.5*	15.0*	15.5*	14.5*	14.0*	14.0*	13.0*	13.0*
	8	15.0*	14.0*	13.5*	13.5*	13.0*	12.5*	12.5*	12.0*	11.5*
	15	12.5*	12.0*	11.0*	11.5*	10.5*	10.0*	10.0*	9.5*	9.0*